U.S. DEPARTMENT OF COMMERCE
National Technical Information Service
PB-301 064

System Identification of Tall Vibrating Structures

Hawaii Univ at Manoa, Honolulu Dept of Civil Engineering

Prepared for

National Science Foundation, Washington, DC Engineering and Applied Science

Jul 79

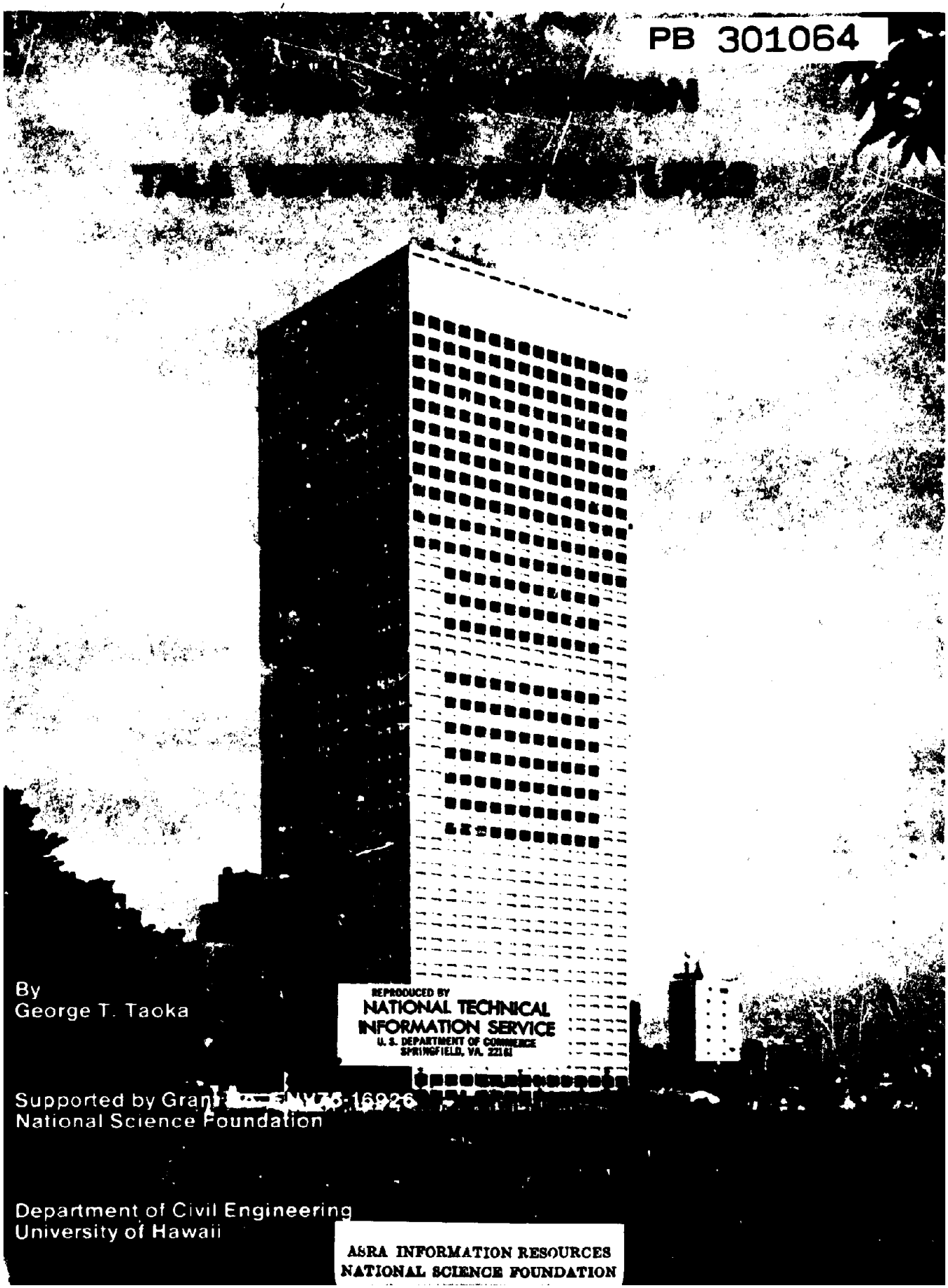

By
George T. Taoka

Supported by Grant [illegible] ENV76-16926
National Science Foundation

Department of Civil Engineering
University of Hawaii

50272-101

REPORT DOCUMENTATION PAGE	1. REPORT NO. NSF/RA-790173	2.	3. PB301064

4. Title and Subtitle
System Identification of Tall Vibrating Structures, Final Report

5. Report Date
July, 1979

6.

7. Author(s)
G. T. Taoka

8. Performing Organization Rept. No.

9. Performing Organization Name and Address
University of Hawaii
Department of Civil Engineering
2540 Dole Street
Honolulu, Hawaii 96822

10. Project/Task/Work Unit No.

11. Contract(C) or Grant(G) No.
(C)
(G) ENV7516926

12. Sponsoring Organization Name and Address
Engineering and Applied Science (EAS)
National Science Foundation
1800 G Street, N.W.
Washington, D.C. 20550

13. Type of Report & Period Covered
Final

14.

15. Supplementary Notes

16. Abstract (Limit 200 words)

An investigation of the comparative accuracy of four different system identification methods for estimating frequency and damping parameters from identical ambient vibration records of tall structures is reported. Ambient vibration responses under natural wind conditions of five tall structures in Tokyo and Yokohama were recorded. The ambient data thus obtained were analyzed by four system identification methods: filtered correlation, spectral moments, spectral density, and two-stage least square. Factors that greatly affect the values of parameter estimates obtained from the ambient vibration record are record length, signal-noise ratio in the record, filter shape, and filter cutoff bandwidth. The filtered correlogram method was easy to program and generally produced reasonably accurate vibrational parameter estimates. The spectral moments method was also easy to program and produced parameter estimates consistent with those of the filter correlogram method. Spectral density estimates are consonant with those from the other two methods. The two-stage least square method requires greater effort in programming and in analyzing data than the filtered correlogram or spectral moments methods. Building pictures, equations, data, graphs and references are included.

17. Document Analysis a. Descriptors

Earthquakes
Buildings
Earthquake resistant structures
Skyscrapers
Ambient pressure
Structural engineering

b. Identifiers/Open-Ended Terms

Japan
Filter correlogram
Spectral moments
Least square (two stage)
Spectral activity

c. COSATI Field/Group

18. Availability Statement	19. Security Class (This Report)	21. No. of Pages
NTIS		124
	20. Security Class (This Page)	22. Price PC A06 MF A01

(See ANSI-Z39.18) See Instructions on Reverse OPTIONAL FORM 272 (4-77)
(Formerly NTIS-35)
Department of Commerce

SYSTEM IDENTIFICATION OF TALL VIBRATING STRUCTURES

by

George T. Taoka

Final Report

Supported by

The National Science Foundation

through Grant No. ENV-16926

Department of

Civil Engineering

University of Hawaii at Manoa

Honolulu, Hawaii

July, 1979

TABLE OF CONTENTS

LIST OF TABLES

LIST OF FIGURES

I. INTRODUCTION

Investigations into the full scale dynamic testing of tall structures have been performed on many new buildings, especially when these are located in seismically active zones. References [1], [2], and [3] are examples of tall buildings that have been tested in this manner. While full scale testing of a new structure using rotating vibration shakers is probably the most desirable method for estimating its dynamic parameters, it is frequently difficult to obtain permission from the owner to test a building in this manner. The cost of such a test and the possibility that slight visually observable non-structural cracking may result are generally cited as reasons why such tests are generally not performed on a new structure.

Ambient vibration measurements, however, can be performed on any tall structure inexpensively without causing any damage. Such measurements may be performed quickly and easily by a small team of investigators with a minimum of interference to the occupants of a building. After ambient response data have been recorded and suitably digitized for a structure, two questions confront the investigator:

a) what is the "best" way to analyze this data to identify structural response parameters, i.e., which is the "best" system identification method; and

b) by how much do these parameter estimates evaluated under very low levels of excitation differ from the values to be expected when the structure is subjected to much higher levels of excitation, due to vibration shakers, or under severe wind or

earthquake conditions?

This investigation is concerned with attempting to seek some answers to these two very fundamental questions, with emphasis on the former. Before the general theory underlying some of these methods is presented, the relatively recent history of ambient vibration analysis will be briefly discussed.

The application of statistical techniques to estimate vibration parameters from random response data appears to have first developed in Japan in the mid 1950's. In 1954, Takahashi and Husimi [4] published a paper whereby the frequency and damping parameters of a one degree of freedom system excited by a white noise were obtained by correlation and spectral density functions. The correlation function was approximately an exponentially decaying cosine function, and the spectral density function had a corresponding sharp peak at the natural frequency. The damping parameter was estimated by the logarithmic decrement of the correlation function.

In 1957, Hatano and Takahashi [5] used this method to estimate dynamic parameters of dams. The application to towers, buildings, and other structures excited by wind and microtremors was obvious. However, the modeling of a structure as a one degree of freedom system was a severe limitation, since most structures respond in several degrees of freedom under low level excitation. It was obvious that some form of filtering of the original data would be necessary before the correlation technique could be successfully applied to vibration of actual structures. The work of Cherry and Brady [6] demonstrated that if more than one mode of vibration were present in the record,

the envelope of the correlation function would exhibit irregular behavior while generally decaying exponentially, making estimation of damping difficult.

Ward and Crawford [7] used analog filtering techniques to isolate individual response modes of buildings excited by wind. While this gave satisfactory results, information on higher modes is frequently lost by analog filtering of response records. Thus the tendency has been for investigators to apply digital band-pass filters to random ambient data rather than analog filters.

Several methods of analyzing digitally filtered ambient vibration data have been proposed in the literature. All of these assume that the input function is stationary for a short duration and can be represented by fairly wide band-limited white noise. The Cherry-Brady autocorrelation approach [6] has been used by Davenport, Hogan, and Vickery [8] to analyze records from a tall building, where a trapezoidal band-pass filter was applied to the response data before the autocorrelation function was computed. Taoka and Scanlan [9] used a Gaussian filter in conjunction with the autocorrelation function to estimate structural response parameters of seven tall structures.

Vanmarcke [10] has proposed a method of estimating parameters using properties of spectral moments. Gersch, Nielsen, and Akaike [11] have developed a maximum likelihood technique for determining these values. A comparison of these techniques has been performed on an actual ambient vibration record of nine story steel building by Foutch [12]. Gersch has also proposed a two-stage least square method of analysis [13], which is simpler to apply than the maximum likelihood

technique.

With respect to the difference in levels of excitation, Tanaka [14] has compared the period and damping values determined from earthquake records and from wind excitation for a group of buildings in Japan. In this country, Trifunac [15] and Udwadia [16] have presented comparisons of ambient and forced vibration test of structures. Hudson [17] and Schiff [18] have surveyed the state of the art in random vibration measurements due to wind and microtremor excitation. Ibanez has also presented an extensive review of this subject [19].

While substantial effort has been expended on the dual problems of analyzing random vibration data and of the comparison of ambient response estimates with values obtained from shaker or earthquake excitation, additional work needs to be done in this area, especially in regards to the response of very tall structures. More comparisons of estimates obtained by analyzing actual response data by different methods are required to properly evaluate advantages and disadvantages of each method proposed to compute parameter values by different methods of time series analysis.

In the summer of 1974, the author served as a Visiting Research Professor at Tokyo Institute of Technology (Tokyo Kogyo Daigaku) at the invitation of the Japan Society for the Promotion of Science. During this period, the author was able to record the ambient vibration responses under natural wind conditions of seven tall structures in Tokyo and Yokohama with the help of Professor Hiroyoshi Kobayashi of Tokyo Institute of Technology. These records were suitably digitized and processed in a manner such that they were ready for time series

analysis on a digital computer.

In early 1975, the author submitted a proposal to the National Science Foundation to analyze the data and compare any dynamic structural parameter estimates with values obtained for these same structures during rotating vibration shaker tests.

After incorporating the suggestions of reviewers, the emphasis of the investigation was shifted to a study of the various system identification techniques available to analyze data. The comparison of values obtained by different methods from the same data became the primary focus of this research proposal.

Since the actual funding was reduced by about one-third from the original request, the scope of this project was reduced to an investigation of only five of the original seven structures. It was also decided that the study of digital filtering would be limited to two fundamental and easily constructed windows, so that errors in parameter estimates due to filtering of the experimental data would be minimal.

The four system identification methods for analyzing ambient data to be investigated are:

1. filtered correlation method
2. spectral moments method
3. spectral density method
4. two-stage least square method.

Since all these methods will be applied to the same data, filtered using the same window, differences in parameter estimates will be primarily due to the system identification procedures employed. This

will give an indication of how accurately each procedure estimates the desired dynamic parameters for actual experimental data, instead of for simulated data.

This research proposal was granted by the National Science Foundation in August of 1976. This document is the final report summarizing the result obtained by the author during the course of his investigation, funded by this research grant.

II. DIGITAL FILTERING OF THE AMBIENT RESPONSE RECORD

The discrete time series obtained from digitizing a response record generally represented the structural response in more than a single mode of vibration. A direct computation of the autocorrelogram of the response series $\{y_n\}$ would therefore result in a function exhibiting highly irregular behavior, due to the presence of energy concentrations at more than one natural frequency. It was therefore necessary to filter the response records in order to investigate structural parameters associated with individual modes.

A filtered time series $\{u_n\}$, where

$$u_n = u(nh) \qquad n = 0,1,2,\text{---}, N-1 \tag{1}$$

can be obtained from the original series $\{y_n\}$ by passing it through a nonrecursive filter defined by the following operation:

$$u_n = h_o y_n + \sum_{k=1}^{m} h_k \, (y_{n+k} + y_{n-k}) \tag{2}$$

where $h_k = h_{-k}$, due to the symmetry of the filter.

The frequency response function H(f) of the filter is defined as [20]

$$H(f) = h_o + 2 \sum_{k=1}^{m} h_k \cos (2\pi f_k \Delta t) \; . \tag{3}$$

The filter weights $\{h_k\}$ are obtained as the inverse Fourier transform of Equation (3).

$$h_k = \int_{-\infty}^{\infty} H(f) \cos (2\pi f_k \Delta t) \, df \tag{4}$$

Once the filter weights are known, the filtering can be performed in the time domain as specified by Equation (2).

Not all of the terms of the resulting output series $\{u_n\}$ should be used for further analysis, however. It is desirable to construct a new series $\{u_\ell^1\}$ by essentially truncating m terms from both ends of $\{u_n\}$,

$$u_\ell^1 = u_{m+\ell} \qquad \ell = 1,2,3,\text{---}, N - 2m \quad . \tag{5}$$

The new series $\{u_\ell^1\}$ now has only N - 2m number of terms, and is relatively free from the effect of transient conditions, if the value of h_k is negligible for $k > m$.

The autocorrelogram of the truncated filtered series $\{u_\ell^1\}$ can then be used to estimate the damping associated with the mode in question, as will be discussed later.

Digital filtering can also be performed in the frequency domain with the use of a Fast Fourier Transform (FFT) algorithm. If $\{Y(f)\}$ and $\{H(f)\}$ are the complex Fourier Coefficients of the discrete Fourier Transform of $\{y_n\}$ and $\{h_k\}$, respectively, then filtering in the frequency domain can be performed as follows:

1. Compute $\{Y(f)\}$ by applying FFT to $\{y_n\}$,
2. Specify the filter frequency response $\{H(f)\}$,
3. Multiply $\{Y(f)\}$ and $\{H(f)\}$ to obtain $\{U(f)\}$,
4. Compute $\{u_n\}$ by applying inverse FFT to $\{U(f)\}$.

Filtering by multiplication in the frequency domain using the FFT is generally more economical than filtering by convolution in the time domain. Stockham [21] and Brigham [22] both summarize the advantages of this indirect method.

Two filters have been utilized in this investigation: the Gaussian Filter and the Trapezoidal Filter. The Gaussian Filter is

defined by

$$H(f) = \exp\left[-\alpha\left[\frac{f-f_c}{f_c}\right]^2\right] \qquad |f-f_c| \leq \frac{C}{2}$$
$$H(f) = 0 \qquad |f-f_c| > \frac{C}{2} . \tag{6}$$

The frequency characteristics for this filter are shown on Figure (1a), where B is the half-power bandwidth and C the cutoff bandwidth.

The trapezoidal filter's frequency response is indicated on Figure (1b), where H(f) is unity in the passband and decreases linearly on both sides of the passband. It is also assumed zero for $|f-f_c| > \frac{C}{2}$.

Papoulis [23] has an extensive discussion of the properties of Gaussian Filters. An example of its application in geophysics is given by Dzienwonski, Bloch, and Landisman [24]. This filter was chosen because of its nearly ideal optimum properties [23], and the ease with which it could be programmed on a digital computer.

In Equation (6), f_c denotes the center frequency of the Gaussian filter. The half-power bandwidth is denoted by B, and the cutoff bandwidth by C, as shown in Figure (1a). By centering the filter at a spectral peak, and adjusting the cutoff bandwidth C to isolate only a single peak, the filtered spectrum of individual modes could be studied.

The square of the absolute value of the filter gain is given by

$$|H(f)|^2 = \exp\left[-2\left[\frac{f-f_c}{f_c}\right]^2\right] \qquad |f-f_c| \leq \frac{C}{2}$$
$$|H(f)|^2 = 0, \quad |f| < f_c - \frac{C}{2}, \qquad |f-f_c| > \frac{C}{2} \tag{7}$$

For $\alpha = 3.0$, $B \tilde{=} 0.34C$

and the frequency response of the filter is truncated at a level of

-26 decibels. (See Jenkins [20]).

The value of B, and consequently of C, was determined by trial and error for each computer run. Starting with a relatively narrow bandwidth, the value of B was subsequently widened with each computer run until the shape of the resulting autocorrelation curve "stabilized" into an exponential cosine decay function. Generally, however, as wide a bandwidth value B as could be used without overlapping into a second spectral peak was used, for reasons that will be explained in the next section.

For the fundamental modes, the resulting damping estimate proved to be relatively insensitive to the value assigned to B, provided that

$$B \geq \frac{1}{6} f_c \quad . \tag{8}$$

For most of the damping estimates, a value of B approximately equal to $\frac{1}{3} f_c$ was used in the final computer analysis. For higher modes, the values of B and C were generally kept small to prevent nearby spectral peaks from interfering with the mode being analyzed.

The trapezoidal filter, shown in Figure (1b), has an advantage over the Gaussian filter in that it is flat in the passband B and therefore equal to unity in this region. However, because of discontinuities of its derivatives at four points, its impulse response function h_n in the time domain has a somewhat longer decay time, and its integral has somewhat longer rise time than the impulse response function of the Gaussian filter. The significance of the length of the rise time will now be briefly explained.

Since the filter impulse response weights h_k have anticipatory

components on the negative time scale h_{-k}, the total rise time t_R of the integral of the impulse response can be separated into two parts.

Half of the rise time (t_R / 2), corresponding to a rise from 0.5 to approximately 1.0 occurs during the first (m+1) terms of the record (n=0,m). The other half appears at the end of the record, and corresponds to a decay from approximately 1.0 to 0.5, for n=(N-m) to n=N.

Therefore, the "usable" portion of the filtered record $\{u_n\}$ has only (N-2m) terms, rather than (N) terms. This results because m terms are truncated from both the beginning and ending of the $\{u_n\}$ terms, because these "end portions" include the rather long rise times of the impulse response function integral of the trapezoidal filter. The effect of these "two-sided tails" is graphically illustrated in Figure (2).

Thus a good "rule of thumb" for the choice of filter to use is this:

1) If the ambient vibration record is long, use the trapezoidal filter, because of its constant value of unity in its passband. Truncating 2m terms from the original time series still yields a long record to analyze.
2) If the record is relatively short, however, use the Gaussian filter. While its value is not constant in the passband, its impulse response function decays rapidly, and less terms will have to be truncated from the original time series. The shortened record will still be long enough to give valid estimates of frequency and damping parameters.

III. APPLICATION OF THE RAW SPECTRUM ESTIMATE FOR FREQUENCY DETERMINATION

In most ambient vibration studies, three assumptions are made concerning the nature of the input forces, system characteristics, and output response. These are listed below (Schiff [25]):

1. The spectrum of the input forcing function, due primarily to wind loading, is almost flat or of constant amplitude with respect to frequency in the relatively narrow frequency bands surrounding the natural frequencies of interest.
2. The physical system may be modeled by linear equations with constant coefficients.
3. The output response is stationary and ergodic.

Under these assumption, if $H(\omega)$ is the system frequency response function, and $x(t)$ and $y(t)$ represent the input and response functions, respectively, then the spectral estimates of the input and response, $G_0(\omega)$ and $G(\omega)$, are related by

$$G(\omega) = |H(\omega)|^2 \, G_0(\omega). \tag{9}$$

From Assumption 1, $G(\omega)$ is assumed proportional to $|H(\omega)|^2$ in a narrow region surrounding a natural frequency. Assumption 3 implies that the system characteristics may be estimated from one relatively long record.

All three conditions were tacitly assumed in this investigation. Since the input spectra for the different records were not available, no estimate could be made concerning the degree to which Assumption 1 might not have been satisfied for these records. Assumption 2 is generally valid for the small amplitudes of vibration caused by wind

or microtremor excitation. From a visual inspection of the individual records, it appeared that the responses could reasonably be assumed to be nearly stationary over the time intervals for which the ambient responses were recorded.

Therefore, the shape of the square of the magnitude of the system response function, $|H(\omega)|^2$, may be assumed to be nearly proportional to the shape of the output response spectrum $G(\omega)$. Thus knowledge of the characteristics of $G(\omega)$ implied knowledge of the system response parameters inherent in the absolute value of the system response function $|H(\omega)|$.

If $y(t)$ is a continuous ambient response record, let

$$y_n = y(nh) \qquad n = 0,1,2,---, N-1 \tag{10}$$

be the discrete values of the response digitized at equi-spaced times

$$T_n = nh \qquad n = 0,1,2,---, N-1 \tag{11}$$

where $h = \Delta t$ is the constant digitizing interval.

Let discrete values along the frequency axis be defined by

$$f_k = \frac{k}{Nh} \qquad k = 0,1,2,---, N-1. \tag{12}$$

Then the discrete values of the complex Fourier components $\{X_k\}$ corresponding to frequencies $\{f_k\}$ are given [26] by:

$$Y_k = \sum_{n=0}^{N-1} y_n \exp\left(-j \frac{2\pi kn}{N}\right). \tag{13}$$

These complex Fourier components can be easily calculated by a Fast Fourier Transform algorithm. The raw spectral density estimates $G_y^1(k)$ are defined as follows:

$$G_y^1(k) = \frac{2h}{N} |Y_k|^2 . \tag{14}$$

Since values computed from Equation (13) do not give consistent estimates of the true Fourier coefficients, these values are usually smoothened by convolving them with appropriate weighting coefficients averaged over adjacent discrete values [27]. This is necessary because the original finite time series defined by Equation (10) is pictured as a portion of an infinite time series that is seen through a rectangular, or "box car" window function in the time domain. The corresponding Fourier coefficients given by Equation (13), therefore, are the results of a convolution of the true Fourier coefficent estimates with the Fourier transform of the rectangular window function. The value of the raw spectral density estimates computed from Equation (14) will thus tend to have pronounced "side lobes" near the spectral peak lobes, indicating a "leakage" of energy from the peak frequency band to adjacent frequency bands.

Such a smoothening procedure, however, automatically widens the bandwidth and reduces the peak value corresponding to a spectral lobe, resulting in a tendency to overestimate the amount of damping associated with a natural frequency.

The natural frequency estimates were therefore computed directly from the unsmoothered spectral density estimates $G_y^1(k)$, using the following interpolation method due to Lanczos [28]. The following discussion differs slightly from that given in Reference [28], employing the magnitude of the Fourier coefficients rather than algebraic values of sine and cosine components.

Assume that the largest absolute values of the Fourier coefficients near a spectral peak are given by $|Y_k|$ and $|Y_{k+1}|$.

Form the following pairs of weighted sums:

$$Z_k = |Y_{k-1}| + |2Y_k| + |Y_{k+1}|$$
$$Z_{k+1} = |Y_k| + |2Y_{k+1}| + |Y_{k+2}| \tag{15}$$

The quotient q_k is now defined as

$$q_k = \frac{Z_k}{Z_{k+1}} \quad . \tag{16}$$

The parameter ϵ is determined by

$$\epsilon = \frac{2 - q}{1 + q} \quad . \tag{17}$$

The value of the natural frequency coresponding to the position of a spectral peak can now be estimated as

$$f_{estimate} = \frac{k + \epsilon}{Nh} \quad . \tag{18}$$

Equation (18) was used to determine the natural frequency estimates in this report. Although the raw spectral estimates tended to have pronounced "side lobes" on both sides of a spectral peak, it was found that the determination of the natural frequency estimates for the first three modes of vibration in a record could be carried out in a very straightforward manner.

IV. APPLICATION OF THE FILTERED AUTOCORRELOGRAM ESTIMATE

The theoretical basis for the use of the autocorrelation function to estimate structural response parameters has been reviewed by Cherry and Brady [6]. They credit Hatano and Takahashi [5] for introducing this technique into the study of full scale structures.

Hudson [17] and Schiff [18] have both reviewed the present state of the art in this field. Filtered autocorrelation functions have been used by Ward and Crawford [7] and by Davenport and Hogan [8] to study the response of tall buildings due to wind excitation.

The following brief discussion of the general theory involved is taken from Cherry and Brady [6], and is included here for completeness.

If $h(\tau)$ is the system response function due to a unit impulse applied at $\tau = 0$, then the relation between an input function $x(t)$ and the resulting output response $y(t)$ is given by

$$y(t) = \int_0^\infty h(\tau)\, x(t-\tau)\, d\tau \tag{19}$$

For a lightly damped single degree of freedom oscillator having a natural circular frequency ω and a small critical damping ratio ζ the system response function is defined as

$$h(\tau) = \frac{e^{-\zeta\omega\tau}}{\omega\sqrt{1-\zeta^2}} \sin\left[\sqrt{1-\zeta^2}\,\omega\tau\right], \qquad \tau \geq 0 \tag{20}$$

It is assumed that $h(\tau) = 0$ for $\tau < 0$.

The autocovariance function for a function $y(t)$ is defined by

$$C_y(\tau) = \lim_{T\to\infty} \frac{1}{T} \int_{-\frac{T}{2}}^{\frac{T}{2}} y(t)\, y(t+\tau)\, dt \tag{21}$$

It can be shown that if the input function x(t) is composed of "white noise" with constant spectral density G_0, that the output autocovariance function is given by

$$C_y(\tau) = \frac{\pi G_0}{2\zeta\omega^3} \left[e^{-\zeta\omega\tau} \left(\cos \sqrt{1-\zeta^2}\ \omega\tau + \frac{\zeta}{\sqrt{1-\zeta^2}} \sin \sqrt{1-\zeta^2}\ \omega\tau \right) \right] \qquad (22)$$

Equation (22) represents a cosinusoidal function with exponential decay. The decay of the envelope of the autocovariance estimate of the output response can thus be used to estimate the critical damping ratio ζ of the system.

Note that for $\zeta << 1$, the sine expression in the parenthesis is very small compared to the cosine expression, and $C_y(\tau)$ approaches a damped exponential cosine function.

The unbiased autocovariance estimate of a time series $\{ y_n \}$ where n varies from 1 to N is given by

$$C_x(k) = \frac{1}{N-k} \sum_{n=1}^{N-k} y_n\, y_{n+k} \quad , \qquad 0 \leq k \leq M \qquad (23)$$

The corresponding autocorrelogram estimate is given by

$$R_y(k) = \frac{C_y(k)}{C_y(0)} \qquad 0 \leq k \leq M \qquad (24)$$

In both Equations (23) and (24), the integer M, the maximum lag number, is kept small compared to N, the number of points in the series.

In this investigation, the autocorrelation estimate $R_y(k)$ was computed indirectly by first forming the spectral density estimate,

and then computing the inverse transform of the filtered spectral density, by applying the Fast Fourier Transform algorithm twice.

The procedure is summarized below.

1. Subtract the mean value from the original series, and add N zeroes to obtain a 2N augmented series.
2. Filter the original series y(t) to obtain a filtered series u(t).
3. Form the raw spectral estimates of the filtered series $G_u^1(k)$.
4. Form the biased estimate of the autocovariance function corresponding to the filtered function $\{u_n\}$ by finding the inverse Fourier transform of
$$G_u^1(k) = |H(f)|^2 G_y^1(k). \qquad (25)$$
5. Multiply each $C_u^1(k)$ by the factor $\left(\frac{N}{N-k}\right)$ to obtain an unbiased estimate $C_u(k)$.
6. Divide each $C_u(k)$ by $C_u(0)$ to obtain the normalized autocorrelogram estimate $R_u(k)$.

It should be noted that the nonrecursive filtering process by which $\{u_n\}$ is derived from $\{y_n\}$ according to Equation (2) is affected by the transient conditions in the first m terms, introducing some error in these initial terms of $\{u_n\}$, unless these m terms have already been removed from the ends of the filtered time series as discussed earlier. As a consequence, the resulting envelope of the autocorrelogram estimate $R_y(k)$ may not exhibit exponential decay in the region $0 \leq k \leq m$.

The "usable" region from which the critical damping ratio may be

estimated is for k within the limits

$$m \leq k \leq M. \tag{26}$$

The logarithmic decrement method [29] was used to estimate the critical damping ratio in each mode. The value is determined by

$$\zeta = \frac{1}{2\pi q} \ln \left(\frac{A_p}{A_{p+q}} \right) \tag{27}$$

where A_p is the peak amplitude at cycle p and A_{p+q} is the peak amplitude q cycles later. It should be noted that if τ_n corresponds to the time lag $\tau = \tau_n$, then

$$\tau_m \leq \tau_p \leq \tau_{p+q} \leq \tau_M \tag{28}$$

Since τ_m is inversely proportional to the cutoff bandwidth C of the filter, τ_m could be made small by using as wide a cutoff bandwidth C as possible. This is a consequence of the "uncertainty principle" discussed by Papoulis [23].

The value τ_m may be interpreted as the minimum time lag required for the autocorrelation function to "stablize" because of the filtering operation indicated by Equation (2).

Four important factors can influence the accuracy of the damping parameters estimated by the filtered correlogram method presented above. These are

1. the ambient response record length
2. the signal to noise ratio for a given mode
3. the shape of the filter
4. the filter bandwidth.

Assuming that the record is stationary, the longer its length is, the better its correlogram estimate will generally be. Since the

maximum lag time is generally only a tenth (conservative value) to a quarter of its total length [30], and since the damping ratio estimate obtained from Equation (27) generally increases in accuracy as the number of cycles q increases, the filtered record, after truncating its m terms at both ends, should be as long as possible. A minimum of five peaks should be used in Equation (27).

It is self evident that the signal to noise ratio should be at a maximum for best results. This requires that data be recorded from different building levels for different modes. From previous analytical studies of a building, the level at which each mode appears to exhibit its maximum relative amplitude is usually known in advance. In order to estimate parameters for this mode, data should be collected at this level. Thus, a typical set of levels for which data should be taken for a tall structure might be as follows:

1. top of building for first mode
2. 40% level for second mode
3. 70% level for third mode.

It should be noted that the values shown above are only approximate, listed for purposes of illustration only.

The filter gain should be a real symmetrical function, reasonably flat in a relatively small passband about its center frequency, and should roll off gradually to negligible levels outside a wider cutoff bandwidth.

The filter bandwidth has a significant effect on the resulting damping estimate. The cutoff bandwidth C (Figure 1) is inversely proportional to the filter rise time t_R (Figure 2). Thus C should be

as wide as possible without including more than a single mode in the passband. The resulting rise time will then be as short as possible, allowing for a longer correlogram maximum lag time. The inverse relationship existing between bandwidth and rise time is discussed by Schwartz [31].

V. SPECTRAL MOMENTS METHOD

In 1972, Vanmarcke [10] proposed a spectral moments method for estimating frequency and damping parameters of a randomly excited system. The method depends on the computation of the zeroeth order, first order, and second order moments of the power spectral density function of the response of a structure to "white noise excitation". The original method proposed by Vanmarcke has been slightly modified in this investigation to correspond to the response of a structure to "band-limited white noise," rather than pure "white noise".

The zeroeth order moment gives the area under the power spectral density function. The first order moment is a function of its centroid, and the second order moment gives a measure of variability or dispersion about a spectral peak indicating a central frequency.

If $y(t)$ is a stationary random process with zero mean value, its autocorrelation function $R(\tau)$ is defined by

$$R(\tau) = E\,[y(t)\; y(t+\tau)]. \tag{29}$$

The "one-sided" Fourier Transform pair of formulas relating $G(\omega)$ and $R(\tau)$ is given by

$$G(\omega) = \frac{2}{\pi} \int_0^\infty R(\tau)\, \cos(\omega\tau)\, d\tau \tag{30}$$

$$R(\tau) = \int_0^\infty G(\omega)\, \cos(\omega\tau)\, d\omega \tag{31}$$

where $G(\omega)$ is the "one-sided" power spectral density function of the autocorrelation function of the zero-mean process $y(t)$. The mean square value $\langle y(t)^2 \rangle$ is obtained by setting $\tau = 0$, in Equation (31),

giving

$$R(0) = \int_0^\infty G(\omega)\ d\omega \tag{32}$$

The spectral moments are

$$\lambda_0 = \int_0^\infty \omega^0\ G(\omega)\ d\omega = \int_0^\infty G(\omega)\ d\omega \tag{33}$$

$$\lambda_1 = \int_0^\infty \omega^1\ G(\omega)\ d\omega \tag{34}$$

$$\lambda_2 = \int_0^\infty \omega^2\ G(\omega)\ d \tag{35}$$

Vanmarcke has introduced the following quantities related to the spectral moments above.

$$\omega_1 = \frac{\lambda_1}{\lambda_2} \tag{36}$$

$$\omega_2 = \left\{ \frac{\lambda_2}{\lambda_0} \right\}^{1/2} \tag{37}$$

Note that ω_1 and ω_2 as defined have dimensions of circular frequency. For a physical interpretation, ω_1 is the location of the centroid or center of mass of the spectral density function, and ω_2 is the radius of gyration of this function. The parameter ω_2 will be directly related to ω_n, the natural circular frequency of vibration. The following dimensionless parameter

$$q = \left\{ 1 - \frac{\lambda_1^2}{\lambda_0 \lambda_2} \right\}^{1/2} \tag{38}$$

will be directly related to the percentage of critical damping ζ of

the vibrating system.

If $x(t)$ is the input and $y(t)$ the output of a linear system, the relationship between $x(t)$ and $y(t)$ is given by

$$y(t) = \int_0^\infty h(\tau)\, x(t-\tau)\, d\tau \tag{39}$$

where $h(\tau)$ is the impulse response function of the system, with $h(\tau) = 0$ for $\tau < 0$. The system transfer function $H(\omega)$ is defined to be the Fourier transform of the impulse response function $h(\tau)$.

If $G_0(\omega)$ is the power spectral density function of the stationary "white noise" input $x(t)$, and $G(\omega)$ is the output spectral density function, the equation defining these relationship is

$$G(\omega) = |H(\omega)|^2 \; G_0(\omega). \tag{40}$$

For a single degree of freedom system with natural circular frequency ω_n and damping ratio coefficient ζ, the square of the absolute value of the system transfer function is given by

$$|H(\omega)|^2 = \frac{1}{(\omega_n{}^2 - \omega^2) + 4\zeta^2\omega_n{}^2\omega^2} \; . \tag{41}$$

It can then be shown that the following relationships exist:

$$\lambda_0 = \frac{\pi G_0}{4\zeta\omega_n{}^3} \tag{42}$$

$$\omega_2 = \omega_n \tag{43}$$

$$q^2 = \frac{4\zeta}{\pi}\; [1 - 1.1\zeta + 0(\zeta^2)]. \tag{44}$$

When $|\zeta| << 1$, it can be seen that

$$q^2 \simeq \frac{4\zeta}{\pi} \tag{45}$$

for very light damping [$\zeta \leq 0.15$]. Thus the natural circular frequency and critical damping ratio is given by

$$\omega_n = \left(\frac{\lambda_2}{\lambda_0} \right)^{1/2} \tag{46}$$

$$\zeta = \frac{\pi}{4} q^2 = \frac{\pi}{4} \left(1 - \frac{\lambda_1^2}{\lambda_0 \lambda_2} \right). \tag{47}$$

Since the output function y(t) is filtered by a band-limited window function between circular frequencies ω_a and ω_b, the effect of excluding frequencies outside of (ω_a, ω_b) will now be discussed. It will be convenient to define dimensionless band limits

$$\Omega_a = \frac{\omega_a}{\omega_n}, \quad \Omega_b = \frac{\omega_n}{\omega_b}. \tag{48}$$

Vanmarcke has demonstrated that the natural frequency is still given by

$$\omega_n = \left(\frac{\lambda_2}{\lambda_0} \right)^{1/2} \tag{49}$$

However, the critical damping ratio is corrected according to the relationship

$$\zeta = \left(\frac{1 + \Omega_a}{1 - \Omega_b} \right) \frac{\pi}{4} \left(1 - \frac{\lambda_1^2}{\lambda_0 \lambda_2} \right) \tag{50}$$

for the special case when $\Omega_a = \Omega_b$. This condition will be utilized in this investigation.

VI. POWER SPECTRAL DENSITY METHOD

This method is based on analyzing the power spectral density function of the response spectra. In the output power spectrum, the spectral density becomes maximum at a frequency $\omega\sqrt{1-2\zeta^2}$, and the damping coefficient ζ can be calculated as follows, knowing the frequencies f_1 and f_2 where the spectral densities become $1/\lambda$ of its maximum.

$$\zeta \simeq \frac{A}{2}\left(1 - \frac{3}{8}A^2\right) \tag{51}$$

where,

$$A = \frac{f_2^2 - f_1^2}{f_2^2 + f_1^2} \cdot \frac{1}{\sqrt{\lambda - 1}} . \tag{52}$$

In practice, $\lambda = 2$ is usually used for simplicity.

Equation (52) is derived from the power spectral density function

$$S(\omega) = \frac{S_0}{(\omega_0^2 - \omega^2) + 4\zeta^2\omega_0^2\omega^2} . \tag{53}$$

Although the power spectral analyses for the microtremor records in actual buildings have often been conducted recently, only a few examples of damping estimates of the buildings have been reported.

This method has been used by Tanaka, Yoshizawa, Osawa, and Morishita [14] to estimate period and damping parameters of some buildings in Japan.

The power spectral density function is defined as the Fourier transform of the true autocorrelation function derived from a vibration record of infinite length of time. When the length of the record is finite, we cannot estimate the true autocorrelation function for arbitrarily long lags. Furthermore, it is said that the use of

lags longer than a moderate fraction, say 10 per cent, of the length of the record is usually not desirable. In the practical cases, therefore, we can only compute the so called the apparent autocorrelation function from a record of relatively short length. However, a good estimation of smoothened values of the true power spectrum can be obtained from the Fourier transform of a modified apparent autocorrelation function, which is the product of the apparent autocorrelation and a suitable even function called the lag window. It is apparent that when this process of analysis is adopted for determining the damping value of a structure, a much larger value than the true one would be obtained. However, if the effect of smoothing in the process could be known and the corrections for this influence could be made on the apparent damping value, the true value of damping could be obtained. With the above expectations in mind, we now examine the effect of smoothing and discuss ways of determining the desired correction to the damping estimate.

In the present investigation, the so called 'hamming' type lag window expressed by Equation (54) was used.

$$\omega(\tau) = 0.54 + 0.46 \cos \frac{\pi\tau}{T_m} \qquad \text{for } |\tau| < T_m \qquad (54)$$
$$= 0 \qquad \text{for } |\tau| > T_m$$

where, τ is a time lag and T_m is the maximum lag which we desire to use.

The corresponding frequency function is

$$W(\omega) = 0.54\, W_0(\omega) + 0.23 \left[W_0\left(\omega + \frac{\pi}{T_m}\right) + W_0\left(\omega - \frac{\pi}{T_m}\right)\right] \qquad (55)$$

where,

$$W(\omega) = 2T_m \frac{\sin \omega T_m}{\omega T_m} \quad . \tag{56}$$

The modified autocorrelation function is the product of $\phi(\tau)$ and $w(\tau)$, and its Fourier transform is represented by the convolution integral of the power spectrum for each time function. This operation implies smoothing of the response power spectrum $G(\omega)$ with the spectral window $W(\omega)$ as a weighting function. The smoothened spectral function is then expressed by

$$P(u) = K \int_{-\infty}^{\infty} \frac{1}{(1 - u'^2)^2 + 4\zeta^2 u'^2} \left[Y_0(u - u') + \frac{23}{54} \{Y_0(u - u' + \frac{1}{2f_0 T_m}) + Y(u - u' - \frac{1}{2f_0 T_m})\}\right] du' \tag{57}$$

where,

$$K = \frac{1.08 T_m G_0}{\omega_n^4} \quad , \qquad Y_0(u-u') = \frac{\sin \omega_n T_m (u-u')}{\omega_n T_m (u-u')} \quad , \qquad u = \frac{\omega}{\omega_n} \quad , \qquad u' = \frac{\omega'}{\omega_n} \quad .$$

This method has been used by Kobayashi and Sugiyama [32] to estimate the structural dynamic parameters of the five structures investigated in this report. The results of this analysis is reported in a later chapter.

VII. TWO STAGE LEAST SQUARES METHOD

A fourth method of analyzing ambient vibration data for parameter estimation is the two-stage least square correlation function method, to be referred to hereinafter by the initials 2SLS. It was developed by Gersch and Foutch [33], and is an improvement of the maximum likelihood estimation for structural parameter estimation developed by Gersch, Nielsen, and Akaike [11].

The use of the 2SLS procedure is based on the assumption that the structure under consideration can be accurately described in terms of an n degree of freedom lumped mass-spring-damper model excited by a white noise. Displacement, velocity or acceleration vibration data sampled at uniform intervals for digital computer analysis is known to have a representation in terms of an AR-MA (mixed autoregressive moving average) discrete time series model. The coefficients of the AR-MA model can be expressed in terms of the structure's natural frequency and damping parameters. The 2SLS procedure is a statistically efficient procedure for estimating the parameters of the AR-MA model. Statistically efficient estimates of the natural frequency and damping parameters can in turn be computed from the statistically efficient AR-MA parameter estimates. Estimates of the statistical reliability of the structural system parameter estimates are also readily obtained from the AR-MA parameter estimates.

Much of the background material for this paper appears in recent related papers [33], [34], [13], so the description of the problem considered and the time series background of 2SLS methods are only

briefly described here. The results of 2SLS correlation function method applied to ambient response data taken from three floors of the World Trade Center Building will appear later in this report.

The structural system is assumed to be represented by an n degree of freedom lumped mass-spring-damper white noise excited stochastic differential equation

$$M\ddot{z}(t) + C\dot{z}(t) + Kz(t) = f(t) . \tag{58}$$

The input $f(t)$, an approximation to a random wind force, is assumed to be a zero mean n component white noise vector with covariance matrix $E[f(t)f'(s)] = D\delta(t-s)$, [35]. Assume that $z(t) = [z_1(t), z_2(t),\ldots, z_n(t)]'$ is the vector of displacements with $z_i(t)$ being the relative displacement of the ith mass in the model of Equation (58) to the ground, and the $z_j(t)$, the displacement of the jth mass is observed. (Velocity or acceleration measurements can be used with equally good results, [34].) Further, assume that only a regularly sampled noise contaminated version of $z_j(t)$ is available for analysis. Let $z_j(kT_s)$ $k = 0,\pm1,\ldots$ be the regular samples of the vibration data and $n(kT_s)$ be independent noise samples with T_s the sampling interval. The observed vibration data for some particular mass point is represented by the discrete time series $y_t = z_j(tT_s) + n(tT_s)$, $t = 0,\pm1,\ldots$ The problem is: Given a finite sample $\{y_t, t = 1,\ldots N\}$ of noise contaminated vibration data, obtain estimates of the parameters f_j, ζ_j, $j = 1,\ldots n$, the natural frequency and damping parameters of the structure described in Equation (58).

The regularly sampled noise contaminated vibration data is known to be exactly represented in the AR-MA model,

$$\sum_{i=0}^{2n} \alpha_i y_{t-i} = \sum_{i=0}^{2n} \beta_i x_{t-i}, \quad \alpha_0 = 1, \quad \beta_0 = 1 \tag{59}$$

where $\{x_t\}$ is a zero mean uncorrelated sequence with variance σ_x^2. A useful relationship between the AR-MA time series model parameters a_i, $i = 1,\ldots 2n$ and the natural frequency and damping parameters f_j, ζ_j, $j = 1,\ldots n$ is given by,

$$\sum_{i=0}^{2n} a_i \mu^{2n-i} = \prod_{j=1}^{2n} (\mu-\mu_j)(\mu-\mu_j^*) \tag{60}$$

where μ_j, μ_j^* are the complex conjugate root pairs of the characteristic equation of the AR parameters satisfy,

$$\mu_j = \exp(-2\Pi f_j \zeta_j T_s + i2\Pi f_j T_s \sqrt{1-\zeta^2_j}\,). \tag{61}$$

Next our attention is directed to the estimation of the AR-MA parameters $\{a_i, b_i\}$ $i = 1,\ldots 2n$ by the 2SLS method.

Convention or ordinary LS statistical parameter estimates are expressed in the form

$$y = X'\theta + e \tag{62}$$

where y is an N vector of observations, X' is a known Nxp matrix, θ is a p vector of unknown parameters which are to be estimated and e is a zero mean vector of N independent random variables each with variance σ^2. The normal equation for the LS estimation of θ, are

$$\begin{aligned} Xy &= [XX']\hat{\theta} \\ \hat{\theta} &= [XX']^{-1} Xy \end{aligned} \tag{63}$$

where it is assumed that the rank of X is p so that the pxp matrix inverse of [XX'] exists.

The unknown parameters $\{b_i, a_i \quad i = 1,\ldots 2n\}$ of the AR-MA time series model can be expressed in an ordinary LS model OLS form [33],

by making the associations

$$Xy = [cyx(1) \quad -cyy(1) \quad \ldots \quad cyx(2n) \quad -cyy(2n)], \tag{64}$$

$$\theta = [\, b_1 \quad a_1 \quad \ldots \quad b_{2n} \quad a_{2n} \,], \tag{65}$$

$$[XX'] = \begin{bmatrix} C(0) & C(1) & \ldots & C(2n-1) \\ C'(1) & C(0) & \ldots & C(2n-2) \\ \cdot & \cdot & & \cdot \\ \cdot & \cdot & & \cdot \\ \cdot & \cdot & & \cdot \\ C'(2n-1) & \ldots & & C(0) \end{bmatrix}, \tag{66}$$

$$C(k) = \begin{bmatrix} cxx(k) & -cxy(k) \\ -cyx(k) & cyy(k) \end{bmatrix}. \tag{67}$$

In Equation (66) the 4n x 4n matrix [XX'] is in block Toeplitz form and cyy(k), k = 0,1,... is the sample covariance function computed from the observed data $\{y_t,\ t = 1,\ldots N\}$ in the usual manner by the formula

$$\bar{y} = \frac{1}{N} \sum_{t=1}^{N} y_t; \quad cyy(k) = \frac{1}{N} \sum_{t=1}^{N-k} (y_{t+k} - \bar{y})(y_t - \bar{y}). \tag{68}$$

In Equation (67), cxx(k), cxy(k), cyx(k) are input and cross-covariance functions.

The statistical properties of OLS parameter estimation, i.e. consistency, and asymptotic unbiasedness and efficiency for AR-MA time series parameter estimation was well treated by Astrom [36]. The OLS procedure described above is the second stage of our 2SLS procedure. Because only the time series $\{y_t,\ t = 1,\ldots N\}$ is observed, the covariance functions cxx(k), cxv(k), cyx(k) necessary for the OLS stage must be computed by something other than the direct sample function computations in Equation (68). They are in fact obtained

from the cyy(k) data in the first LS stage. That material is discussed next.

The AR-MA model in Equation (59) has alternative equivalent representations as an AR and as an MA or impulse response model, (64). These models are represented by

$$\sum_{i=0}^{2n} a_i y_{y-i} = \sum_{i=0}^{2n} b_i x_{t-i} \qquad \text{(AR-MA)} \qquad (69)$$

$$\sum_{i=0}^{\infty} \tilde{a}_i y_{t-i} = x_t \qquad \text{(AR)} \qquad (70)$$

$$y_t = \sum_{i=0}^{\infty} h_i x_{t-i} \qquad \text{(MA)} \qquad (71)$$

where x_t is an uncorrelated sequence with variance σ_x^2.

In the first LS stage a "long" but finite order AR model

$$\sum_{i=0}^{\tilde{p}} \tilde{a}_i y_{t-i} = x_t, \quad \tilde{a}_0 = 1 \qquad (72)$$

is fitted to the cyy(k) k = 0,1,... data by the Levenson-Durbin-Akaike procedure [37]. This computation also yields an estimate of the variance of the $\{x_t\}$ time series, $\hat{\sigma}_x^2$, so that the input covariance function can be represented as $cxx(k) = \hat{\sigma}_x^2 \delta_{k,0}$ where $\delta_{r,s}$ is the Kronecker delta (which is one if r = s and zero otherwise).

A recursive formula for computing the MA parameters $\{h_i\}$ from the AR parameters a_i in Equation (71) follows easily using operator notation. Identify the delay operator z, $zx_t = x_{t+1}$, $z^{-1}x_t = x_{t-1}$. Then the AR and MA models in Equation (71) can be written $\tilde{a}(z)y_t = x_t$ and $y_t = h(z)x_t$ respectively where $\tilde{a}(z)$ and h(z) are polynomials in the operator z. Multiply the second form by $\tilde{a}(z)$ to get $\tilde{a}(z)y_t = \tilde{a}(z)h(z)x_t$. Compare this form with the first form to get the result

$\tilde{a}(z)h(z) = 1$. This latter operator or transform domain equation is transformed to the time domain to obtain the desired recursive formula for h_t,

$$h_0 = 1, \quad h_t = -\sum_{t=i}^{\tilde{p}} \tilde{a}_i h_{t-i} \qquad t = 1,2,... \tag{73}$$

Next, multiply the MA model in Equation (71) by x_{t-k} and take expectations to obtain the known result for the input-output covariance function in terms of impulse respose

$$cyx(k) = \sigma_x{}^2 h_k \qquad k > 0 \tag{74}$$

$$cxy(k) = \begin{cases} \sigma_x{}^2 & k = 0 \\ 0 & k > 0 \end{cases} \tag{75}$$

Thus given the original cyy(k) data and the results from the first LS stage, we have all the covariance function information, cyy(k), cxx(k), cxy(k), cyx(k) k = 0,1,... required for computation of the second LS stage. If n is a large number, numerical instabilities may be encountered in the inversion of the 4n x 4n block Toeplitz matrix [XX']. A block Toeplitz matrix inversion routine due to Akaike achieves inversion of the 4n x 4n matrix recursively requiring only inversion of 4 x 4 matrices.

Once the AR-MA time series parameters are known, the structural system parameter estimates and an evaluation of their statistical reliability can be computed from them [11], [34]. The roots μ_j, $\mu_j{}^*$ of the characteristic Equation (60) can be computed by a packaged subroutine. The μ_j, $\mu_j{}^*$ then yield the convenient dimensionless parameters δ_j, λ_j

$$\delta_j = 2\Pi f_j r_j T_j = (-1/2)\log(\mu_j \mu_j{}^*)$$

$$\lambda_j = 2\pi f_j T_j \sqrt{1-\zeta_j^2} = \tan^{-1} \frac{\left|\mu_j - \mu_j^*\right|}{\mu_j + \mu_j^*} \tag{76}$$

The right-hand side of Equation (76) can be expanded in a Taylor series whose linear part is

$$[da_1, \ldots . da_{2n}] = S[d\delta_1, d\lambda_1, \ldots d\delta_n, d\lambda_n]$$

where dx denotes the total differential of x. Define the 2n x 1 column vectors $a = [a_1, \ldots a_{2n}]'$, $ct = [\delta_1, \lambda_1, \ldots \delta_n, \lambda_n]'$ and the covariance matrix of the a parameter estimates by V_{AR}. Then the covariance matrix of the ct parameter estimates V_{ct} and V_{AR} are related by [11], [34],

$$V_{ct} = S^{-1} V_{AR} S^{-1}$$

$$= \begin{bmatrix} \mathrm{var}(\delta_1) & \mathrm{cov}(\delta_1,\lambda_1) & \ldots & \mathrm{cov}(\delta_1,\lambda_n) \\ \mathrm{cov}(\lambda_1,\delta_1) & \mathrm{var}(\lambda_1) & \ldots & \mathrm{cov}(\lambda_1,\lambda_n) \\ . & . & & . \\ . & . & & . \\ . & . & & . \\ \mathrm{cov}(\lambda_n,\delta_1) & \ldots & & \mathrm{var}(\lambda_n) \end{bmatrix} \tag{77}$$

The matrix V_{AR} is a submatrix of the AR-MA parameter variance-covariance matrix corresponding to the a_i $i = 1,\ldots 2n$ parameters. The AR-MA parameter estimate variance-covariance matrix, the reciprocal of the Fischer information matrix may be computed from the AR-MA parameters, [11].

Finally, the coefficients of variation c_{f_j} and c_{ζ_j} $j = 1,\ldots n$ of the natural frequencies and their damping are given by

$$c_{f_j} = \frac{\Delta f_j}{f_j} = \frac{\Delta \lambda_j}{\lambda_j}$$

$$c_{\zeta_j} = \frac{\Delta\zeta_j}{\zeta_j} = \frac{\Delta\delta_j}{\delta_j} + \frac{\Delta\lambda_j}{\lambda_j} \qquad j = 1,\ldots n \tag{78}$$

The quantities $\Delta\delta_j, \Delta\lambda_j$ in the Equation (78) are the standard deviations of the δ_j, λ_j parameter estimates. They can be computed as the square roots of the diagonal elements of V_{ct}.

VIII. BASIC GUIDELINES FOR EARTHQUAKE RESISTANT DESIGN OF TALL BUILDINGS IN JAPAN

GENERAL DESCRIPTION

The earthquake resistant design of tall buildings has always been a subject of primary importance to architects and structural engineers in Japan, since earthquakes occur frequently in all parts of the country. Prior to 1963, the Japanese Building Code restricted the height of high rise buildings to 31 m, a relatively low height restriction by American standards.

In 1964, the Japanese Building Code was revised to permit the height of high-rise buildings to exceed 31 m, providing the safety of the structures under earthquake loading could be assured. The Ministry of Construction would give its approval if a dynamic analysis of the structure had been performed during its design stage for earthquake loading, and its maximum stresses and deformations resulting from the dynamic analysis were within safe design limits.

The first high-rise building constructed in Japan is called the Kasumigaseki Building located in downtown Tokyo. It has 36 stories and rises to a height of 147 m, and was completed in 1968. Its earthquake resistant design was performed by the Muto Institute of Structural Mechanics under the direction of the world-renowned Dr. Kiyoshi Muto. Since 1968 there have been a multitude of high-rise buildings completed in Japan.

Since the reader may not be familiar with the general provisions for earthquake resistant design of tall buildings in Japan, its main

features will be briefly discussed here. The following edited excerpt is taken from a report by Dr. T. Hisada of the Kajima Institute of Construction Technology [38].

INTRODUCTION

In January 1964, the building height limitation, which had been stipulated in the Japanese Building Code since 1921, was repealed. The revisions permit the construction of buildings exceeding 31 meters (100 feet) in height, provided that the buildings are constructed in accordance with the provisions of density control as well as sky exposure restrictions.

As is commonly known, the seismic code for low buildings cannot be applied to high-rise buildings, since they respond differently to earthquake loading. Also the wind velocity at higher levels has a different profile from that close to the ground and this fact must be considered in the structural design of tall buildings.

To account for these differences, the Structural Standard Committee of the Architectural Institute of Japan (AIJ) worked to draft a document stipulating the guide lines to be utilized in structural design of tall buildings and published it in March, 1964 with revisions in 1967 and 1971.

In order to insure the structural safety of tall buildings, an Examination Board was set up in the Ministry of Construction in September 1964. The Board was transferred from the Ministry of Construction to the Building Center of Japan in 1965 to perform preliminary evaluations of the structural safety of tall buildings.

Since its inception, the Examination Board has investigated and approved the structural design of more than 250 high-rise buildings. These buildings have been designed in accordance with the principal items described in the guide lines mentioned below.

Since no seismic code is at present in force governing the provisions for the safety of tall buildings, the role the Board plays is important and the results of the examinations performed by the Board is highly significant.

AIJ GUIDE LINES FOR ASEISMIC DESIGN OF TALL BUILDINGS

1) Scope of Application
   a) These guide lines are applicable to the structural design of a tall building with a height exceeding 45 meters above ground level.
   b) These guide lines need not be applied to tall buildings which are designed on the basis of the results of special engineering studies.
2) Rules for General Planning
   a) It is generally desired that structures have simple cross sections in both plan and elevation views.
   b) The foundation of a tall building should be supported on firm ground.
   c) Structural elements to resist horizontal forces should be designed so as to minimize torsional effects.
   d) The structure of a building should be easily amenable to rational analysis.

e) The structure of a building should have both adequate strength and rigidity under the applied loadings.

f) The deformation of a building under seismic loadings should be limited in order not to endanger the public or cause inconvenience to occupants of the building.

3) Seismic Analysis

The seismic analysis of the structure may be performed in the following steps:

a) The design base shear coefficient C_B (ratio of total design seismic force on the building to its total weight including effective live loads) of the building should be first evaluated. The value of C_B is considered to decrease hyperbolically with an increase of the fundamental period of the structure and is to have a minimum value of 0.05.

b) The distribution of the story shear coefficients is assumed for each story of the building in proportion to the value calculated for the base shear coefficient.

c) The dimensions of structural menbers and details of the structural joints are then designed. On the basis of this preliminary structural design, the strength, rigidity and behavior of the structure in the elastic and inelastic ranges are evaluated for each story for the assumed seismic and wind loading. It is desirable to perform experiments on the structure or portions of the structure to confirm their design characteristics, when-

ever necessary.

d) Dynamic analysis on the structure is then performed using strong earthquake accelerograms appropriate to the seismicity and ground condition of the site and its responses under earthquake loadings are computed and examined. If necessary, the preliminary structural design is modified and the revised structural responses are computed. This iterative procedure is repeated until a sound structural design of the building is formulated.

e) Large horizontal seismic coefficients should be considered for the design of parapets, interior and exterior ornamentary objects, water tanks, chimneys and similar unusual structures or structural elements.

4) Items to be considered in Design of Structural Members and Connections

In tall buildings, steel or composite construction is generally used in the entire structure or partly in a composite structure. Reinforced concrete construction is sometimes used for basement foundations. The usual type of a structure is that of a space frame with or without seismic shear walls or bracings.

Items to be considered in the design of structural members and connections in tall buildings are mentioned below:

a) High strength steel may be used for structures.

b) In case of steel construction, special attention should

be given to prevent local buckling of the structural members.

c) In case of reinforced concrete or composite columns, attention should be given to prevent failure due to shear and buckling of reinforcing steel bars due to spalling of covering concrete under cyclic loads.

d) The connection between column and girder in a space frame structure should be carefully designed, because stress concentration usually occurs there. The effect of the deformation of this connection to the rigidity of the entire frame should also be considered.

e) When the lateral distortion of the frame under earthquake is large, the reduction of the rigidity and strength of a column due to additional moment caused by the lateral distortion and axial force should be considered.

f) The floor should be safely designed to provide proper strength and rigidity in its plane.

g) Besides those items mentioned above, structural details shall be carefully designed so that the whole structure has sufficient ductility.

SUMMARY OF STRUCTURAL DESIGN OF HIGH-RISE BUILDINGS

The structural design and the related dynamic analyses of over 250 high-rise buildings thus far examined by the Board are summarized below.

1) A steel structure is generally adopted for high-rise buildings

up to about 60 stories. However, a steel encased reinforced concrete (composite) structure is often used for buildings up to about 20 stories in height. Recently a 18 story reinforced concrete buildings was constructed in Tokyo.

2) The usual type of structure is a space frame (ductile moment resisting) with or without shear walls or bracings.

3) All high-rise buildings have basement floors of 2 to 5 stories. Many buildings have mat footings located on firm layers (the Tokyo gravel layer in case of Tokyo) but some have pier footings.

4) The fundamental periods of vibration of the buildings are in the range of 0.7 to 6 seconds, increasing with the building heights.

5) The design base shear coefficients C_B (most are story shear coefficients of the first story or of the first or second basement story) decrease with the increase of the fundamental periods of vibration T_1. The relation between C_B and T_1 is generally in the range of $C_B = 0.36/T_1 - 0.18/T_1$ and the values of C_B are not less than 0.05.

6) The story shear coefficient of each story increases with the building height and the ratio of the story shear coefficient of the top story to the base coefficient is in the range of 2 to 4.

7) In many cases, the damping factors (fraction of critical damping) used in the dynamic analyses are 5% and 2% for composite and steel structures, respectively.

IX. RECORD DATA AND BUILDING DETAILS

DATA COLLECTION PROCEDURE

The vibration sensors used in this investigation were three horizontal velocity meters manufactured by the Hosaka Instrument Company of Japan. The analog signals were subjected to low pass filtering effectively eliminating frequencies greater than 10 Hz.

The resulting signals were than digitized at a constant interval of 0.04 seconds, which gives a Nyquist frequency of 12.5 Hz. For the World Trade Center Building, a record length for each sensor of approximately 6,000 points, or four minutes, was recorded on each floor. For the other three buildings, as well as for the Tokyo Tower, 4,500 points, or three minutes of data, were continuously recorded.

The method for recording the ambient vibration data was the same for all the structures, so the method will only be described in detail for the World Trade Center Building. Data were collected on the 40th floor (1st mode), 28th floor (3rd mode), and 16th floor (2nd mode) for this building.

On each floor level, the three vibration sensors, were placed as shown in Figure (3). Sensor #1 was placed at the geometric center of the cross section, facing North-South. Sensor #2 was placed at the Northern tip of the cross section, facing East-West. Sensor #3 also faced East-West, but was located at the Southern tip of the cross section. Thus, if $y_1(t)$, $y_2(t)$, and $y_3(t)$ were the output from the three sensors, the North-South, East-West, and Torsional responses were given by

$$y_{N-S}(t) = y_1(t) \tag{79}$$

$$y_{E-W}(t) = 1/2\ [y_2(t) + y_3(t)] \tag{80}$$

$$y_T(t) = 1/2\ [y_2(t) - y_3(t)] \tag{81}$$

The ambient responses for this building were subjected to both the Gaussian and the Trapezoidal filters. For the Gaussian filter, the cutoff bands were 0.546 Hz, 0.638 Hz and 1.096 Hz for the 40th floor (1st mode), 16th floor (2nd mode), and 28th floor (3rd mode). For the Trapezoidal filter, the cutoff bands were the same as for the Gaussian filter. The unit passbands, however, were 0.363 Hz, 0.394 Hz, and 0.607 Hz for the 40th, 16th, and 28th floors, respectively.

TOKYO WORLD TRADE CENTER BUILDING

The Tokyo World Trade Center Building is located in the Hamamatsucho, Minato-ku section of the city. It is located adjacent to the train stations for the Japan National Railways and for the monorail to Tokyo International Airport. In addition, the building itself houses a terminal for medium distance buses. It consists of a low-rise block and a tall tower. The low-rise block contains exhibition halls, transportation facilities, and an energy center, as well as extensive underground parking facilities.

The tower portion contains offices, shops, banks, and other service facilities. It rises 40 stories to a height of 152.2 meters at roof level. A small structure on the roof raises the overall height to 156.0 meters. The tower is a steel frame, almost symmetrical in plan view, being 51.4 m (E-W) by 48.8 m (N-S) in cross section. The area of a typical floor is 2,458 m^2. There is a restaurant at

the top level which overlooks the city. Construction started in July, 1967, and the structure was completed in February, 1970.

Details of the building are given in Figures (3) and (4). Vibration tests on this structure have been reported by Muto [39].

The structural details of the other three buildings will only briefly be described.

INTERNATIONAL TELE-COMMUNICATIONS CENTER

This building is located in the Nishi Shinjuku area of Tokyo. This part of the city contains a large number of tall structures, and is well known for its many hotels and restaurants. The 52 story triangular Shinjuku Sumitomo Building, and the famous Keio Plaza Hotel are located close to this building. This structure houses the equipment for international telephone transmission to and from Tokyo.

This building is a steel frame which rises 32 stories to a height of 170 meters. It is almost square in plan view, with plan dimensions 51 m by 54 m. Its structural framing consists of closely spaced columns lying on the perimeter of the cross section. Its vibrational characteristics and design features have also been reported by Muto [40].

Records were taken from the 32nd floor for the fundamental modes and the 17th floor for the other modes. Its structural details are shown in Figures (5) and (6).

ASAHI TOKAI BUILDING

The Asahi Tokai Building is a steel frame high-rise structure

located in the Ohtemachi section of Tokyo. It is a 30 story building with a total height of 119 m. There is a concrete foundation of three floors below ground level. It is essentially square in cross section, with plan dimensions 36 m by 35 m. Each typical floor has a cross sectional area of 1,249 m^2. Its dynamic characteristics are described by Ichinose [41]. Its structural details are shown in Figure (7).

Data for this building were taken on the 22nd and 14th floors.

YOKOHAMA TENRI BUILDING

The last building studied in this investigation is not located in Tokyo, but in the port city of Yokohama, Japan. It is also a steel frame whose cross section is perfectly square, being 27 meters on each side. Its structural framing system consists of a "tube in tube" design. It consists of 27 stories and rises to a height of 103 m. There are also three basement floors below ground level. Its structural details are shown in Figure (8). Vibration test for this building are described in a report by Tamano [42]. Ambient data were recorded on the 27th, 20th, and 13th floors.

X. THE TOKYO TOWER

GENERAL DESCRIPTION

The television tower called the Tokyo Tower is located in the Shiba Park section of Tokyo. The geodetic coordinates of the tower are 139° 44'55" E and 35° 39'20" N. The site in which this tower stands occupies an area of 21,003 m^2. The tower was constructed over a period of about eighteen months from June 1957, to December 1959. It is used for broadcasting and receiving television, and due to the construction of this tower, the effective distance of the electronic wave transmission extends to a radial distance of 110 km from Tokyo. Besides serving as a television transmitter, the tower is open to the public for sight-seeing during normal working hours.

As can be seen in Figure (9), the tower is an isolated free-standing steel-framed tower composed of two parts; that is, a primary tower with a height of 253 m and another one of a height of 80 m being added on the top of the former. The latter tower may be divided into two parts, i.e., the super-gain-antenna of 60 m in height and the super-turn-antenna of 20 m in height. Thus, the total height of the tower is 333 m above ground level which is at an elevation of 18 m above the mean sea level.

It is of some interest to compare this tower with the Eiffel Tower in Paris. The height of the Tokyo Tower is taller than that of the latter tower which is 312 m high. The total weight of steel used in the Eiffel Tower is 7,300 tons, whereas in the Tokyo Tower it is 3,600 tons. The number of rivets in the former tower is 2,500,000

and that in the latter is 1,200,000. Therefore, the Tokyo Tower was constructed with approximately half of the amount of the materials that were used in constructing the Eiffel Tower. A design requirement for this tower was that under any circumstances, the maximum deformed slope at the top of the antenna was to be less than $\pm$ 2°- 3°, which is a necessary requirement for television transmission.

The present Tokyo Tower is built over a six-story building having a total floor area of 21,500 m^2, as shown in Figure (10). At a height of 120 m, there is a two-story observation-platform with total area of 1,320 m^2 and above this, an operation-platform of an area of 132 m^2 is situated at a height of 223 m. Travel up and down between the building beneath the tower and the observation-platform is made possible by means of three elevators, each capable of carrying 23 persons, as well as by stairway. This tower was designed so as to allow the addition of another platform at a height of 66 m, if it becomes necessary to do so in the future.

The floor of the observation-platform is formed on the V-shaped deckplates by plastering the mortar with wire-meshes inside. The surface of the floor is covered by an asphalt compound called Astiles. The outer surfaces of the platform are formed by glass windows, but, the walls surrounding the lift-shaft and the staircases are constructed of mortar with laths inside and finished with special paint or flexible panels. The ceiling and the roof are made of ribbed iron plates. The walls of the elevator shaft are of flexible boards and in a part of these walls there exist glass windows. The stairs are of iron, and the metal netting is used surrounding the staircase.

The floor of the room for the transmitter is constructed in the same way as in the case of the observation-platform, but, finished with colored-concrete. The walls of this room are made of flexible panels.

The floor of the room controlling the elevator shaft is made of striped steel plates, and the walls are of sandwich panel construction. The roof is covered with ribbed iron plates.

CONNECTION OF STRUCTURAL MEMBERS

With the exception of the antenna-tower, most of the parts of the tower were constructed by riveting the steel members together or by tightening them with bolts.

Up to height of 130 m from the ground, all members are connected by rivets and painted to resist corrosion. This portion was constructed by the Matsuo Bridge Manufacturing Co., Ltd. In the part lying above this and up to a height of 253 m, all members are galvanized and the connection was made by means of bolts. All the members in this part were tightened by polished bolts with spring washers to prevent them from being loosened.

The supporting tower of the antenna was constructed in the workshop by welding the portions, each 10-12 m long. After that, the welded tower was annealed in a furnace at a temperature of 625° C for four to six hours, depending on the thickness of the steel member, for the purpose of relieving the internal stresses. The field connection of this tower was done by using bolts.

The construction work of the bolted parts and the antenna parts

were carried out by the Shin-Mitsubishi Heavy Industry and Ship Building Co., Ltd.

FOUNDATION DESIGN

According to the results of several borings down to depths of 25-30 m, it was found that the uppermost layer was formed by the K vato loam of a thickness of 4-6 m, and beneath this layer, there lay alternate layers of sand and sandy clay, for which the standard penetration number N was about 10. However, the sand and gravel layer which lay at depths deeper than 20-26 m was dense and hard enough to support the foundation of this tower, where the value of N was greater than 50.

The load test which was made on the base of the foundation revealed that the deflection was of an order of 3 mm when the load intensity was 180 ton/m^2. In the design of the foundation, however, a bearing stress of 50 ton/m^2 was taken as the maximum permanent load.

In the test of lateral loading on the deep foundation, a force which was equivalent to 50 tons was applied horizontally at the top of the foundation, with the result that the lateral shift at the top was about 5-10 mm for this load case.

Under each footing at the corner of the square foundation, eight piers were driven by the patented method of deep-foundation of the Kida Construction Co., Ltd. These circular piers were 2 m in diameter and 3.5 m at their bases. A bearing load of 500 tons can be resisted by one pier, therefore a load of 4,000 tons can be taken by one footing. For an actual load of 1,250 tons acting on one footing under

ordinary load, the safety factor is greater than 3. During an extraordinarily strong wind, such as of a velocity of 90 m/sec, under typhoon conditions, an uprooting force will act on the foundation. When this force is only in one direction, it will be of an order of 700 tons. Under this loading this force is easily counteracted by the dead weight of the foundation alone. Thus, the foundation of this tower is exceptionally well designed to safely withstand the extremely large lateral forces which can be expected under typhoon or earthquake conditions.

The design of this tower, as well as its dynamic response to vibration test and under typhoon conditions, has been reported by Naito, Nasu, Takeuchi, and Kubota [42] in a Waseda University Engineering Report. Details of the response characteristics of this tower will be presented later in this report.

XI. EXPERIMENTS WITH DIGITAL FILTERING AND PARAMETER ESTIMATION

Records containing the first three modes of vibration in the North-South direction of the World Trade Center (WTC) were subjected to both the Gaussian and the Trapezoidal digital filters, to determine how the characteristics of each filter may affect the values of the parameter estimates.

Each of these three records were first filtered by a Gaussian Filter and then by a Trapezoidal Filter with the same center frequency and cutoff bandwidth. These filtered records were then analyzed by the Filtered Correlogram Method and the Spectral Moments Method to estimate frequency and damping parameters. The results of these experiments are shown in Table 1.

An inspection of Table 1 reveals that the digital filter used had negligible effect on the estimates of the natural frequencies obtained by the Filtered Correlogram or Spectral Moments methods. The minor differences vary by less than one percent. The filter chosen, however, resulted in wide differences in the estimation of the critical damping ratio for each mode. While only a small difference was noted in values estimated by the Filtered Correlogram method of analysis, the Spectral Moments method resulted in values of damping parameters by Gaussian Filtering being only half of the values obtained by Trapezoidal Filtering. Since the Trapezoidal Filtered estimates appeared to be consistent in both methods of analysis, it appears that the Gaussian Filter has the effect of seriously lowering the Spectral Moment parameters from their true values. It was thus

TABLE 1
COMPARISON OF PARAMETER ESTIMATES USING
GAUSSIAN AND TRAPEZOIDAL FILTERS
FOR WTC NORTH-SOUTH RECORDS

NATURAL FREQUENCY f_n (Hz)

	GAUSSIAN FILTER	TRAPEZOIDAL FILTER
FIRST MODE		
Filtered Correlogram	0.278	0.278
Spectral Moments	0.279	0.281
SECOND MODE		
Filtered Correlogram	0.859	0.859
Spectral Moments	0.855	0.856
THIRD MODE		
Filtered Correlogram	1.573	1.573
Spectral Moments	1.562	1.569

CRITICAL DAMPING RATIO (ζ_n)

	GAUSSIAN FILTER	TRAPEZOIDAL FILTER
FIRST MODE		
Filtered Correlogram	0.0091	0.0094
Spectral Moments	0.0034	0.0070
SECOND MODE		
Filtered Correlogram	0.0106	0.0116
Spectral Moments	0.0042	0.0072
THIRD MODE		
Filtered Correlogram	0.0172	0.0183
Spectral Moments	0.0068	0.0152

felt that the Trapezoidal Filter should be used in this investigation to compare parameter estimates obtained from different system identification methods. While the Gaussian Filter did not affect the values obtained by the Filtered Correlogram Method, it would probably seriously underestimate damping values obtained by the Spectral Moments method of analysis.

The fact that the Trapezoidal Filter was chosen for analyzing the rest of the structures in this report should not be interpreted as indicating that it is necessarily a "better" filter to use. As has already been mentioned in Section II of this report, a Gaussian Filter may yield more accurate results when the length of the ambient vibration record is relatively short, or when the stationarity property of the record is not satisfied. It is only when long, stationary records are available for analysis, that the Trapezoidal Filter would be the preferred one to use.

The second experiment that was performed on the North-South records of the World Trade Center involved subjecting the records from each of the first three modes, filtered by a Trapezoidal Filter, to system identification analysis by the three methods of Filtered Correlogram, Spectral Moments, and Two-Stage Least Square analyses. The Filtered Correlogram and Spectral Moments methods were used to estimate the parameters from the first three modes of vibration for the North-South direction of the World Trade Center Building. However, only the first two modes were analyzed by the Two-Stage Least Square Method.

The results of this second analytical "experiment" are shown in

Table 2. The frequency estimates obtained form the three analytical procedures appear to be almost identical for the first two modes. However, significant differences occur in the estimates for the critical damping ratio. While the difference between the Filtered Correlogram and Spectral Moments estimates is only 0.2 percent of critical, the difference between the Filtered Correlogam and the Two-Stage Least square estimate is 1.3 percent of critical. It appears that the Two-Stage Least Square estimate is more than double the average estimate obtained by the other two methods. Since the other two methods gave estimates that are consistent for the first mode, the Two-Stage Least Square method appears to overestimate the critical damping ratio for the first mode. The second mode damping ratio estimated by this method appears to be consistent with the other values.

Since the damping estimate obtained for the first mode by this method appears to be in error, the other records for the other structures were not subjected to the Two-Stage Least Square method of parameter estimation.

The power spectrum for a single degree of freedom system is shown in Figure 10, and the unfiltered and filtered two-mode covariance functions for the North-South direction of the World Trade Center Building are shown in Figures 11 and 12. These are the covariance functions subjected to Two-Stage Least Square analysis to obtain the frequency and damping parameters shown in Table 2. The results of this investigation have been reported by Gersch, Taoka, and Liu [13].

TABLE 2
COMPARISON OF PARAMETER ESTIMATES OBTAINED
FROM THREE SYSTEM IDENTIFICATION PROCEDURES
FOR WTC NORTH-SOUTH RECORDS

NATURAL FREQUENCY f_n (Hz)

MODE	FILTERED CORRELOGRAM	SPECTRAL MOMENTS	TWO-STAGE LEAST SQUARE
1	0.278	0.281	0.279
2	0.859	0.856	0.855
3	1.573	1.569	---

CRITICAL DAMPING RATIO (ζ_n)

MODE	FILTERED CORRELOGRAM	SPECTRAL MOMENTS	TWO-STAGE LEAST SQUARE
1	0.009	0.007	0.021
2	0.012	0.007	0.010
3	0.018	0.015	---

XII. COMPARISON OF SYSTEM IDENTIFICATION METHODS

In this section, parameter estimates for the four buildings obtained from the Filtered Correlogram, Spectral Moments, and Spectral Density methods of analysis will be compared. The estimates from the Spectral Density Method were calculated by Professor Hiroyoshi Kobayashi, with the aid of graduate student Nao Sugiyama [32]. It should be noted that each estimate was obtained from the same ambient vibration record, subjected to a Trapezoidal Filter. Thus any differences in these values would be solely due to the different method used to analyze the data.

WORLD TRADE CENTER (WTC)

During its design phase, the theoretical values calculated for the first three natural frequencies of translation were 0.31, 0.99, and 1.92 Hz for the North-South direction, and 0.31. 1.04, and 2.08 Hz for the East-West direction, respectively [39]. No theoretical values were calculated for torsional natural frequencies, or for damping estimates.

The estimates for natural frequencies and critical damping ratios evaluated in this investigation for this building are shown on Table 3. Estimates are shown for three North-South, three East-West, and two Torsional modes of vibration.

With respect to natural frequency estimates, the first and second translational mode estimates are very close, but the Spectral Density estimates for the third translational modes appear to be

TABLE 3
PARAMETER ESTIMATES OF WTC BUILDING

NATURAL FREQUENCY f_n (Hz)

MODE	FILTERED CORRELOGRAM	SPECTRAL MOMENTS	SPECTRAL DENSITY	FORCED VIBRATION
N-S FIRST	0.278	0.281	0.286	0.318
N-S SECOND	0.859	0.856	0.869	0.980
N-S THIRD	1.573	1.569	1.66	1.82
E-W FIRST	0.281	0.285	0.286	0.315
E-W SECOND	0.861	0.872	0.877	0.990
E-W THIRD	1.590	1.600	1.64	1.85
TORSION FIRST	0.345	0.355	---	---
TORSION SECOND	0.976	0.977	---	---

CRITICAL DAMPING RATIO (ζ_n)

MODE	FILTERED CORRELOGRAM	SPECTRAL MOMENTS	SPECTRAL DENSITY	FORCED VIBRATION
N-S FIRST	0.0094	0.0070	0.008	0.007
N-S SECOND	0.0116	0.0072	0.008	0.013
N-S THIRD	0.0183	0.0152	0.016	0.014
E-W FIRST	0.0100	0.0096	0.014	0.009
E-W SECOND	0.0096	0.0104	0.014	0.013
E-W THIRD	0.0108	0.0094	0.025	0.015
TORSION FIRST	0.0128	0.0119	---	0.008
TORSION SECOND	0.0138	0.0116	---	---

about 3% higher than the estimates obtained from the first two methods. This may indicate a difficulty in carefully determining the shape of the Spectral Density function in the frequency domain for the higher modes of vibration.

With respect to damping estimates, the values of the Spectral Moments and Spectral Density estimates are consistent for the North-South direction, but the Filtered Correlogram estimates are consistently larger than the others. For the East-West direction, the Filtered Correlogam and Spectral Moments values are consistent, with the Spectral Density estimates being much higher in value. The torsional estimates for the two methods were consistent. No torsional estimates were calculated by the Spectral Density method of analysis. The correlograms for this building are shown in Figures 13, 14, and 15.

INTERNATIONAL TELECOMMUNICATIONS CENTER (ITC)

The natural frequency values used in designing this building were 0.233, 0.654, and 1.22 Hz for the North-South and 0.230, 0.645, and 1.20 Hz in the East-West direction for the first three modes of vibration [40].

The values obtained in this investigation are shown in Table 4 for the first two modes of translation and torsion. With respect to frequency estimates, all three methods gave remarkably similar values, with only the second East-West mode estimate from the Spectral Density method being about 1% higher than the others.

The damping ratio estimates are also very close, with the Spectral Density estimates for the first East-West and first Torsional

TABLE 4
PARAMETER ESTIMATES OF ITC BUILDING

NATURAL FREQUENCY f_n (Hz)

MODE	FILTERED CORRELOGRAM	SPECTRAL MOMENTS	SPECTRAL DENSITY
N-S FIRST	0.324	0.324	0.323
N-S SECOND	0.955	0.957	0.952
E-W FIRST	0.311	0.318	0.312
E-W SECOND	0.925	0.928	0.935
TORSION FIRST	0.412	0.415	0.413
TORSION SECOND	1.04	1.05	1.06

CRITICAL DAMPING RATIO (ζ_n)

MODE	FILTERED CORRELOGRAM	SPECTRAL MOMENTS	SPECTRAL DENSITY
N-S FIRST	0.0050	0.0048	0.004
N-S SECOND	0.0070	0.0057	0.007
E-W FIRST	0.0112	0.0115	0.009
E-W SECOND	0.0060	0.0060	0.006
TORSION FIRST	0.0076	0.0091	0.005
TORSION SECOND	0.0144	0.0118	0.013

modes being definitely smaller than the estimates from the other methods. For this building, the parameter estimates from all three methods of system identification gave very similar results.

The correlograms for this building are shown in Figures 16, 17, and 18.

ASAHI TOKAI BUILDING (ATB)

The theoretical natural frequency values used for designing the Asahi Tokai Building were 0.385 and 1.11 Hz for the North-South direction and 0.390 and 1.12 Hz for the East-West direction, respectively. The corresponding theoretical estimates for the critical damping ratios were 0.020 and 0.057 for the North-South modes and 0.020 and 0.058 for the East-West modes.

For the system identification methods, only four modes of vibration were analyzed, due to a relatively low signal to noise ratio, whose effects will be discussed later. These were the first two North-South modes, and the fundamental modes in the torsional and East-West directions. These results are shown in Table 5.

For the natural frequency estimates, the Spectral Moments estimates for the East-West and Torsional modes appear definitely to be in error, being about 7% too high. The remainder of the frequency estimates are valid.

With respect to damping, the Spectral Density estimate for the fundamental North-South mode and the Filtered Correlogram estimates for the East-West and Torsional modes appear to overestimate the true value. Generally speaking, the signal to noise ratio for the records for this building were unfavorably low, generally yielding inaccurate

TABLE 5
PARAMETER ESTIMATES OF ATB BUILDING

NATURAL FREQUENCY f_n (Hz)

MODE	FILTERED CORRELOGRAM	SPECTRAL MOMENTS	SPECTRAL DENSITY	FORCED VIBRATION
N-S FIRST	0.382	0.385	0.374	0.434
N-S SECOND	1.13	1.14	1.15	1.27
E-W FIRST	0.382	0.404	0.374	0.436
TORSION FIRST	0.382	0.405	---	0.562

CRITICAL DAMPING RATIO (ζ_n)

MODE	FILTERED CORRELOGRAM	SPECTRAL MOMENTS	SPECTRAL DENSITY	FORCED VIBRATION
N-S FIRST	0.0052	0.0072	0.026	0.009
N-S SECOND	0.0209	0.0165	0.013	0.012
E-W FIRST	0.0455	0.0287	0.024	0.009
E-W SECOND	0.0473	0.0271	---	0.0073

parameter estimates. The correlograms for this building are shown in Figures 19 and 20.

YOKOHAMA TENRI BUILDING (YTB)

The theoretical natural frequency estimates used in designing the Yokohama Tenri Building were 0.375 and 0.943 Hz for the North-South modes and 0.374 and 1.10 Hz for the East-West modes of vibration, respectively. The corresponding estimates obtained by system identification procedures are shown in Table 6.

The natural frequency estimates are again all very close, with only the second torsional estimate from the Filtered Correlogram method being significantly less than the other values, by 4%. The fundamental North-South Filtered Correlogram method is also about 1% too high. The rest of the results appear to be extremely consistent among all three methods of analysis.

The damping ratio estimates show much wider variation among the three methods of analyses. Four of the six Spectral Density estimates appear to be much lower than those values calculated by the other two analytical procedures. A fifth Spectral Density estimate appears to be considerably higher than it should be. For this building, the Filtered Correlogram and Spectral Moments estimates are in agreement, but the Spectral Density estimates appear to be considerably in error, in estimating damping parameters.

The correlograms for this structure are shown in Figures 21, 22, and 23.

TABLE 6
PARAMETER ESTIMATES FOR YTB BUILDING

NATURAL FREQUENCY f_n (Hz)

MODE	FILTERED CORRELOGRAM	SPECTRAL MOMENTS	SPECTRAL DENSITY
N-S FIRST	0.464	0.459	0.457
N-S SECOND	1.32	1.33	1.32
E-W FIRST	0.454	0.468	0.459
E-W SECOND	1.32	1.34	1.33
TORSION FIRST	0.601	0.603	0.602
TORSION SECOND	1.54	1.60	1.61

CRITICAL DAMPING RATIO (ζ_n)

MODE	FILTERED CORRELOGRAM	SPECTRAL MOMENTS	SPECTRAL DENSITY
N-S FIRST	0.007	0.0075	0.005
N-S SECOND	0.0073	0.0059	0.005
E-W FIRST	0.0129	0.0103	0.006
E-W SECOND	0.0091	0.0074	0.013
TORSION FIRST	0.0125	0.0090	0.003
TORSION SECOND	0.0175	0.0173	0.014

XIII. COMPARISON OF AMBIENT AND FORCED VIBRATION PARAMETER ESTIMATES

Three of the structures investigated were subjected to forced vibration shaker tests. The structures tested under this condition were the World Trade Center, the Asahi Tokai Building, and the Tokyo Tower. Thus for these structures it is possible to compare frequency and damping values obtained under low amplitude ambient vibration with estimates evaluated under large amplitude forced vibration conditions. In addition, frequency estimates for translational modes for the Tokyo Tower observed under typhoon and earthquake loading are also available for comparison purposes.

WORLD TRADE CENTER

Forced vibration tests for the WTC building were conducted by the Kajima Construction Company under the direction of Dr. Kiyoshi Muto. These tests were conducted after the steel frame and curtain walls of the structure, as well as the floor slabs, had been constructed. However, the structure was still not completely finished, and no live load (furniture, equipment, and people) was present on the structure. The results of these tests are also shown on Table 3. The mean value of the natural frequencies evaluated by system identification methods are 0.282, 0.861, and 1.60 Hz for the North-South direction, and 0.284, 0.870, and 1.61 Hz for the East-West modes. The corresponding forced vibration estimates are 0.318, 0.980, and 1.82 Hz for the North-South direction, and 0.315, 0.990, and 1.85 Hz for the East-West direction, respectively. The forced vibration

values are larger by an average value of 14% over the ambient vibration values. This difference can probably be attributed to the absence of live loading in the forced vibration tests. The ambient measurements were taken when the building was fully occupied, so the full live load was present, resulting in shorter natural frequencies.

The mean damping ratios are 0.0081, 0.0089, 0.0165 and 0.0112, 0.0113, 0.0151, for the two translational directions. The corresponding forced vibration estimates are 0.007, 0 013, 0.014 and 0.005, 0.013, 0.015, respectively. No clear pattern emerges from these values. The first and third North-South estimates, and the first East-West estimate evaluated under forced vibration conditions underestimate the corresponding ambient vibration values by about 16%. However, the second North-South values is 46% greater than its ambient counterpart, and the second East-West value is 15% greater. The third East-West mode estimates evaluated under both levels of vibration are identical. The only definite pattern that emerges is that the forced vibration estimates for damping for the first modes are lower than their ambient counterparts, but the second mode values are higher.

ASAHI TOKAI BUILDING

Forced vibration tests for this building were conducted by the Shimizu Construction Company. These tests were also conducted after the building structure had been completely constructed, but before live loads were placed on the structure. Because of low signal to noise ratios for this building, as indicated in Table 9, only the first North-South mode parameter estimates can be expected to be

reliable. The natural frequency estimates obtained by system identification procedures were approximately 14 percent less than the corresponding forced vibration estimates.

The damping estimate for the fundamental North-South mode evaluated by system identification was considerably lower than the forced vibration value. The other damping estimates cannot be considered reliable due to the low signal to noise ratio for the other three modes of vibration.

TOKYO TOWER

Forced vibration tests on the Tokyo Tower were conducted in 1959. In addition to these tests, natural frequency measurements for this tower were recorded during the Ise-Wan Typhoon of September 26 and 27, 1959, and during the earthquake of January 24, 1959. Thus during the year 1959 the natural frequencies of this tower were measured under three levels of dynamic excitation. Only two system identification methods, the Filtered Correlogram and the Spectral Moment procedures, were used to analyze the ambient data from this tower.

The natural frequencies are shown in Table 7. The forced vibration estimates for the North-South modes are 4% and 8% larger than the system identification values for the first two modes, respectively. The third mode estimate, however, is only 2% higher than the ambient vibration value. The values recorded under typhoon conditions are consistently about 2% lower than the forced vibration estimates. The second torsional forced vibration natural frequency is 14% higher than its ambient counterpart.

During the 1959 earthquake, the third North-South mode was

TABLE 7
PARAMETER ESTIMATES OF TOKYO TOWER

NATURAL FREQUENCY f_n (Hz)

MODE	FILTERED CORRELOGRAM	SPECTRAL MOMENTS	FORCED VIBRATION	ISE-WAN TYPHOON
N-S FIRST	0.360	0.357	0.377	0.37
N-S SECOND	0.593	0.595	0.645	0.63
N-S THIRD	1.248	1.249	1.28	1.25
TORSION FIRST	1.438	1.435	---	---
TORSION SECOND	2.043	2.041	2.33	---

CRITICAL DAMPING RATIO (ζ_n)

MODE	FILTERED CORRELOGRAM	SPECTRAL MOMENTS
N-S FIRST	0.0078	0.0109
N-S SECOND	0.0082	0.0062
N-S THIRD	0.0010	0.0011
TORSION FIRST	0.0025	0.0021
TORSION SECOND	0.0020	0.0019

strongly excited at 1.25 Hz. This value agrees exactly with the estimates for this mode evaluated under ambient and under typhoon conditions. The other modes were not sufficiently excited by the earthquake to be easily identifiable.

No damping estimates were evaluated under forced or typhoon excitation conditions. However, the damping estimates evaluated by the Filtered Correlogram and the Spectral Moments methods appear to be in very good agreement, as indicated in Table 7. It is significant that the third translational mode, and the two torsional modes analyzed, exhibited extremely small values of damping, being less than 0.3 percent of critical.

The first and third North-South modes of vibration are true bending modes, while the second mode is a shear mode. These mode shapes are shown in Figure 24. The correlograms for the Tokyo Tower are shown in Figures 25 and 26.

TABLE 8
SIGNAL TO NOISE RATIO (SNR)
OF WTC AND ITC BUILDINGS

WTC BUILDING	SIGNAL - NOISE RATIO
N-S FIRST	32.8
N-S SECOND	17.3
N-S THIRD	6.9
E-W FIRST	19.9
E-W SECOND	16.4
E-W THIRD	17.3
TORSION FIRST	22.2
TORSION SECOND	14.5
ITC BUILDING	**SIGNAL - NOISE RATIO**
N-S FIRST	47.2
N-S SECOND	22.3
E-W FIRST	23.0
E-W SECOND	22.8
TORSION FIRST	26.3
TORSION SECOND	9.9

TABLE 9
SIGNAL TO NOISE RATIO (SNR)
OF ATB, YTB, AND TOKYO TOWER

ATB BUILDING	SIGNAL - NOISE RATIO
N-S FIRST	26.7
N-S SECOND	7.8
E-W FIRST	7.8
TORSION FIRST	7.7

YTB BUILDING	SIGNAL - NOISE RATIO
N-S FIRST	24.5
N-S SECOND	14.5
E-W FIRST	19.1
E-W SECOND	10.5
TORSION FIRST	13.8
TORSION SECOND	6.5

TOKYO TOWER	SIGNAL - NOISE RATIO
N-S FIRST	29.1
N-S SECOND	13.7
N-S THIRD	78.4
TORSION FIRST	41.3
TORSION SECOND	29.1

XIV. CONCLUSIONS

Prior to analyzing the individual effectiveness of the separate system identification methods, it is necessary to discuss the importance of four factors which greatly affect the values of parameter estimates obtained from an ambient vibration record. These factors are a) the record length, b) the signal-noise ratio in the record, c) the filter shape, and d) the filter cutoff bandwidth.

Generally speaking, the record length should be as long as possible, assuming that the property of stationarity is not seriously violated. If long period non-stationary waves are present in the record, these may be filtered out by a high pass filter. However, the resulting record should be appropriately tapered at both ends to eliminate distortions in the record caused by filter rise times, as discussed earlier in Section II. In this investigation, records of at least three minutes were used for most of the structures, with four minute records being available for the World Trade Center.

The signal-noise ratio is extremely important in determining the accuracy of frequency and damping parameter estimates for any structure. For this reason, the individual mode signal-noise ratios for each structure are listed in Table 8 and 9. These ratios were determined by dividing the peak amplitude at a natural frequency with the average amplitude of the noise in a region of 0.05 Hz on both sides of the natural frequency. It was found in this investigation, that if this ratio exceeded 15, the damping estimate appeared to be reliable. For values of the ratio less than 10, the damping estimates were generally unreliable. Frequency estimates evaluated by the Spectral

Moments method tended also to be inaccurate when this ratio was below 10. For ratios between 10 and 15, the frequency estimates were consistent, but some of the damping estimates were inconsistent. Thus it can probably be said that a value of the signal-noise ratio between 10 and 15 represented a "gray area" where no general statement can be made to cover all cases of parameter estimation.

The filter shape does have a significant effect on the resulting damping parameter estimate. It has been shown earlier, in Section IX, that use of a Gaussian Filter applied to a record prior to analysis by the Spectral Moments method tended to underestimate the true values of the critical damping ratio estimates. The Gaussian Filter most probably would have had a similar effect on parameter estimates obtained by the Spectral Density method. It was for this reason that only the Trapezoidal Filter was used in obtaining parameter estimates for the structures other than the World Trade Center.

The primary focus of this research project was to compare the relative accuracy of four different system identification methods in estimating frequency and damping parameters from identical ambient vibration records of tall structures. Since all records had been subjected to the same Trapezoidal Filter, differences in numerical estimates could be only due to the different analytical procedures applied to the data.

The Filtered Correlogram method proved to be the least sensitive one to changes in filter shape and filter bandwidth. It yielded reliable estimates for long records with signal-noise ratios greater than 15. It was extremely easy to program this method on a digital computer, using Fast Fourier Transform algorithm. With the exception of

the Asahi Tokai Building, this method produces vibrational parameter estimates that appears to be reasonably accurate.

The Spectral Moments method was extremely sensitive to the filter bandwidth chosen. Use of a Gaussian Filter tended to cause damping estimates to be underestimated by as much as 50 percent. Bandwidths greater than 0.1 Hz also tended to produce inaccurate damping values. The accuracy of frequency estimates obtained by this method appears to also depend on the signal-noise ratio of the record. For the East-West and Torsional fundamental modes of the Asahi Tokai Building (Table 5), this method yielded frequency estimates of the order of 7% higher than the other methods produced. These apparent errors can only be attributed to the low signal-noise ratios of these ambient records. For the rest of the structures, parameter estimates evaluated by this method appeared to be consistent with those evaluated by the Filtered Correlogram method. This method was also easy to program on a digital computer.

Since the Spectral Density estimates were evaluated by Professor H. Kobayashi, the author is not able to comment on the relative ease or difficulty encountered in programming this method. Its frequency estimates for the WTC building appear to be between one to two percent higher than those from the other methods. No significant differences are noticeable for frequency estimates from the other three buildings, however. With respect to damping, this method generally gave lower estimates for the buildings than the other two methods gave, by an average of 0.2 percent of critical. The reason this method yielded consistently lower damping estimates cannot be satisfactorily explained at this time.

The Two Stage Least Square method, which was only applied to data from the WTC building, produced frequency estimates that were consistent with the other values. With respect to damping, however, it significantly overestimated the fundamental mode critical damping ratio by a factor of about two. The second mode estimate appeared to be satisfactory. This method requires greater effort in programming and in analyzing the data that the Filtered Correlogram or Spectral Moments methods require.

It is also interesting to notice how the Filtered Correlogram function is affected by changes in filter shape, center frequency, and cutoff bandwidth.

The rounded, "reverse curvature" shape of the envelope of the Filtered Correlogram for the third East-West mode of the WTC building is shown in Figure 14. This record was subjected to a Trapezoidal Filter, but edge effects were not completely eliminated in the truncated filtered record. When a Gaussian Filter was applied to this record, with the same cutoff bandwidth, the resulting curve is shown in Figure 27. In this new Figure, the envelope of the Filtered Correlogram exhibits the normal exponential decay which was not present in Figure 14. This is because all edge effects have now been removed in the truncated record, because of the shorter filter rise time of the Gaussian Filter.

The same effect on the "rounded" appearance of the envelope of the Filtered Correlogram is illustrated in Figure 28 for the second North-South mode for the WTC building. Here again the Trapezoidal Filter rise time was too long to be effectively eliminated in the truncated record.

Figures 29 and 30 also concern the third East-West mode of the WTC building In Figure 29, the bandwidth is so wide that two modes are included in the record, resulting in a "wavy" appearance of the correlogram. In Figure 30, while only one mode is present, the bandwidth is still too wide. This results in the envelope appearing to be composed of a series of straight lines, rather than exhibiting negative exponential decay.

Figure 31 also illustrates two curves evaluated from data from the North-South direction of the Tokyo Tower. The top curve shows the effect on the Filtered Correlogram due to an incorrect filter center frequency. The lower curve illustrates the random fluctuations resulting from the effect of two modes in the same record, due to insufficient filtering.

With the exceptions of the ATB building, whose records exhibited unfavorable signal-noise ratios, measured values of the other three steel buildings appear to range from about 0.5% to about 1.5% under ambient and forced vibration conditions. The higher level of excitation due to forced vibration shaker test of the WTC building did not significantly affect the measured damping estimates.

It is also of interest to compare these measured damping values with estimates reported by other investigators in the literature for steel buildings of similar construction and height.

Davenport, Hogen, and Vickery [8] measured the translational modes of a 100 story steel exterior truss tube design building under ambient conditions. The resulting frequencies for the fundamental modes were 0.147 Hz for the North-South direction and 0.211 Hz for the East-West direction. The corresponding critical damping ratios

were 0.004 and 0.006, respectively, for these modes. These estimates were evaluated from records whose duration were of the order of one hour, which are extremely long for ambient vibration studies. These damping estimates correspond to the lower end of the range of values tabulated in this report.

Hansen, Reed, and Vanmarcke [45] have reported parameter estimates from two 40 story steel structures, measured under severe wind conditions with velocities between 40 to 60 miles per hour. Building "A" is a moment resistant frame, while Building "B" is of a framed tube design. The North-South, East-West, and Torsional fundamental frequencies for Building "A" were measured to be 0.170, 0.190, and 0.187 Hz, while the corresponding critical damping ratios were 0.018, 0.009, and 0.008, respectively. For Building "B", the corresponding fundamental natural frequencies were 0.24, 0.24, and 0.37 Hz. The measured critical damping ratios were 0.020 for the North-South mode, and 0.015 for the East-West mode. No damping estimate was reported for the Torsional mode for this building. The damping estimates reported for Building "A" are similar to those in this report, while those of Building "B" appear higher than the values reported herein.

Ibanez [19] has reported the measured parameter estimates for the twenty-two story steel frame San Diego Gas and Electric Building. The structure was excited by forced vibration shakers, and the measured fundamental frequencies were 0.382 and 0.393 Hz for the translational modes and 0.421 Hz for the Torsional mode. The corresponding critical damping ratio estimates were 0.020, 0.016, and 0.025. These damping estimates are also higher than those tabulated in this report.

Hart and Vasudevan [46] have reported parameter estimates evalu-

ated from records taken during the 1971 San Fernando Earthquake, for three steel structures exceeding twenty stories in height in the Los Angeles area. Estimates were only made for translational modes. For the 34 story 800 West 1st Street Building, the translational fundamental frequencies were 0.345 and 0.296 Hz, and the damping ratios were 0.032 and 0.049. For the 1900 Avenue of Stars Building, the fundamental frequencies were 0.235 and 0.234 Hz, with the damping values of 0.065 and 0.052. The corresponding estimates for the 27 story West 6th Street Building are 0.185 and 0.165 Hz, and 0.074 and 0.030.

If it could be assumed that the normal low amplitude damping estimates for these structures would have fallen in the 0.010 to 0.025 range, then it would appear that the critical damping ratios exhibited by these structures under earthquake conditions may be two to four times larger than would be measured under ambient conditions.

It is recommended that additional structures, constructed of both steel and concrete, be tested under conditions of ambient vibration, forced vibration excitation, and under high wind or earthquake loading. Comparisons of the changes in frequency and damping parameters under these different loading conditions will be of great benefit to future designers of high-rise structures.

XV. ACKNOWLEDGMENTS

The author wishes to acknowledge the excellent cooperation and advice received by several organizations and many individuals during the course of this investigation. The support of the National Science Foundation (NSF Grant ENV-16926) is gratefully appreciated, as well as the cooperation of the University of Hawaii Computing Center. The author also received excellent consulting advice on damping estimation from Professors Robert H. Scanlan of Princeton University and Hiroyoshi Kobayashi of Tokyo Institute of Technology. Professor Will Gersch of the University of Hawaii contributed the material on the Two Stage Least Square method of Analysis in Section VII of this report. The figures were prepared by Mary Kamiya of the Center of Engineering Research at the University of Hawaii, and the manuscript was typed by Lynn Onouye.

The author is also extremely grateful to Professors N. Norby Nielsen and James C.S. Chou for their advice and encouragement during the preparation of this report.

REFERENCES

1. Bouwkamp, J.G. and Clough, R.W., "Dynamic Properties of a Steel Frame Building," Presented at the 1965 Annual Meeting of the Structural Engineers Association of California, published by American Iron and Steel Institute, February 1966.

2. Jennings, P.C., Matthiesen, R.B., and Hoerner, J.B., "Forced Vibration of a 22-Story Steel Frame Building," EERL 71-01, California Institute of Technology, February 1971.

3. Rea, D., Shah, A.A., and Bouwkamp, J.G., "Dynamic Behavior of a High Rise Diagonally Braced Steel Building," EERC 71-5, University of California, August 1971.

4. Takahashi, K. and Husimi, K., "Method to Determine Frequency and Attenuation Constant from the Irregular Motion of an Oscillating Body," Journal of the Institute of Physical and Chemical Research, Japan, Vol. 14, No. 4. 1954.

5. Hatano, T. and Takahashi, T., "The Stability of an Arch Dam Against Earthquakes," Technical Report No. C-5607, Central Research Institute of Electric Power, February 1957.

6. Cherry, S. and Brady, A.G., "Determination of the Structural Dynamic Properties by Statistical Analysis of Random Vibrations," Proceedings of Third World Conference on Earthquake Engineering, Vol. II, 1965.

7. Ward, H.S. and Crawford, R., "Wind Induced Vibrations and Building Modes," bulletin of the Seismologial Society of America, Vol. 56, 1966, pp. 793-813.

8. Davenport, A.G., Hogan, M., and Vickery, B., "An Analysis of Records of Wind Induced Building Motion and Column Strain Taken at the John Hancock Center (Chicago)," BWLT-10-1970, the University of Western Ontario, London, Canada.

9. Taoka, G. and Scanlan, R.H., "A Statistical Analysis of the Ambient Responses of Some Tall Buildings," Princeton University, April 1973.

10. Vanmarcke, E., "Properties of Spectral Moments with Applications to Random Vibrations," Journal of Engineering Mechanics Division, ASCE, Vol. 98, April 1972.

11. Gersch, W., Nielsen, N.N., and Akaike, H., "Maximum Likelihood Estimation of Structural Parameters from Random Vibration Data," Journal of Sound and Vibration, Vol. 31, No. 2, 1973.

12. Foutch, D.A., "A Study of Parameter Estimators of Randomly Excited Structural System," M.S. Thesis, University of Hawaii, May 1973.

13. Gersch, W., Taoka, G.T., and Liu, R., "Structural System Parameter Estimation by a Two-Stage, Least Square Method," Journal of Engineering Mechanics Division, ASCE, October 1976.

14. Tanaka, T., Yoshizawa, S., Osawa, Y., and Morishita, T., "Period and Damping of Vibration in Actual Buildings During Earthquakes," Bulletin of Earthquake Research Institute, Vol. 47, 1969, Tokyo, Japan.

15. Trifunac, M.D., "Comparison Between Ambient and Forced Vibration Experiments," Earthquake Engineering and Structural Dynamics, Vol. 1, 1972.

16. Udwadia, F.E. and Trifunac, M.D., "Ambient Vibration Tests of Full-Scale Structures," Proceedings of Fifth World Conference on Earthquake Engineering, Rome, Italy, 1973.

17. Hudson, D.E., "Dynamic Properties of Full-Scale Structures Determined from Natural Excitations," Presented at the Dynamic Structural Symposium in Honor of N.J. Hoff, Stanford University, June 1971.

18. Schiff, A.J., "Identification of Large Structures Using Data from Ambient and Low Level Excitations," System Identification of Vibrating Structures, ASME Winter Meeting, New York, 1972.

19. Ibanez, P., "Identification of Dynamic Structural Models from Experimental Data," UCLA-ENG-7225, March 1972.

20. Jenkins, G.M. and Watts, D.B., Spectral Analysis and Its Applications, Holden Day, 1968.

21. Stockham, T.G., "High-Speed Convolution and Correlation," AFIPS Spring Joint Computer Conference, 1966, pp. 229-233.

22. Brigham, E.O., The Fast Fourier Transform, Prentice Hall, 1974.

23. Papoulis, A., The Fourier Integral and Its Applications, McGraw-Hill, 1962.

24. Dziewonski, A., Bloch, S., and Landisman, M., "A Technique for the Analysis of Transient Seismic Signals," Bulletin of Seismological Society of America, Vol. 59, No. 1, pp. 427-444, February 1969.

25. Schiff, A.J., "Identification of Large Structures Using Data from Ambient and Low Level Excitations," System Identification of Vibrating Structures, ASME Winter Meeting, New York, 1972.

26. Bendat, J.S., and Piersol, A.G., Random Data: Analysis and Measurement Procedures, Wiley-Interscience, 1971.

27. Bingham, C., Godfrey, M.D., and Tukey, J.W., "Modern Techniques of Power Spectrum Estimation," IEEE Transactions on Audio and Electroacoustics, Vol. AU-15, No. 2, June 1967, pp. 56-66.

28. Lanczos, C., Applied Analysis, Prentice Hall, 1956.

29. Thomson, W.T., Vibration Theory and Application, Prentice Hall, 1965.

30. Jenkins, G.M., "General Considerations in the Analysis of Spectra," Technometrics, Vol. 3, No. 2, May 1961.

31. Schwartz, M., Information Transmission, Modulation and Noise, 2nd edition, McGraw-Hill, 1970.

32. Kobayashi, H. and Sugiyama, N., "Damping Characteristics of Building Structures by Measuring Oscillations due to Microtremors," Tokyo Institute of Technology Report, February 1975.

33. Gersch, W. and Foutch, D.A., "Least Square Estimates of Structural System Parameters Using Covariance Function Data," IEEE Transactions on Automatic Control, Vol. AC-19, No. 6, December 1974, pp. 898-903.

34. Gersch, W., "On the Achievable Accuracy of Structural System Parameter Estimates," Journal of Sound and Vibration, Vol. 34, No. 1, 1974.

35. Lin, Y.K., Probabilistic Theory of Structural Dynamics, McGraw-Hill, New York, N.Y., 1967.

36. Astrom, K.J., "Lectures on the Identification Problem: The Least Squares Method," Report 6806, Division of Automatic Control, Lund Institute of Technology, Lund, Sweden, 1968.

37. Akaike, H., "Power Spectrum Estimation Through Autoregressive Model Fitting," Annals of the Institute of Statistical Mathematics, Vol. 21, 1969.

38. Hisada, T., "Earthquake Resistant Design of High Rise Buildings in Japan," Kajima Institute of Construction Technology, May 1975.

39. Muto, K., Ohta, T., Ashitate, T., and Uchiyama, M., "Vibration Test of WTC Building," Annual Proceedings of the Architectural Institute of Japan, September 1970.

40. Muto,K., Sato, K., Toyama, K., Uyeda, N., and Nagata, S., "High Rise Tube Design of the International Tele-Communications Center," Report of the Architectural Institute of Japan, 1974.

41. Ichinose,K., Fujii, K., Ito, T., Hirose, M., and Yamahara, H., "Vibration Test of the Asahi Tokai Building," Proceedings of the Architectural Institute of Japan, November 1971.

42. Tamano,A., Asahi, K., and Abe, S., "Design of the Yokohama Tenrikyo Building," Report of the Architectural Institute of Japan, 1972.

43. Naito, T., Nasu, N., Takeuchi, M., and Kubota, G., "Construction and Vibrational Characteristics of the Tokyo Tower," Bulletin of the Scientific and Engineering Laboratory, Waseda University, 1962.

44. Personal Communication to the Author from H. Kobayashi, November 1977.

45. Hansen, Robert J., Reed, John W., and Vanmarcke, Erik H., "Human Response to Wind Induced Motion of Buildings," Journal of Structural Division, ASCE, Vol. 99, No. ST7, July 1973.

46. Hart, Gary C. and Vasudevan, R., "Earthquake Design of Buildings-Damping," Journal of Structural Division, ASCE, Vol. 101, No. ST1, January 1975.

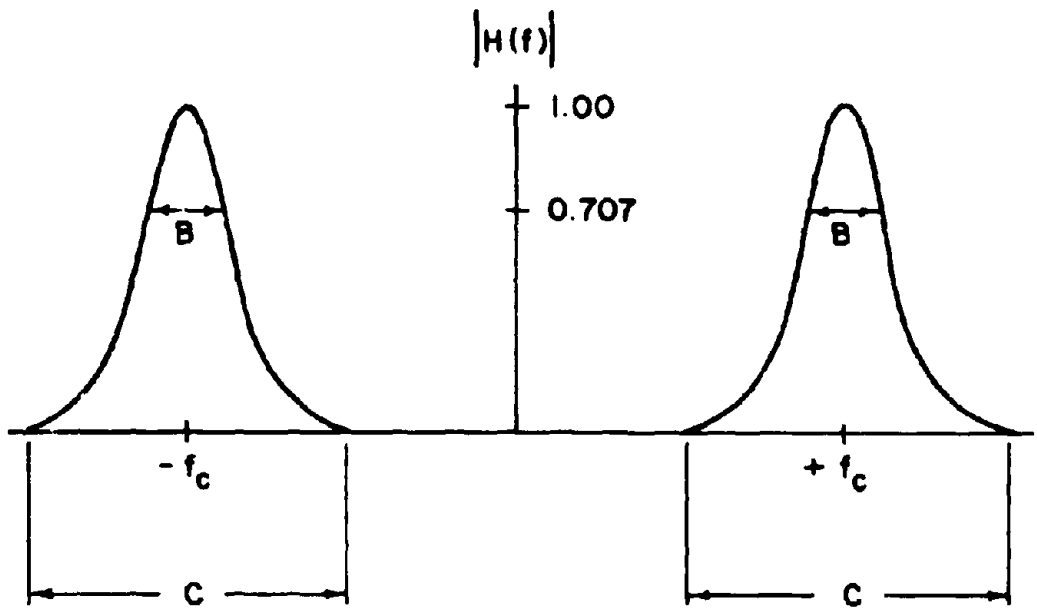

FIGURE I.a. GAUSSIAN FILTER
f_c = CENTER FREQUENCY
B = HALF - POWER BANDWIDTH
C = CUTOFF BANDWIDTH

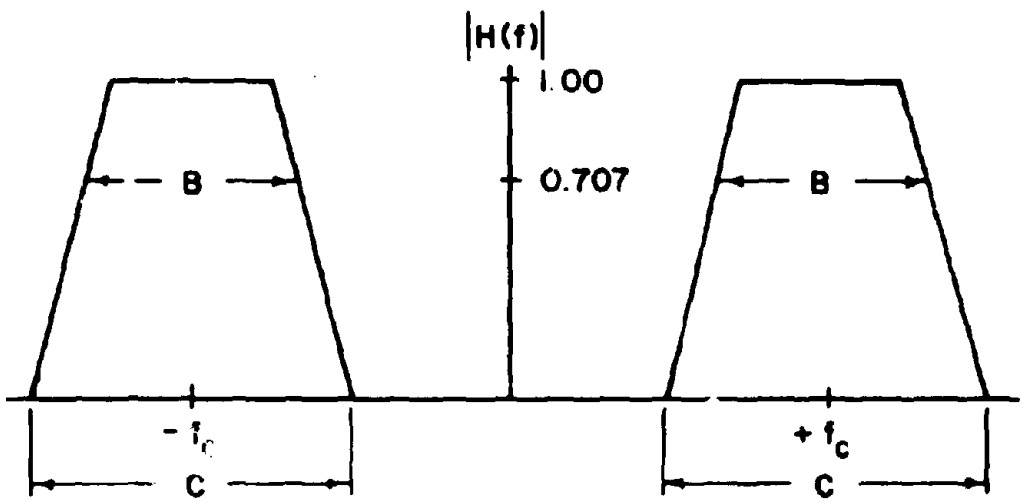

FIGURE I.b. TRAPEZOIDAL FILTER

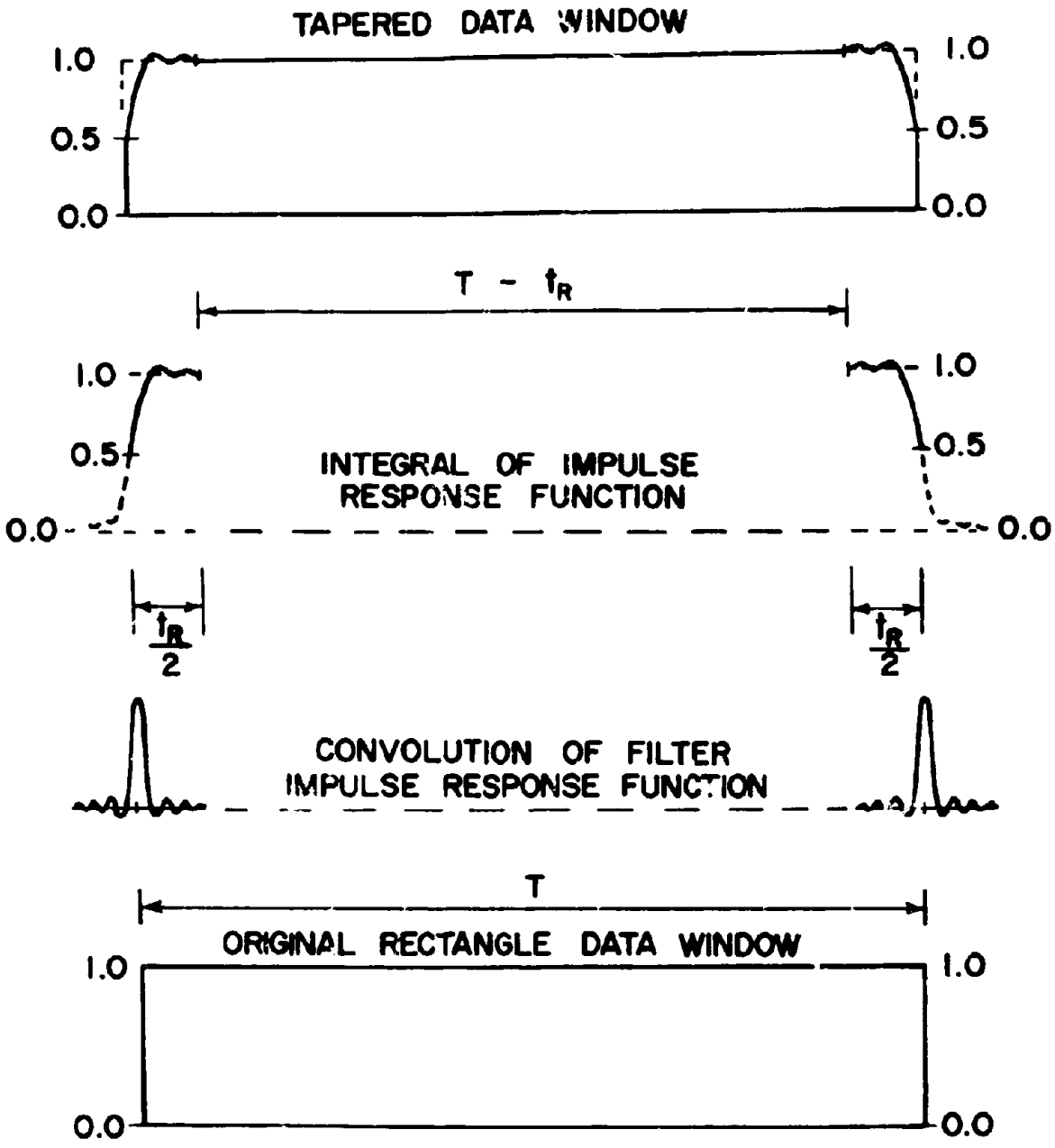

FIGURE 2

TAPERING OF ENDS OF RECTANGULAR
DATA WINDOW DUE TO EFFECTS OF FILTERING

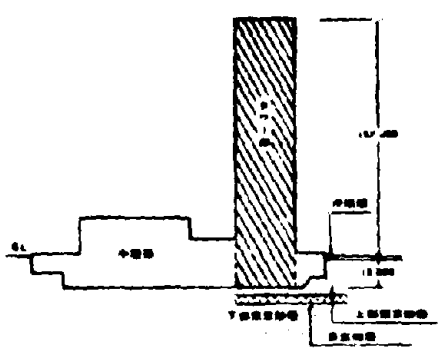

SCHEMATIC OF THE
ENTIRE STRUCTURE

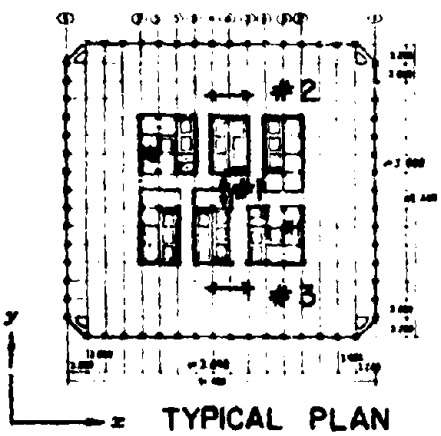

TYPICAL PLAN
VIEW OF TOWER
(NUMBERS REFER TO
POSITIONS OF VIBRATION
SENSORS)

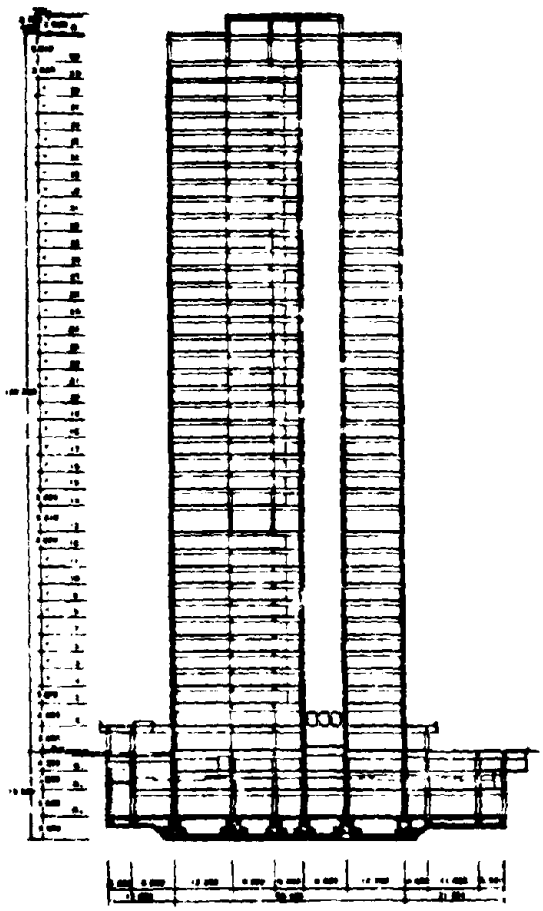

ELEVATION
VIEW
OF TOWER

FIGURE 3
TOKYO WORLD TRADE
CENTER BUILDING

FIGURE 4

TOKYO

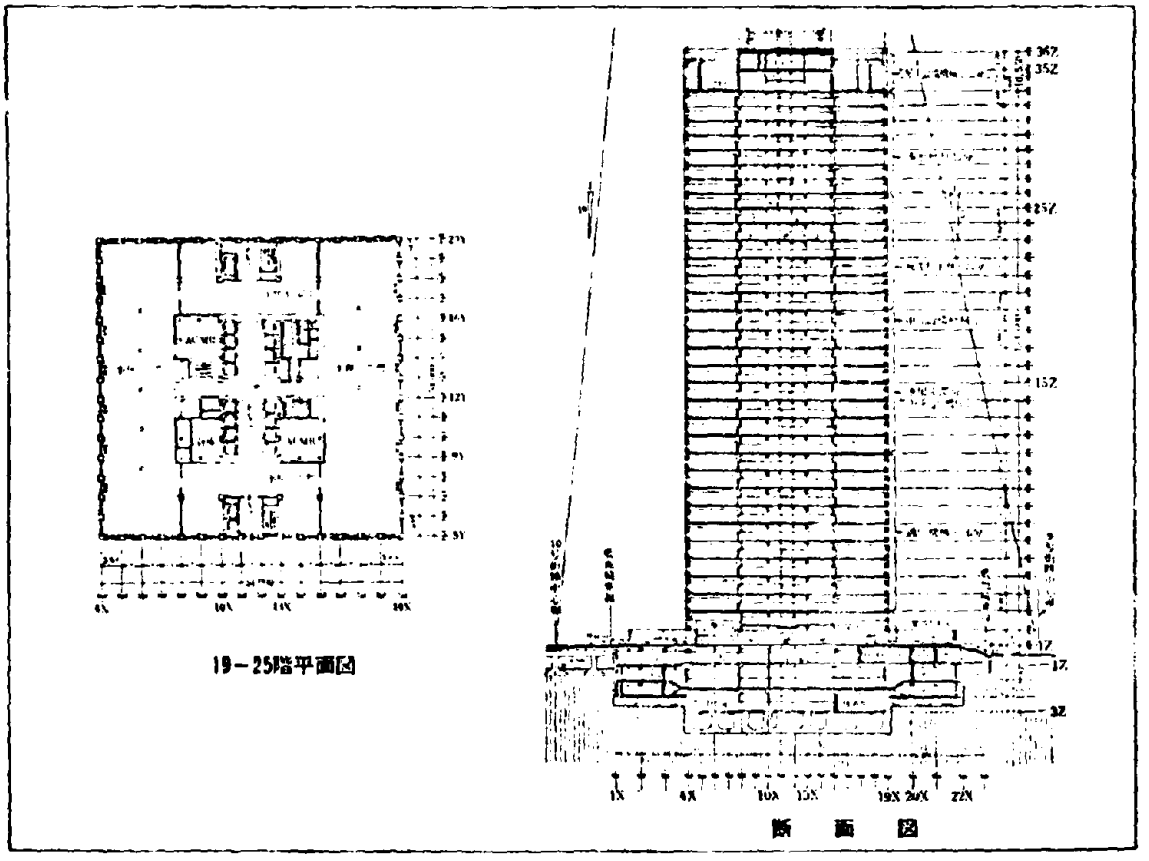

FIGURE 5

DETAILS OF
INTERNATIONAL TELE-COMMUNICATIONS CENTER

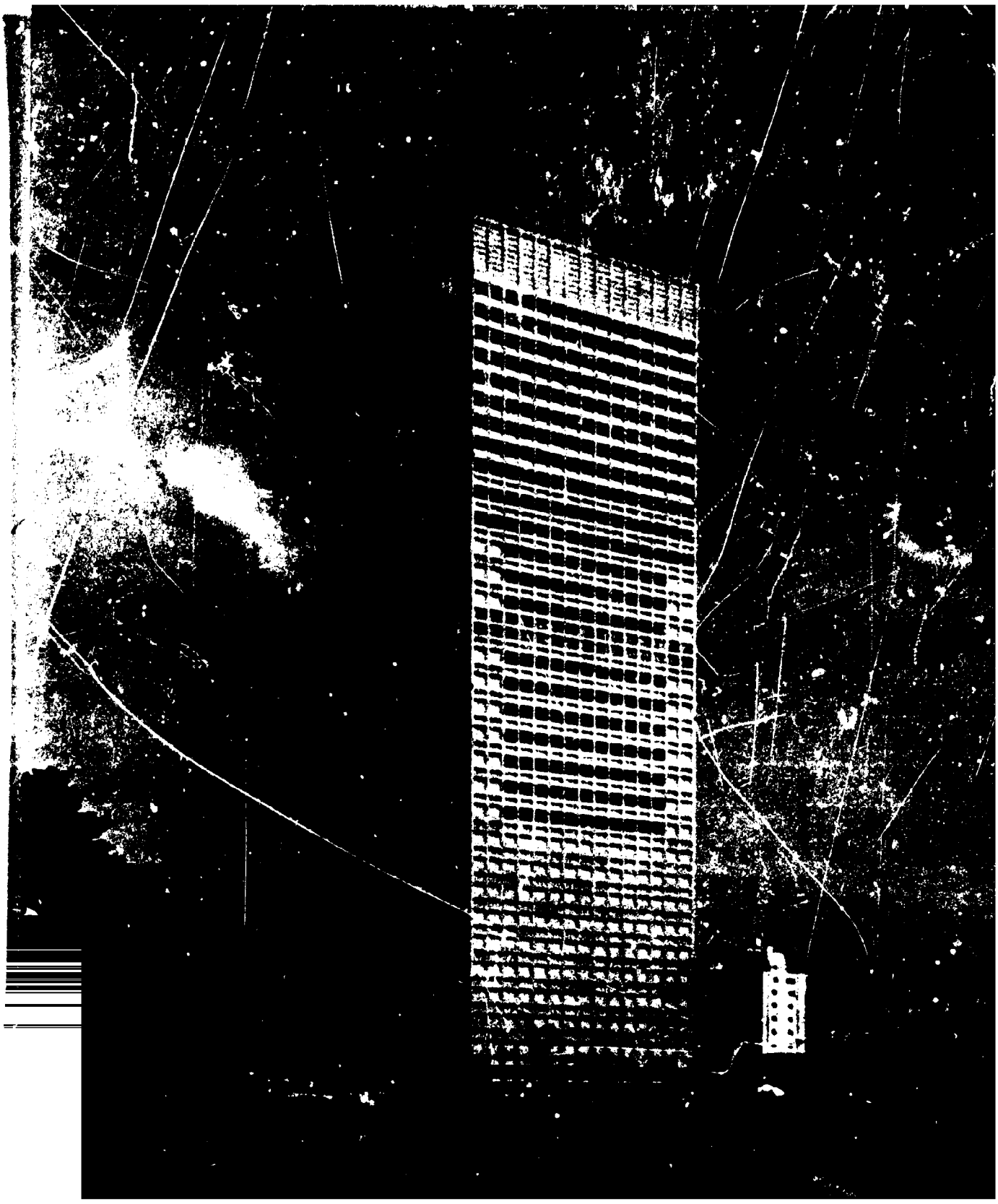

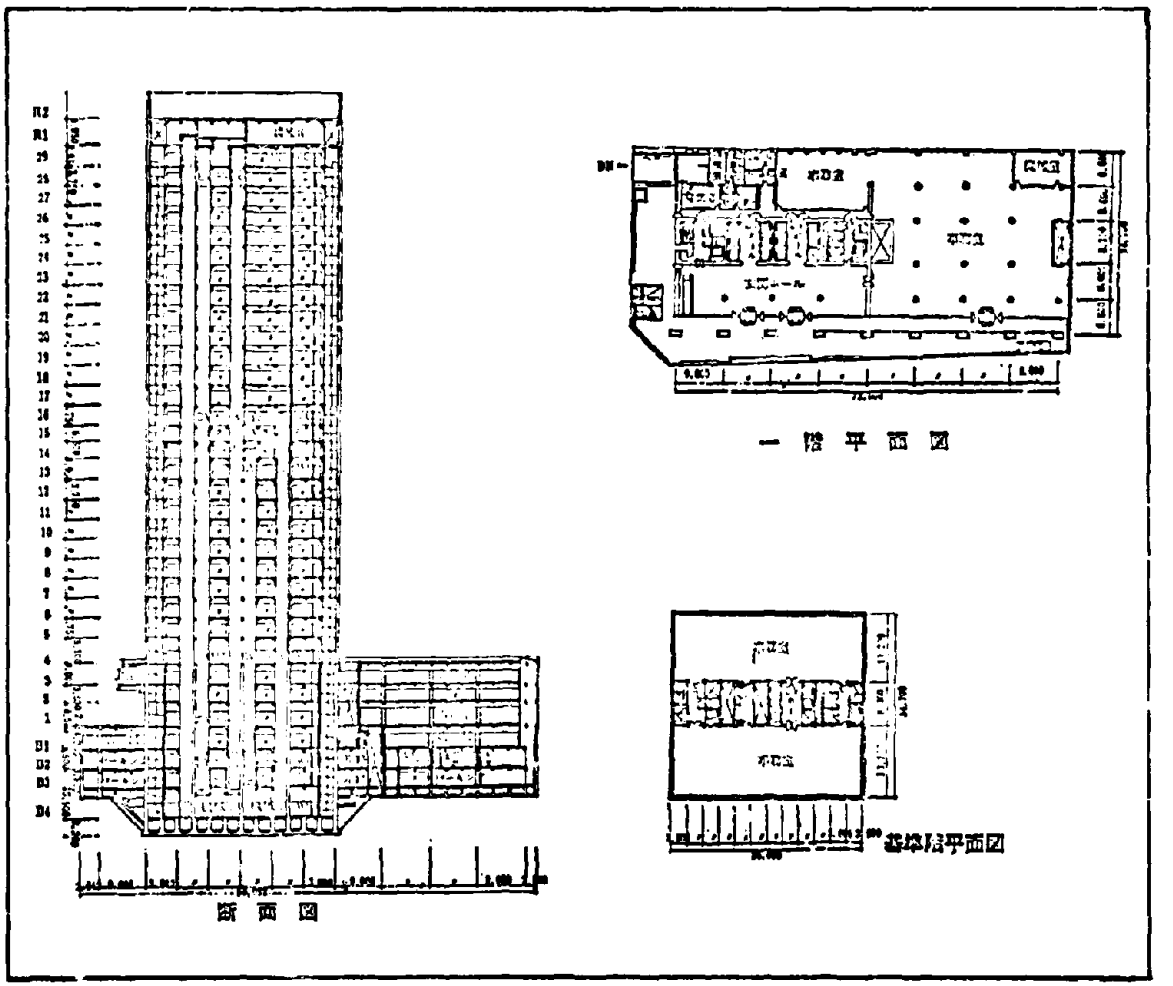

FIGURE 7
ASAHI TOKAI BUILDING

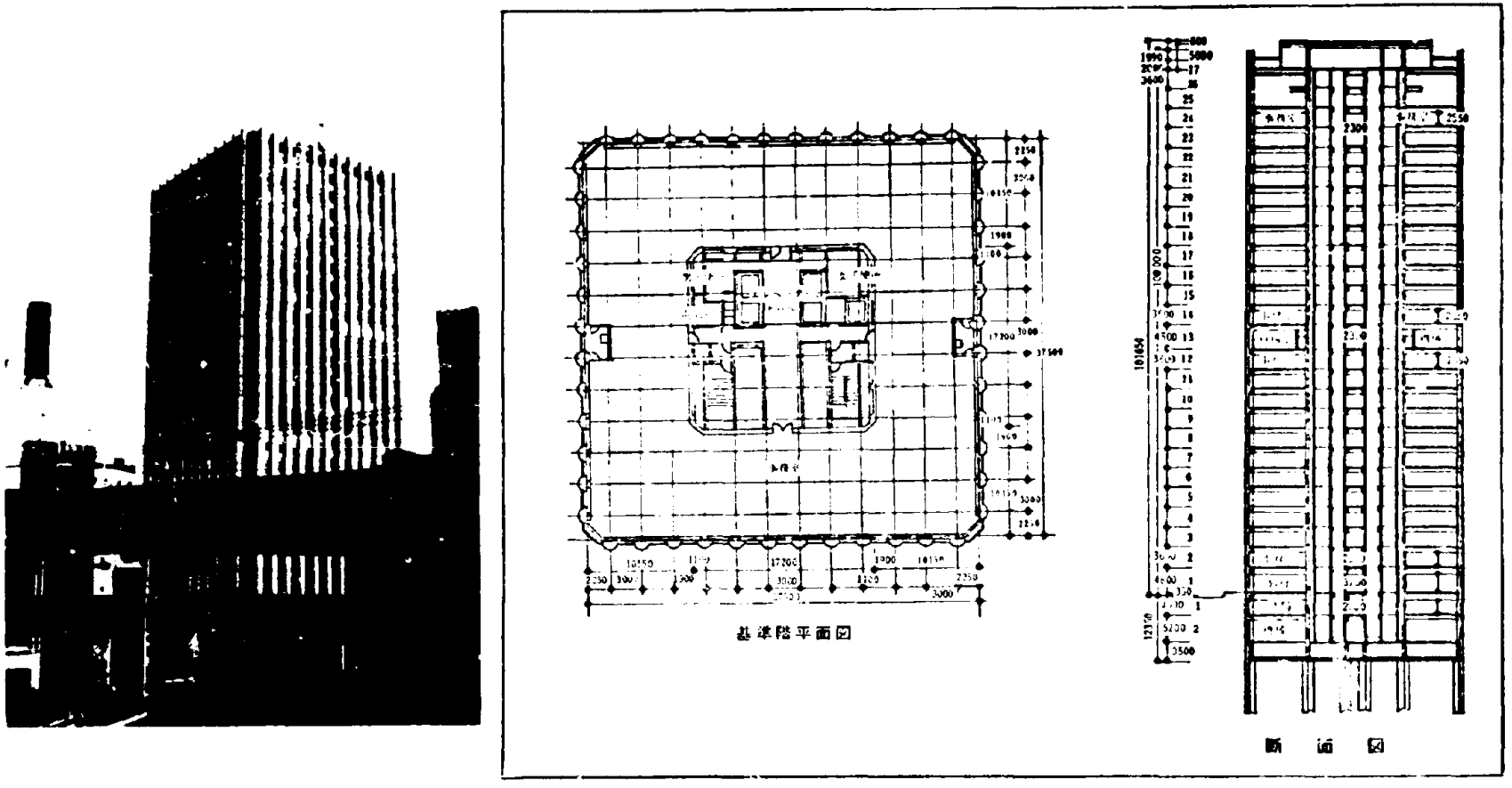

FIGURE 8
YOKOHAMA TENRI BUILDING

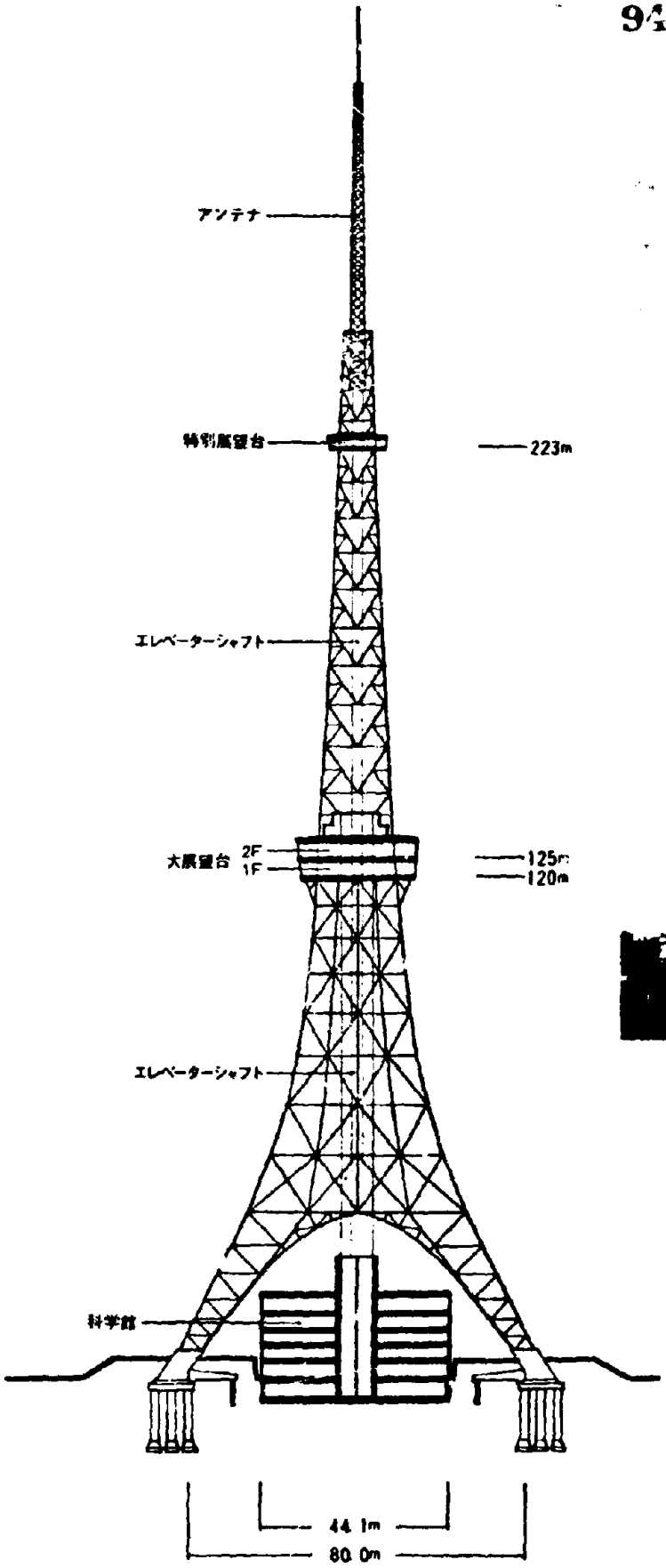

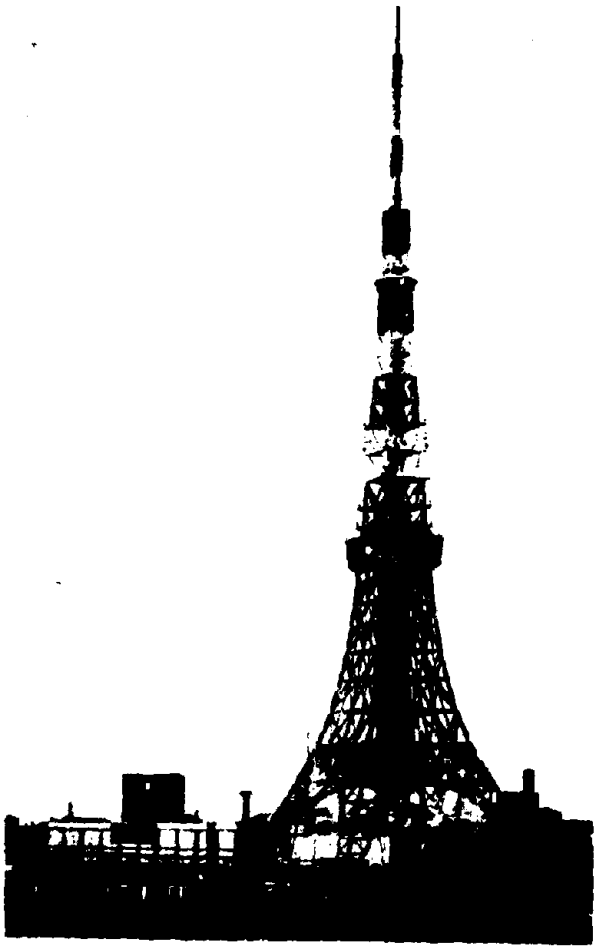

FIGURE 9
TOKYO TOWER

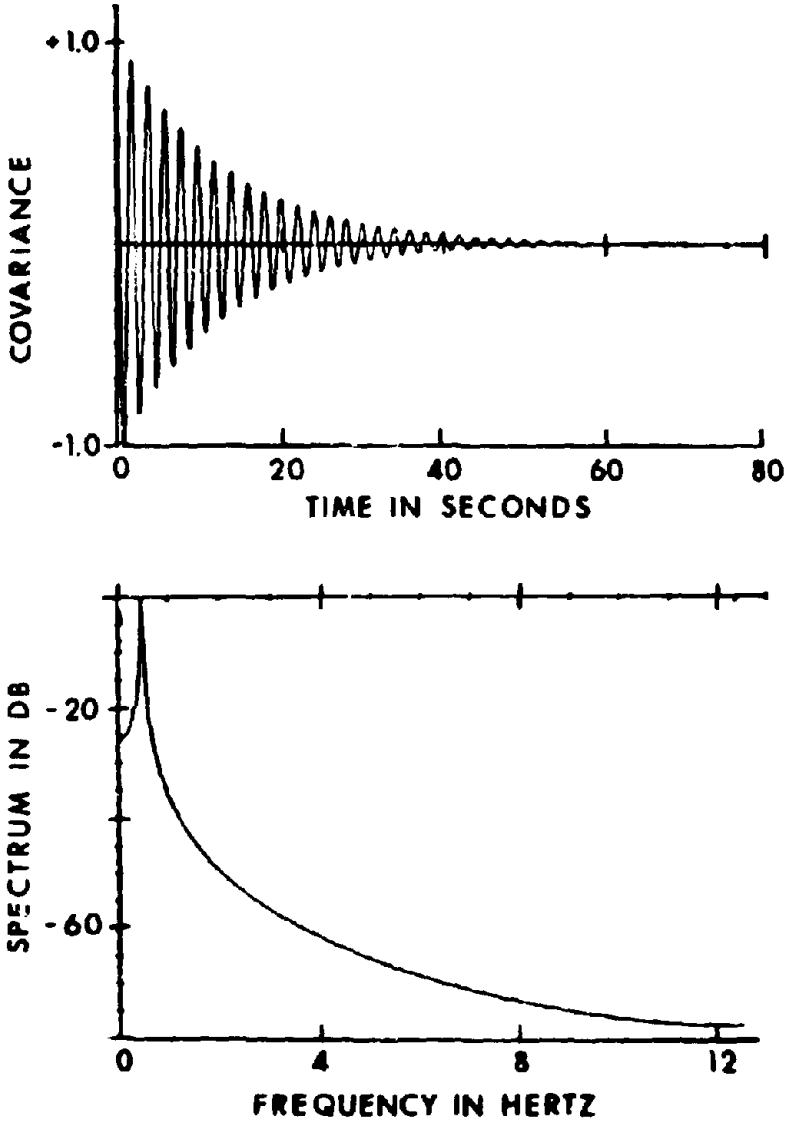

FIGURE 10

WTC N-S FIRST MODE

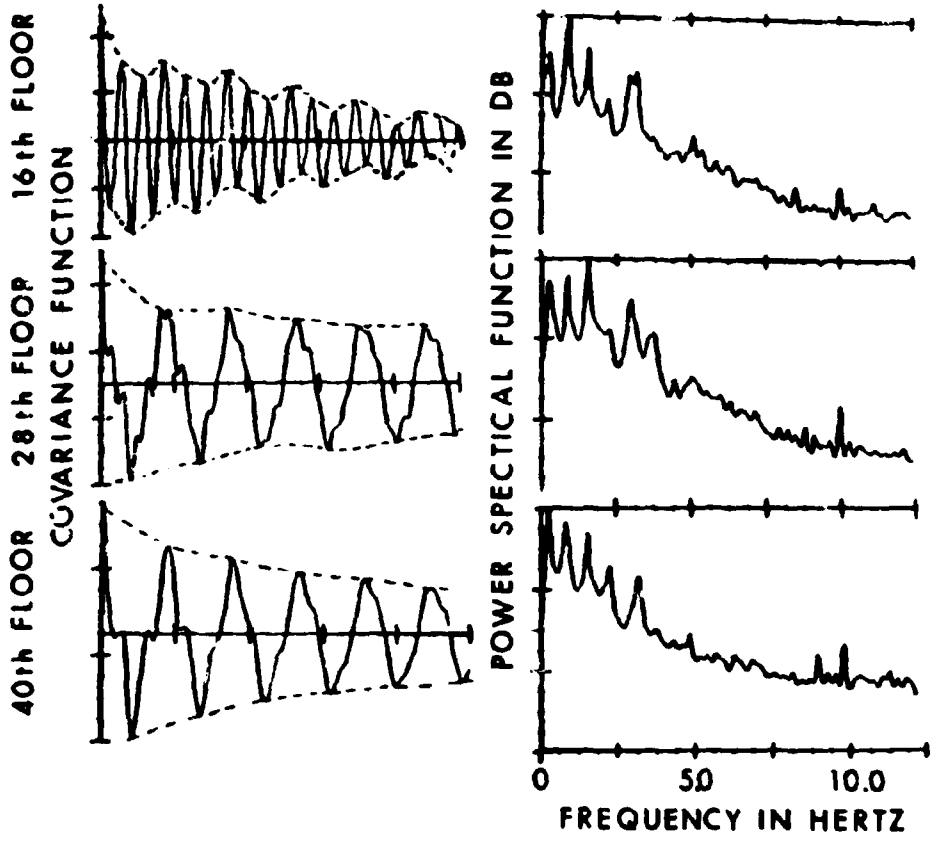

FIGURE 11

WTC N-S MODES

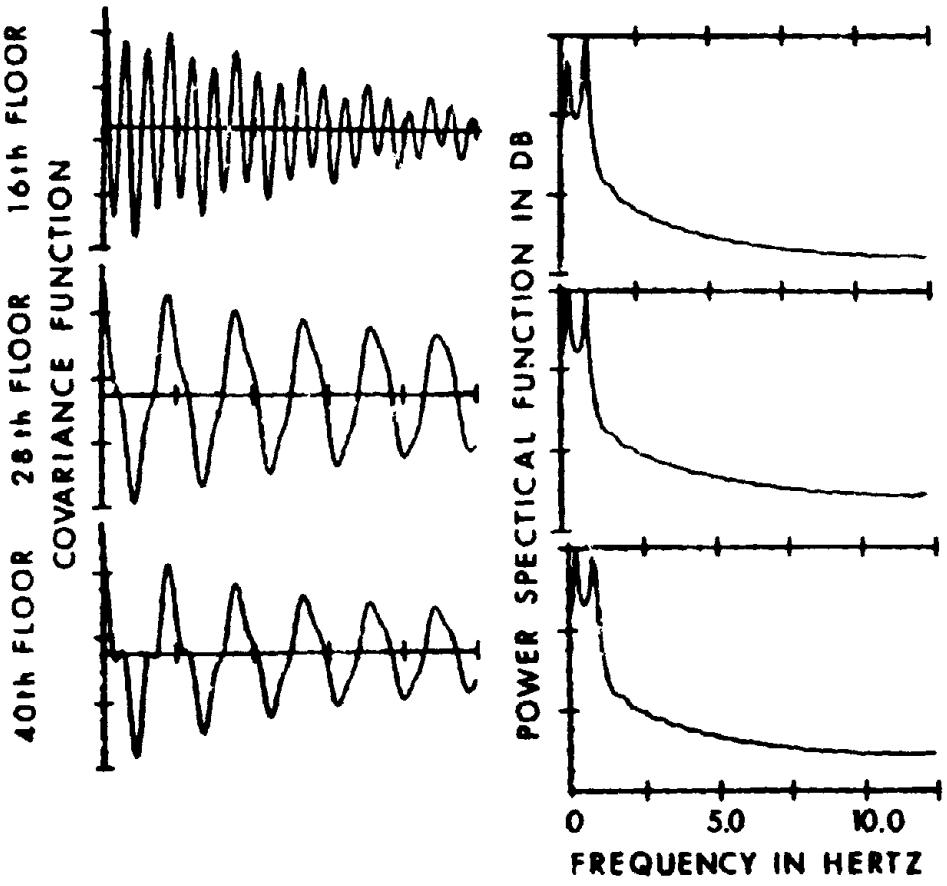

FIGURE 12
WTC N-S MODES

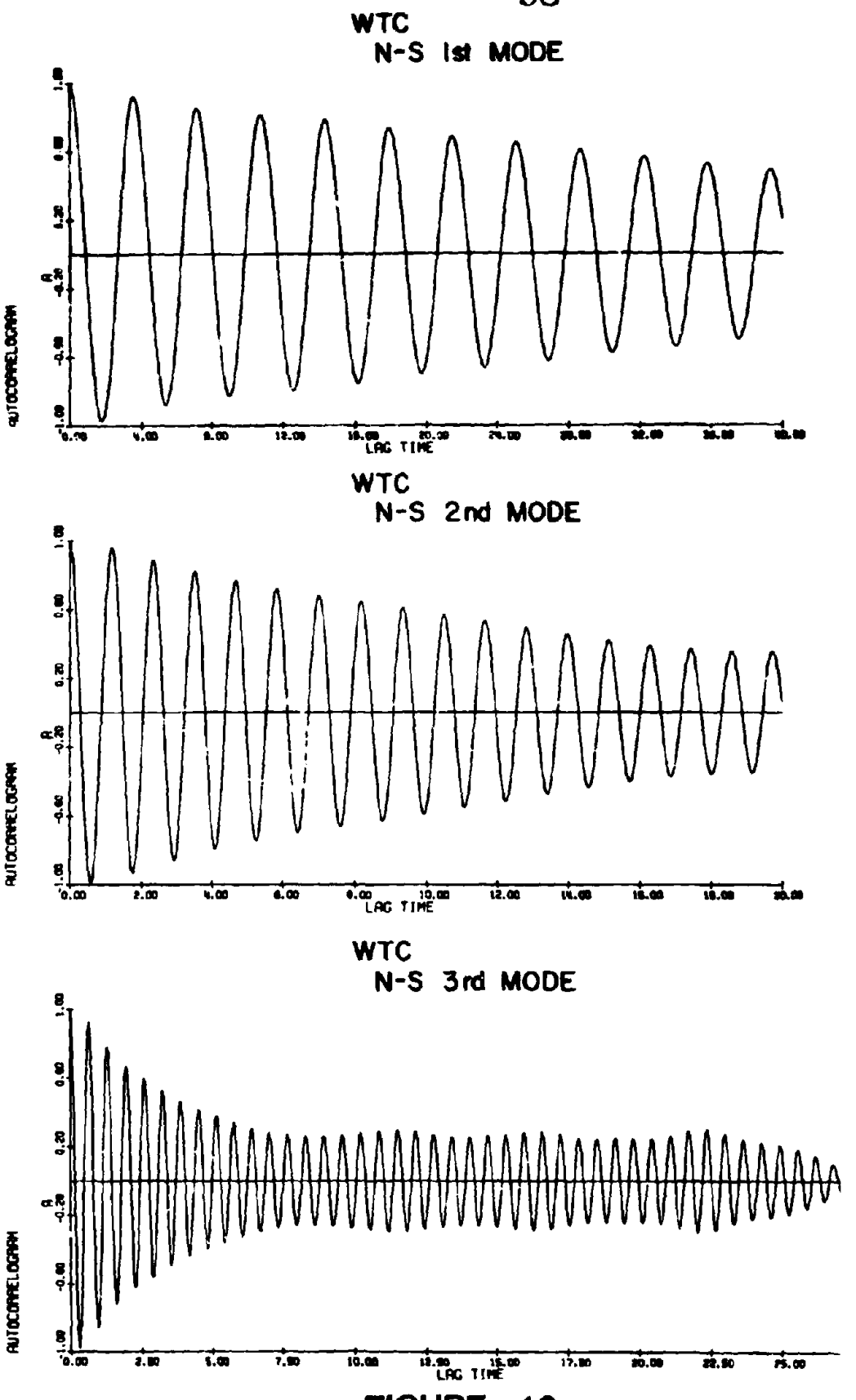
WTC
N-S 1st MODE
AUTOCORRELOGRAM
LAG TIME
WTC
N-S 2nd MODE
AUTOCORRELOGRAM
LAG TIME
WTC
N-S 3rd MODE
AUTOCORRELOGRAM
LAG TIME

FIGURE 13

WTC
E-W 1st MODE

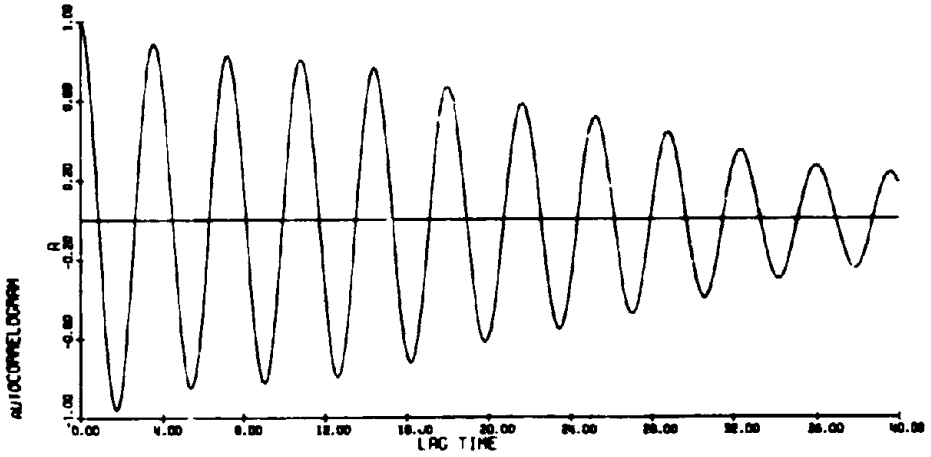

WTC
E-W 2nd MODE

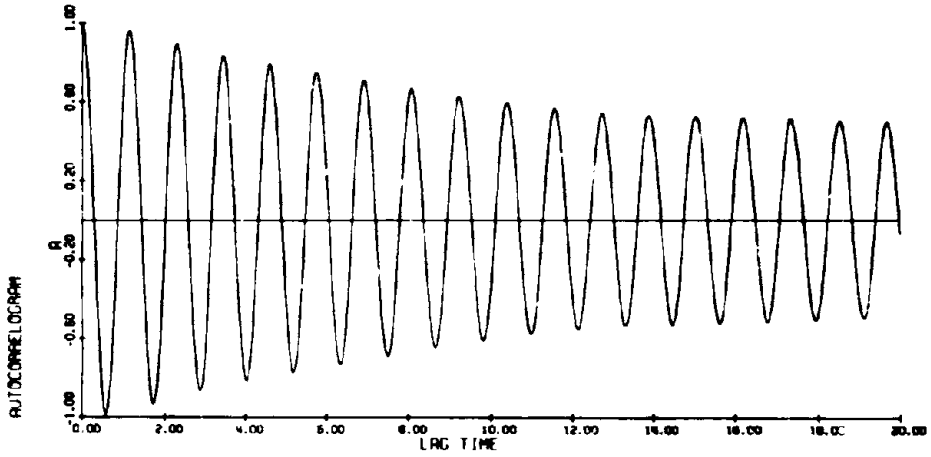

WTC
E-W 3rd MODE

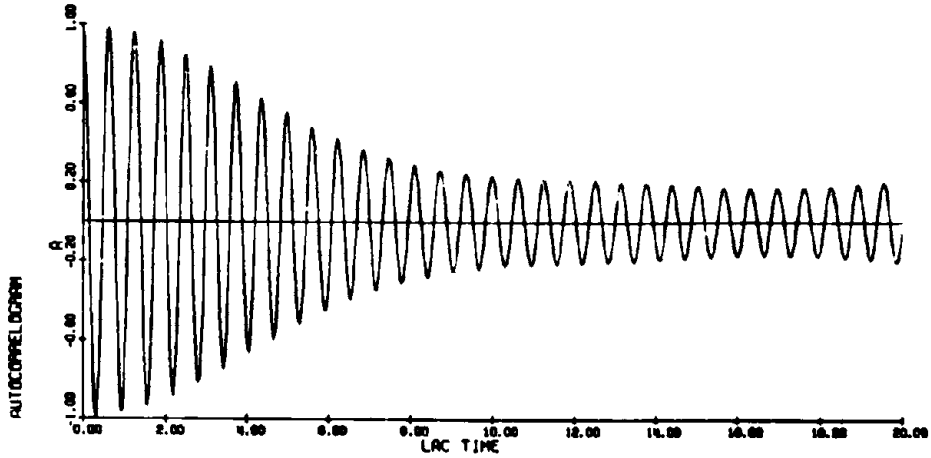

FIGURE 14

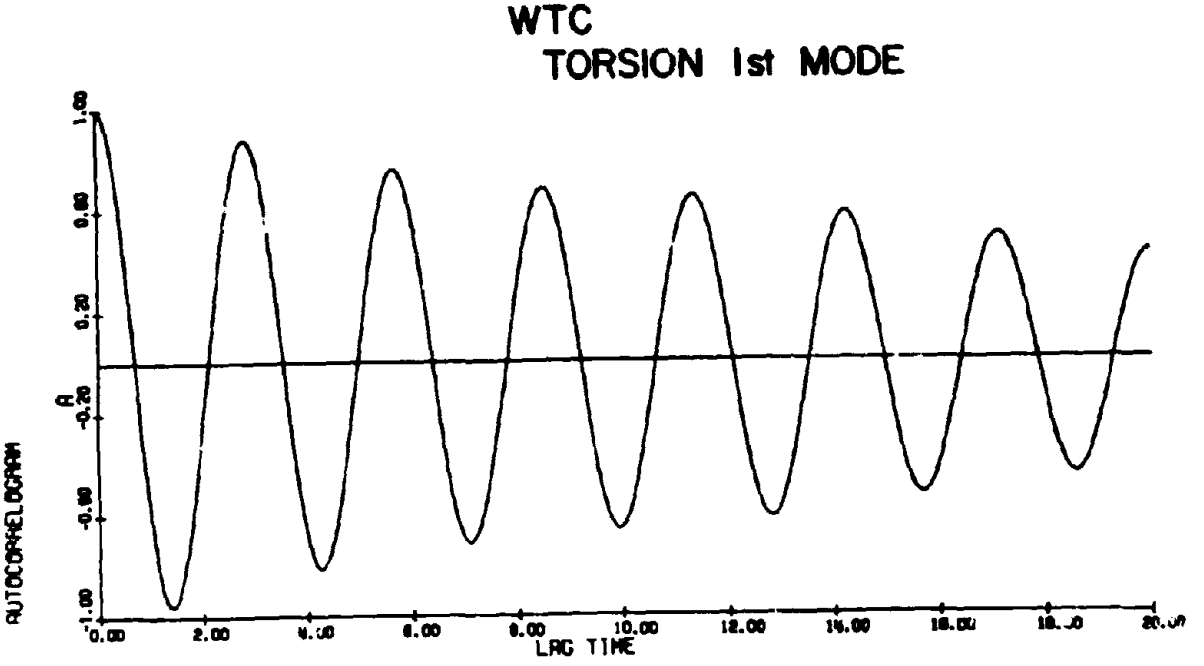
WTC
TORSION 1st MODE
AUTOCORRELOGRAM
A
1.00
0.60
0.20
-0.20
-0.60
-1.00
0.00
2.00
4.00
6.00
8.00
10.00
12.00
14.00
16.00
18.00
20.00
LAG TIME

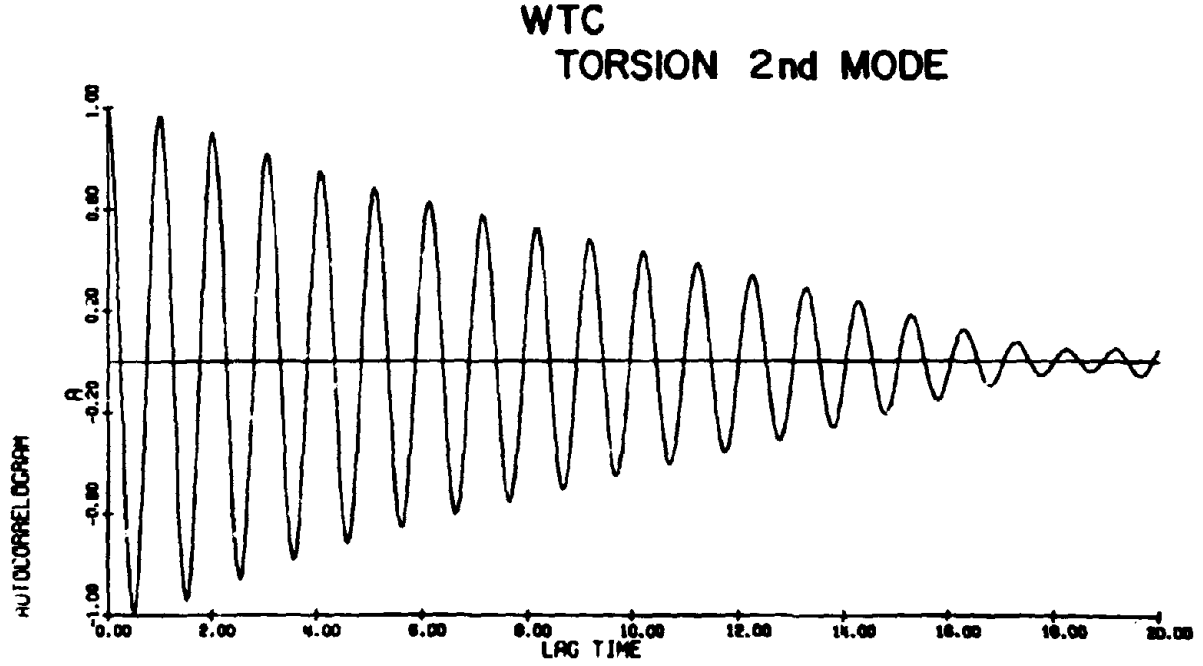
WTC
TORSION 2nd MODE
AUTOCORRELOGRAM
A
1.00
0.60
0.20
-0.20
-0.60
-1.00
0.00
2.00
4.00
6.00
8.00
10.00
12.00
14.00
16.00
18.00
20.00
LAG TIME

FIGURE 15

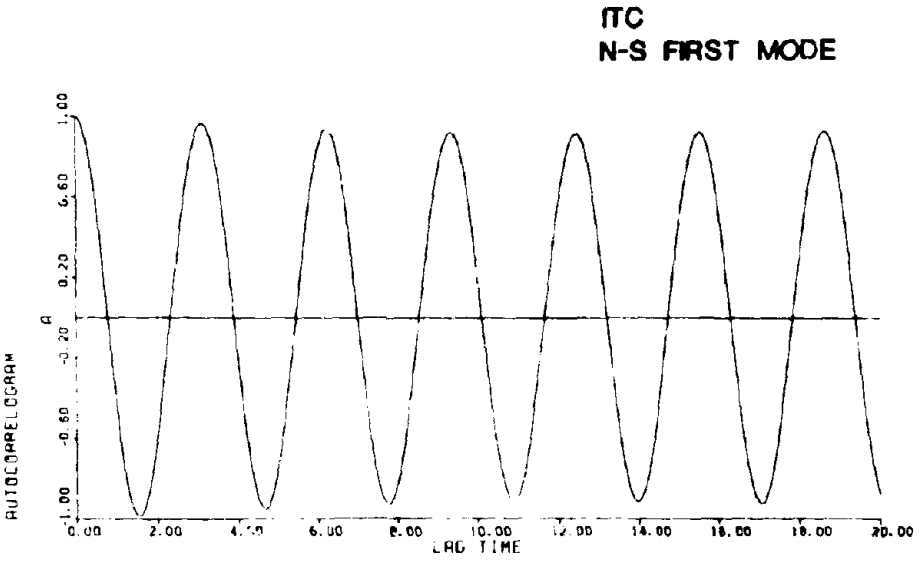
ITC
N-S FIRST MODE
AUTOCORRELOGRAM
R
1.00
0.60
0.20
-0.20
-0.60
-1.00
0.00
2.00
4.00
6.00
8.00
10.00
12.00
14.00
16.00
18.00
20.00
LAG TIME

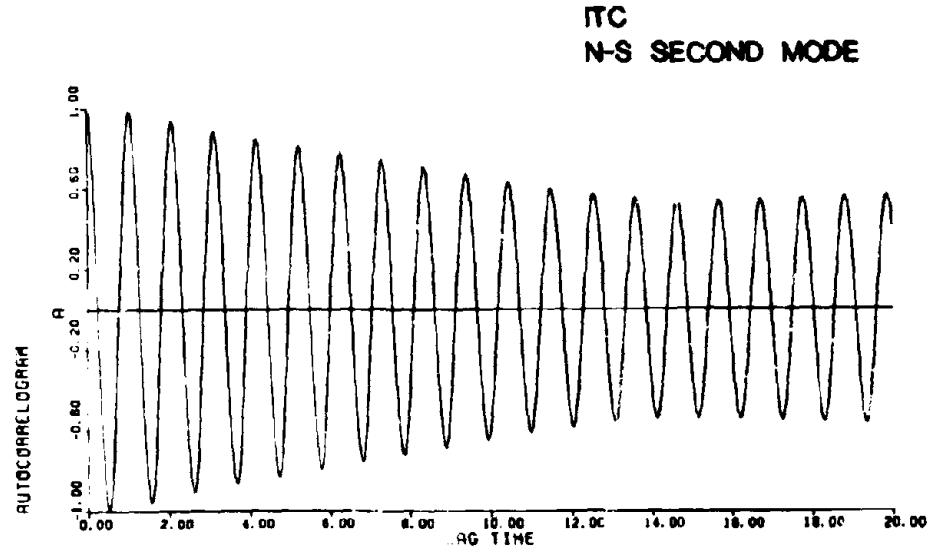
ITC
N-S SECOND MODE
AUTOCORRELOGRAM
R
1.00
0.60
0.20
-0.20
-0.60
-1.00
0.00
2.00
4.00
6.00
8.00
10.00
12.00
14.00
16.00
18.00
20.00
AG TIME

FIGURE 16

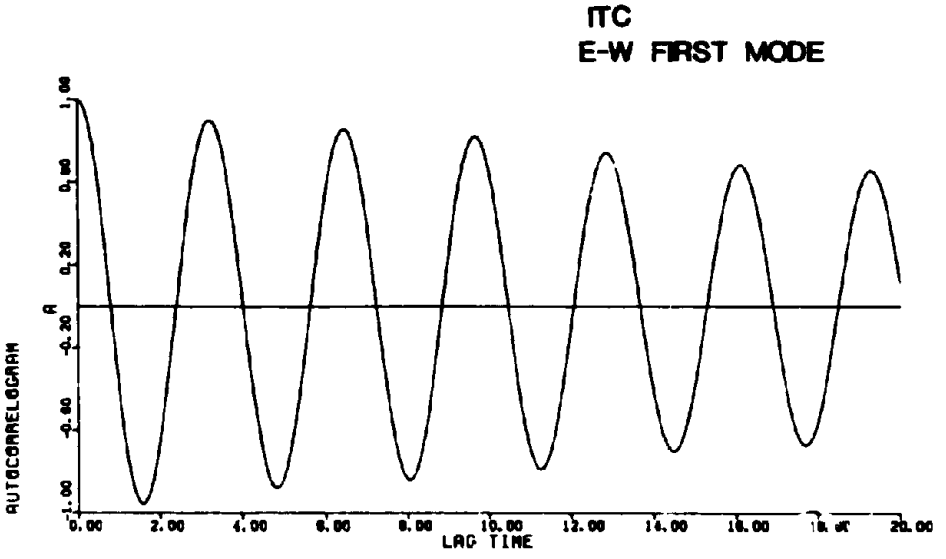
ITC
E-W FIRST MODE
AUTOCORRELOGRAM
A
LAG TIME

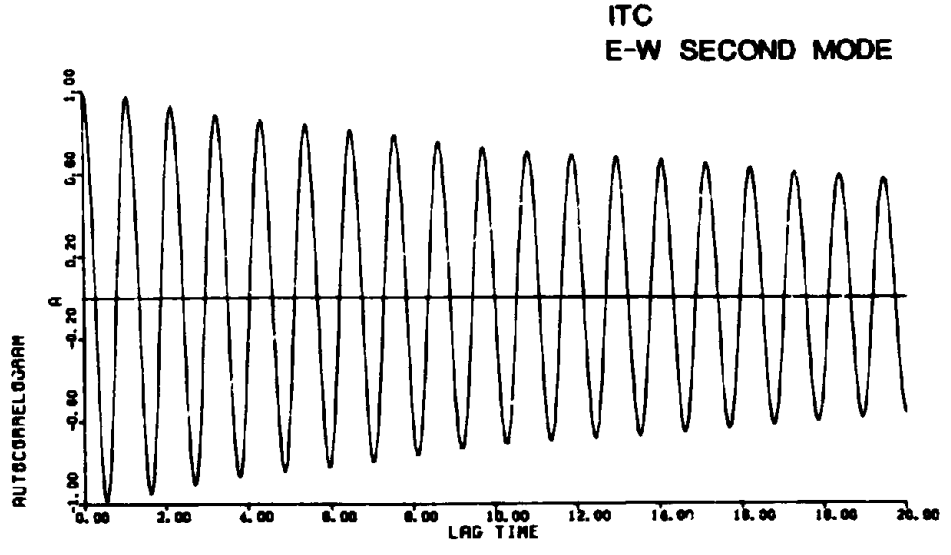
ITC
E-W SECOND MODE
AUTOCORRELOGRAM
A
LAG TIME

FIGURE 17

ITC
TORSION FIRST MODE

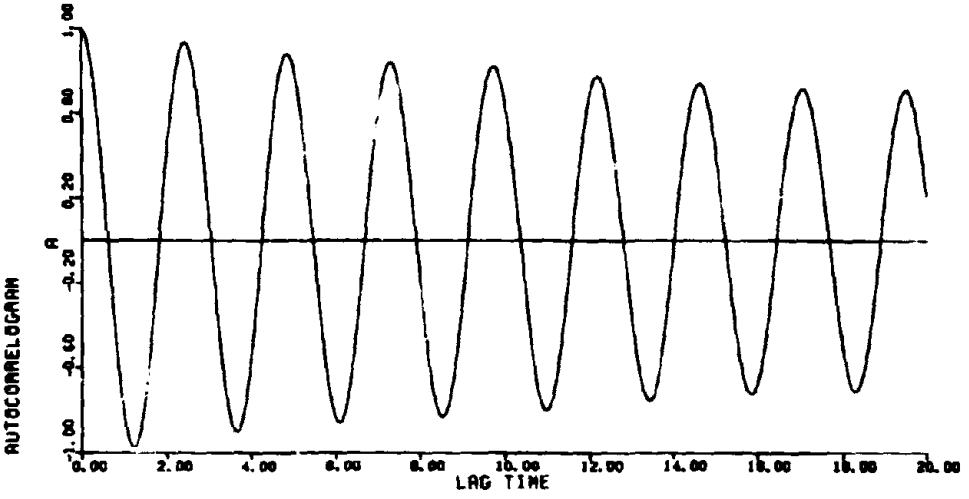

ITC
TORSION SECOND MODE

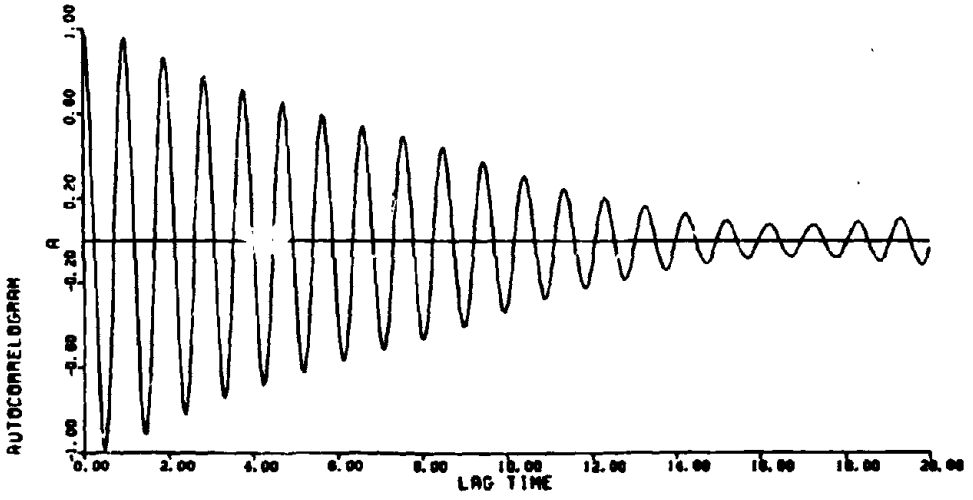

FIGURE 18

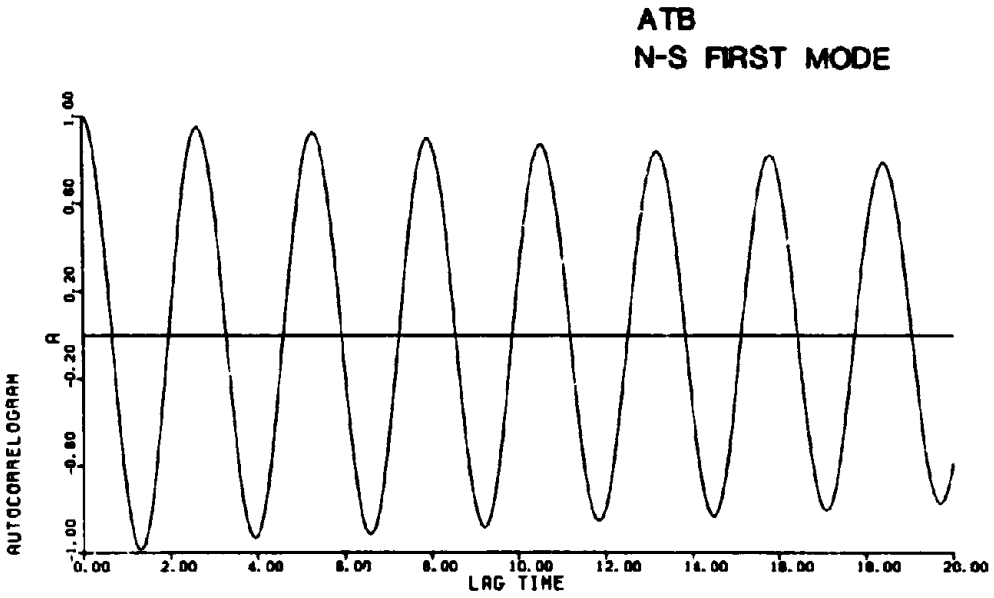
ATB
N-S FIRST MODE
AUTOCORRELOGRAM
A
1.00
0.60
0.20
-0.20
-0.60
-1.00
0.00
2.00
4.00
6.00
8.00
10.00
12.00
14.00
16.00
18.00
20.00
LAG TIME

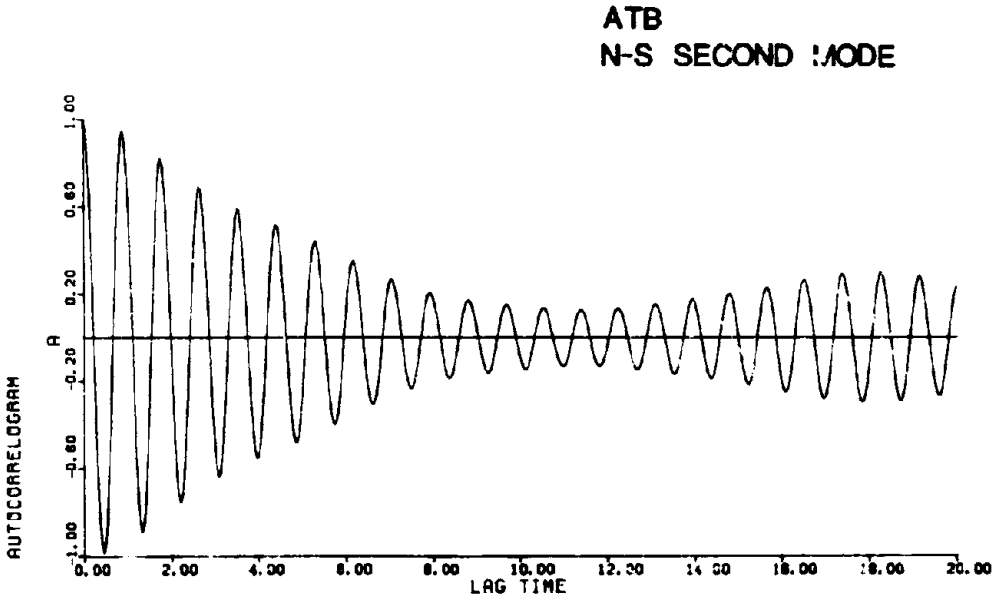
ATB
N-S SECOND MODE
AUTOCORRELOGRAM
A
1.00
0.60
0.20
-0.20
-0.60
-1.00
0.00
2.00
4.00
6.00
8.00
10.00
12.00
14.00
16.00
18.00
20.00
LAG TIME

FIGURE 19

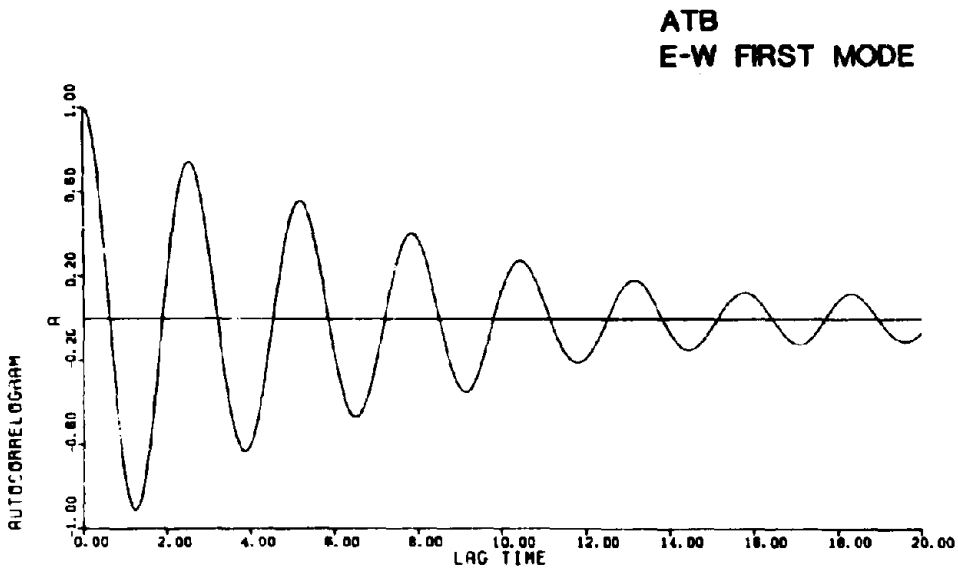
ATB
E-W FIRST MODE
AUTOCORRELOGRAM
A
1.00
0.60
0.20
-0.20
-0.60
-1.00
0.00
2.00
4.00
6.00
8.00
10.00
12.00
14.00
16.00
18.00
20.00
LAG TIME

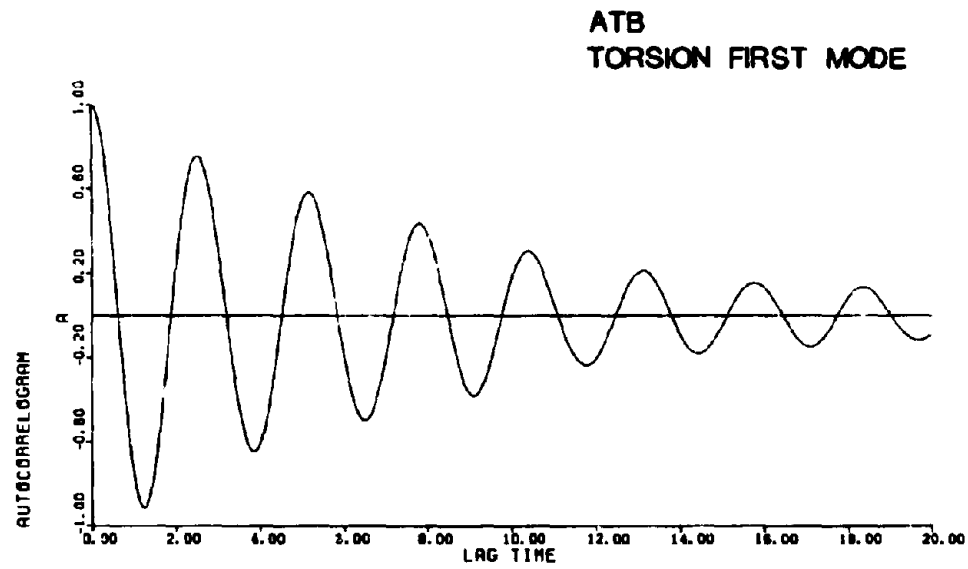
ATB
TORSION FIRST MODE
AUTOCORRELOGRAM
A
1.00
0.60
0.20
-0.20
-0.60
-1.00
0.00
2.00
4.00
6.00
8.00
10.00
12.00
14.00
16.00
18.00
20.00
LAG TIME

FIGURE 20

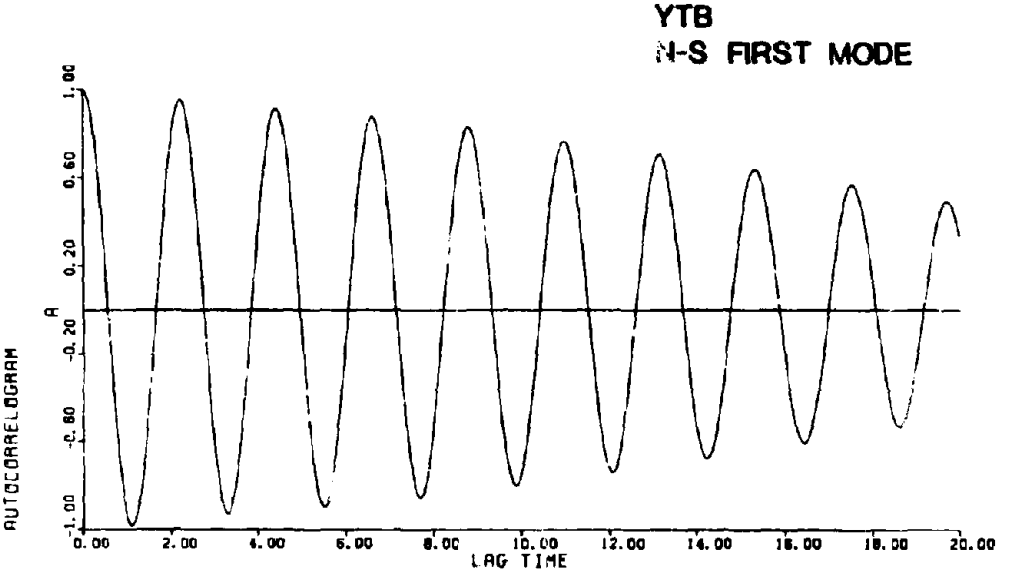
YTB
N-S FIRST MODE
AUTOCORRELOGRAM
A
1.00
0.60
0.20
-0.20
-0.60
-1.00
0.00
2.00
4.00
6.00
8.00
10.00
12.00
14.00
16.00
18.00
20.00
LAG TIME

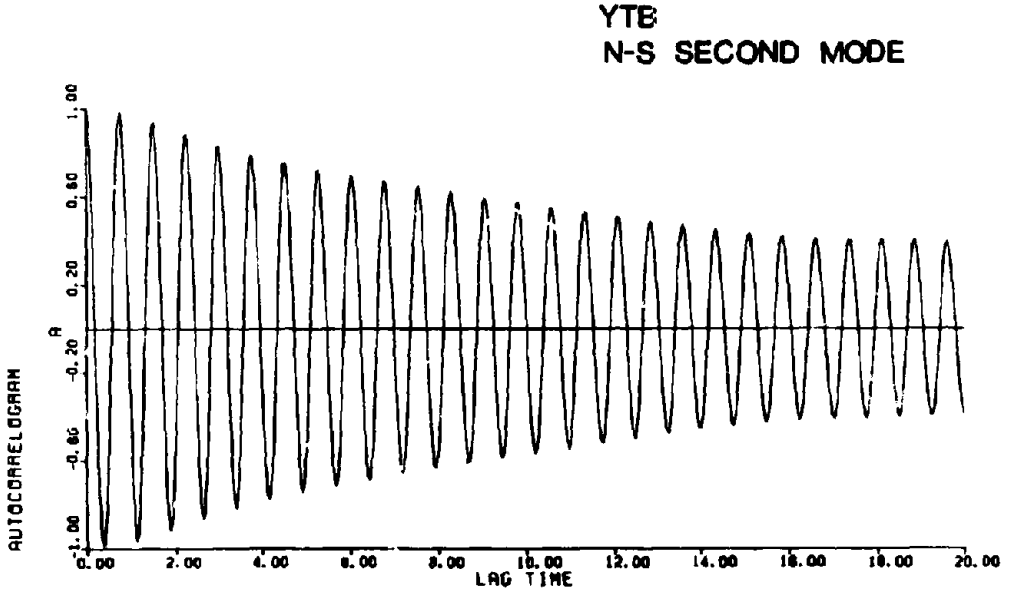
YTB
N-S SECOND MODE
AUTOCORRELOGRAM
A
1.00
0.60
0.20
-0.20
-0.60
-1.00
0.00
2.00
4.00
6.00
8.00
10.00
12.00
14.00
16.00
18.00
20.00
LAG TIME

FIGURE 21

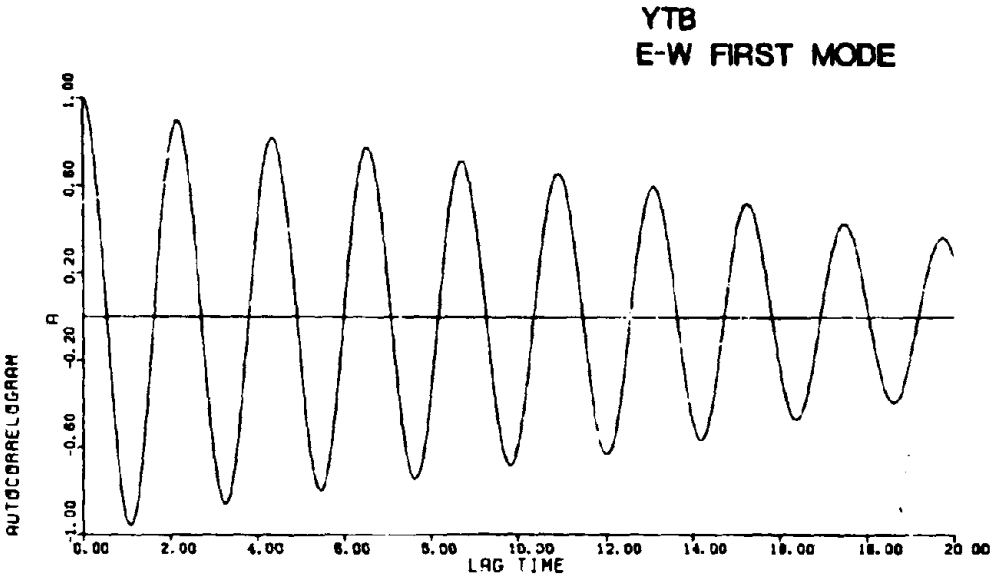
YTB
E-W FIRST MODE
AUTOCORRELOGRAM
R
1.00
0.60
0.20
-0.20
-0.60
-1.00
0.00
2.00
4.00
6.00
8.00
10.00
12.00
14.00
16.00
18.00
20.00
LAG TIME

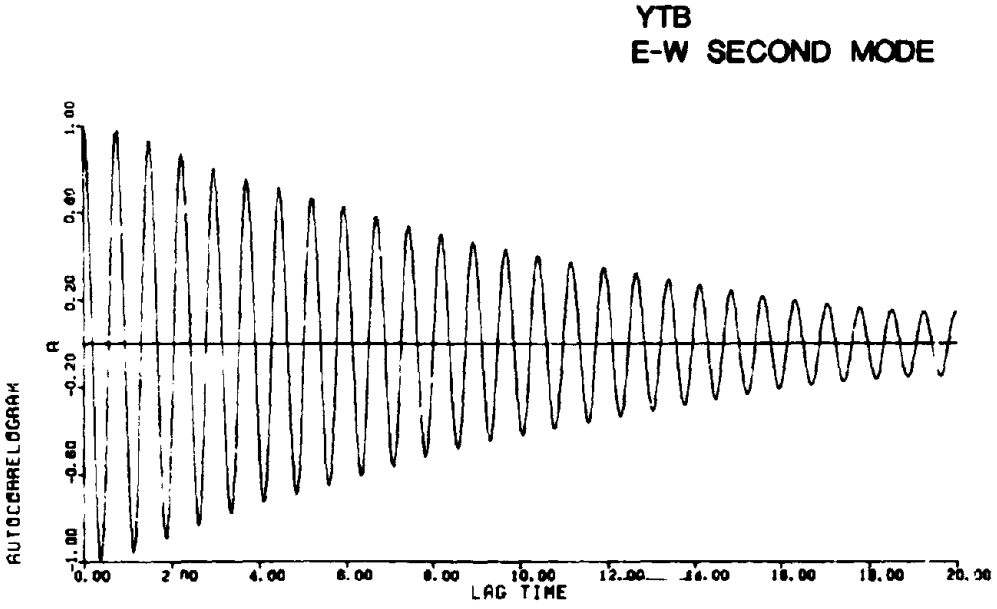
YTB
E-W SECOND MODE
AUTOCORRELOGRAM
R
1.00
0.60
0.20
-0.20
-0.60
-1.00
0.00
2.00
4.00
6.00
8.00
10.00
12.00
14.00
16.00
18.00
20.00
LAG TIME

FIGURE 22

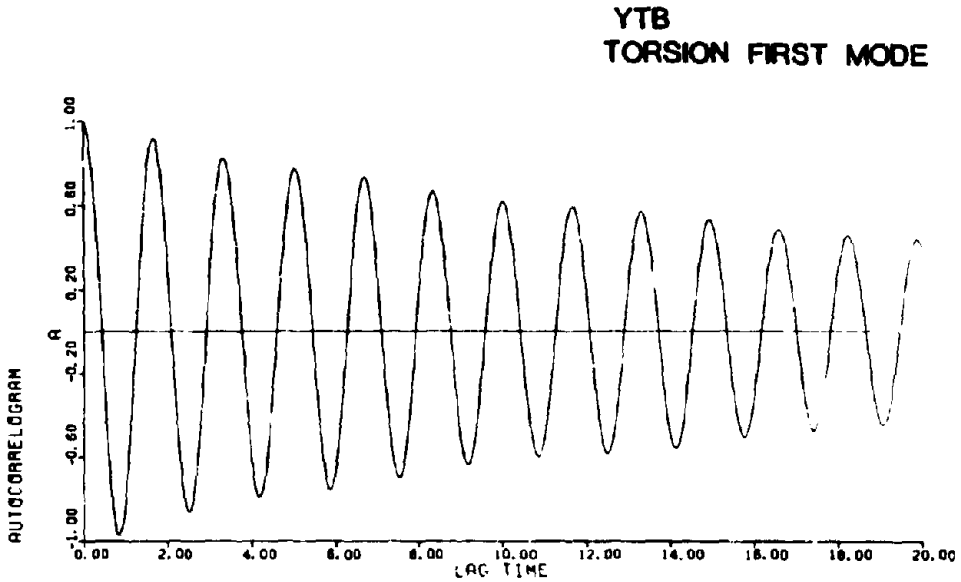
YTB
TORSION FIRST MODE
AUTOCORRELOGRAM
A
1.00
0.60
0.20
-0.20
-0.60
-1.00
0.00
2.00
4.00
6.00
8.00
10.00
12.00
14.00
16.00
18.00
20.00
LAG TIME

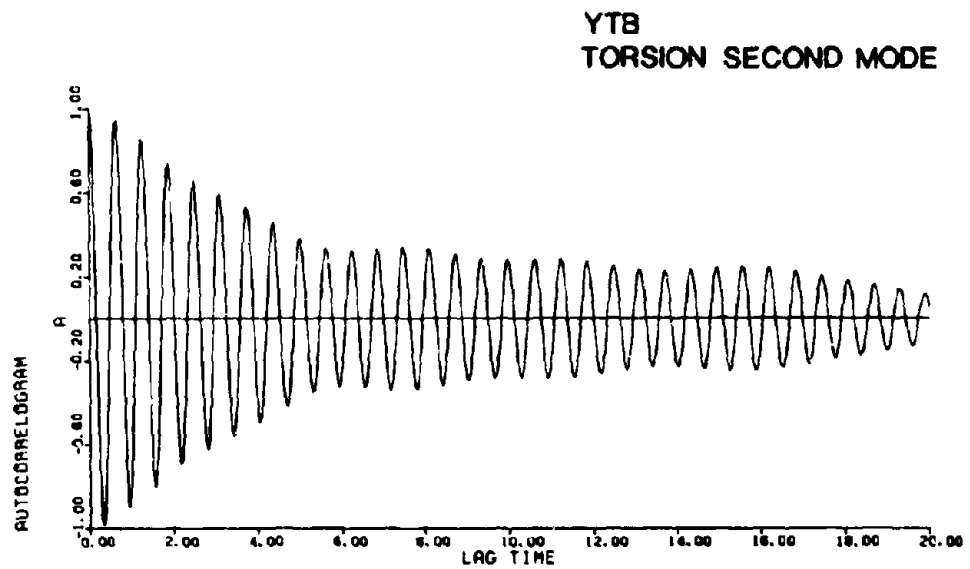
YTB
TORSION SECOND MODE
AUTOCORRELOGRAM
A
1.00
0.60
0.20
-0.20
-0.60
-1.00
0.00
2.00
4.00
6.00
8.00
10.00
12.00
14.00
16.00
18.00
20.00
LAG TIME

FIGURE 23

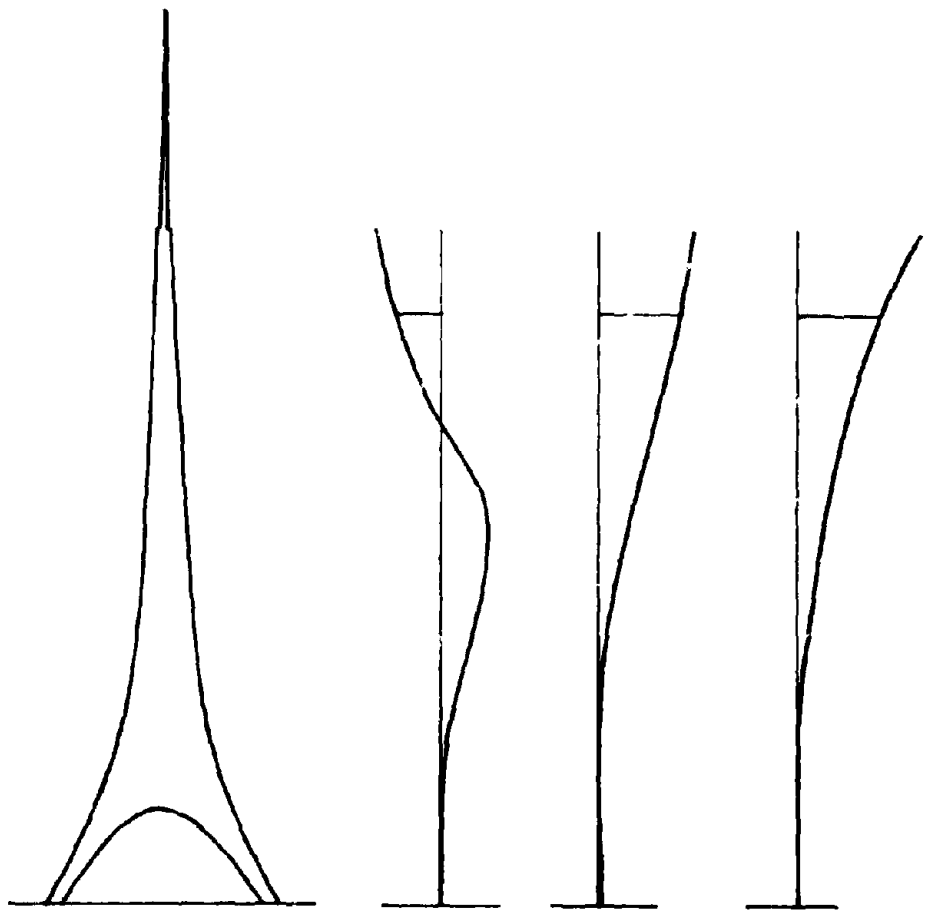

TOKYO TOWER
NORTH-SOUTH MODE SHAPES

FIGURE 24

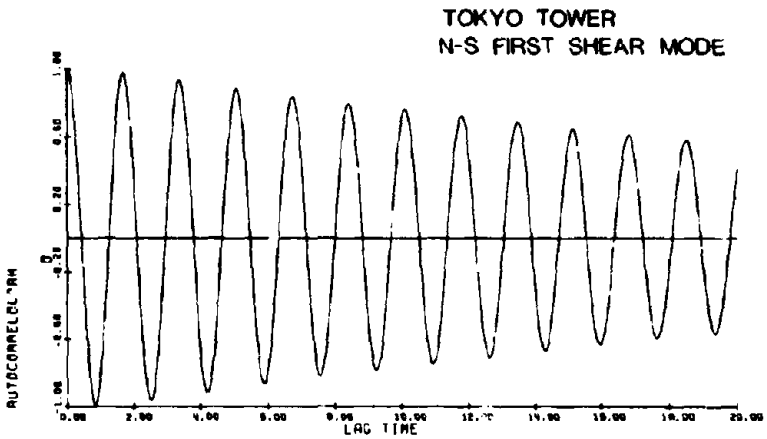
TOKYO TOWER
N-S FIRST SHEAR MODE
AUTOCORRELOGRAM
R
LAG TIME

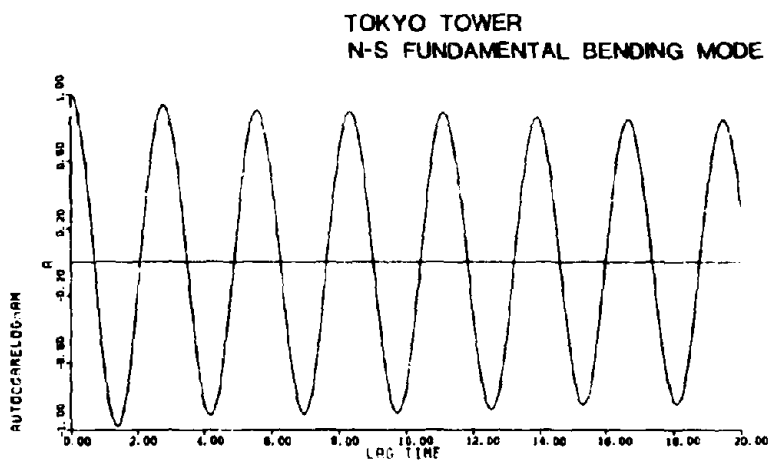
TOKYO TOWER
N-S FUNDAMENTAL BENDING MODE
AUTOCORRELOGRAM
R
0.00
2.00
4.00
6.00
8.00
10.00
12.00
14.00
16.00
18.00
20.00
LAG TIME

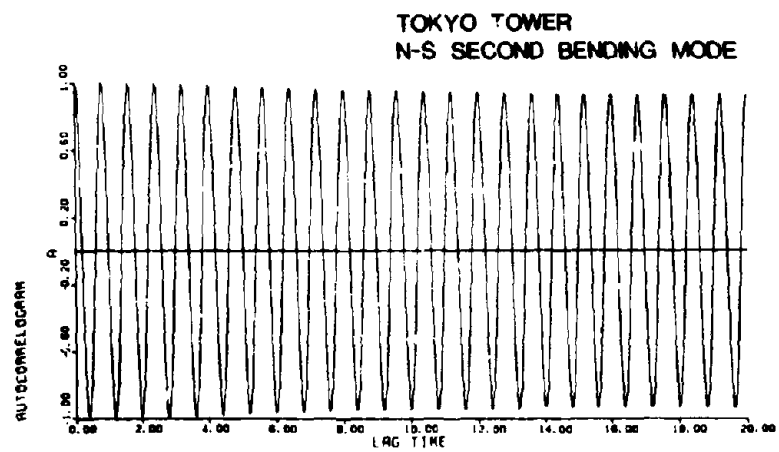
TOKYO TOWER
N-S SECOND BENDING MODE
AUTOCORRELOGRAM
R
LAG TIME

FIGURE 25

TOKYO TOWER
TORSION FIRST MODE

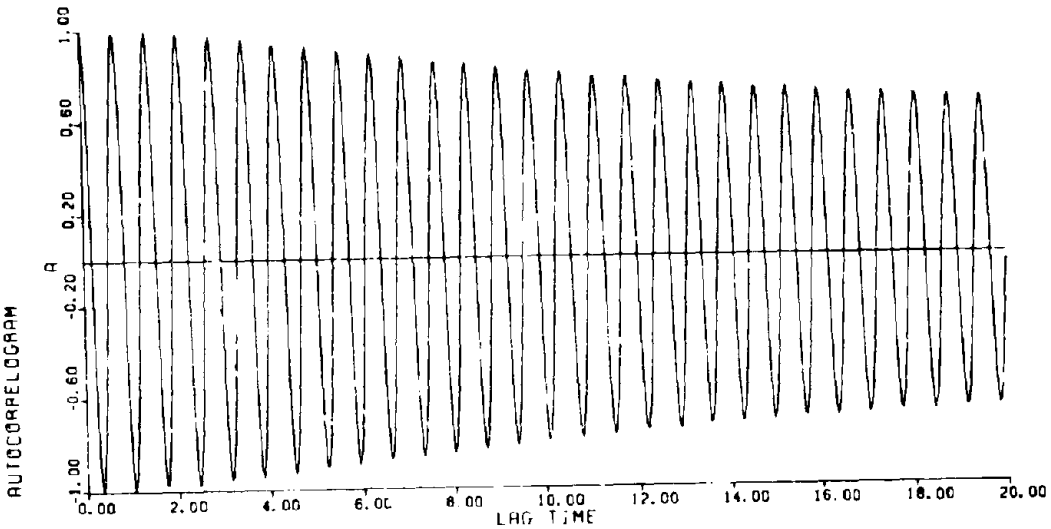

TOKYO TOWER
TORSION SECOND MODE

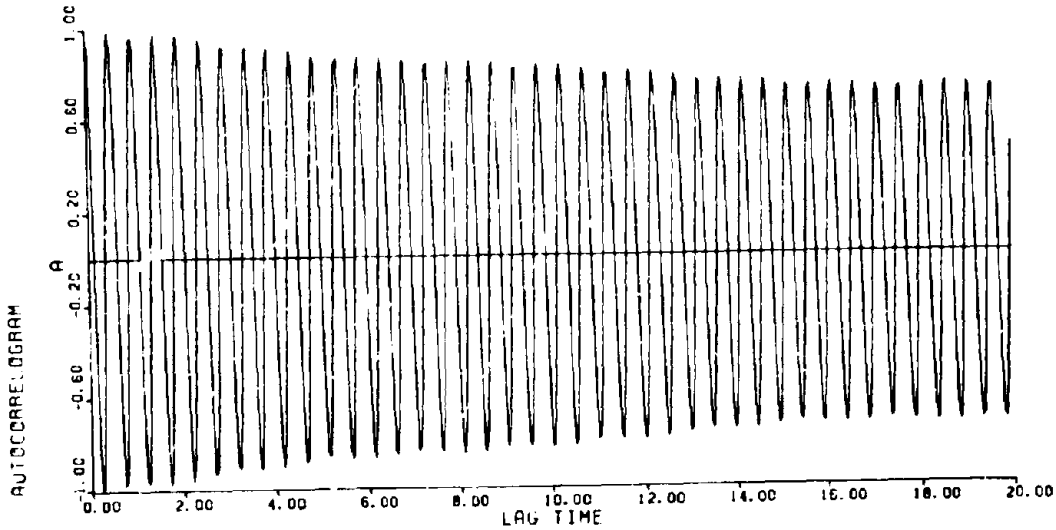

FIGURE 26

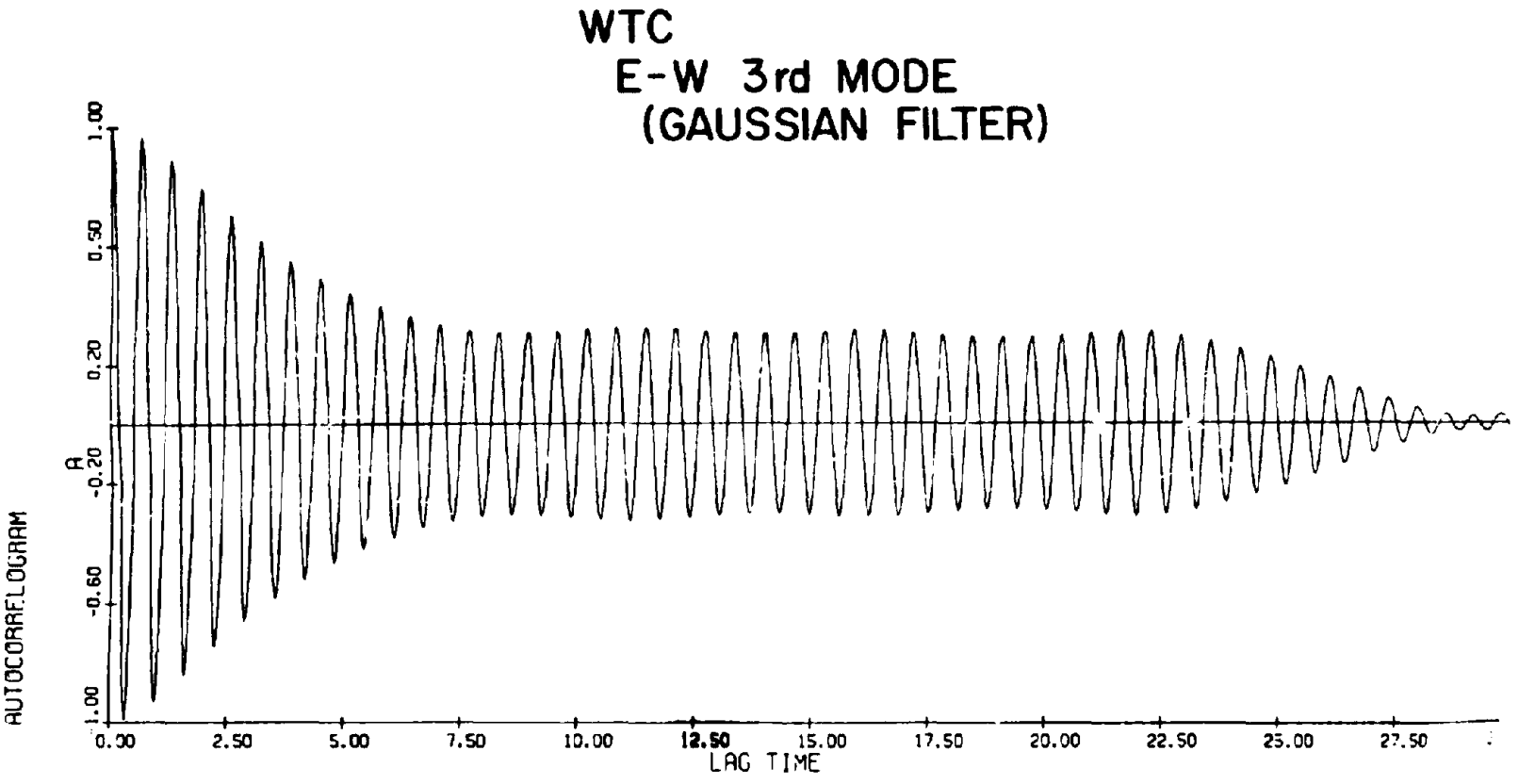
WTC
E-W 3rd MODE
(GAUSSIAN FILTER)
AUTOCORRELOGRAM
A
1.00
0.60
0.20
-0.20
-0.60
-1.00
0.00
2.50
5.00
7.50
10.00
12.50
15.00
17.50
20.00
22.50
25.00
27.50
LAG TIME

FIGURE 27

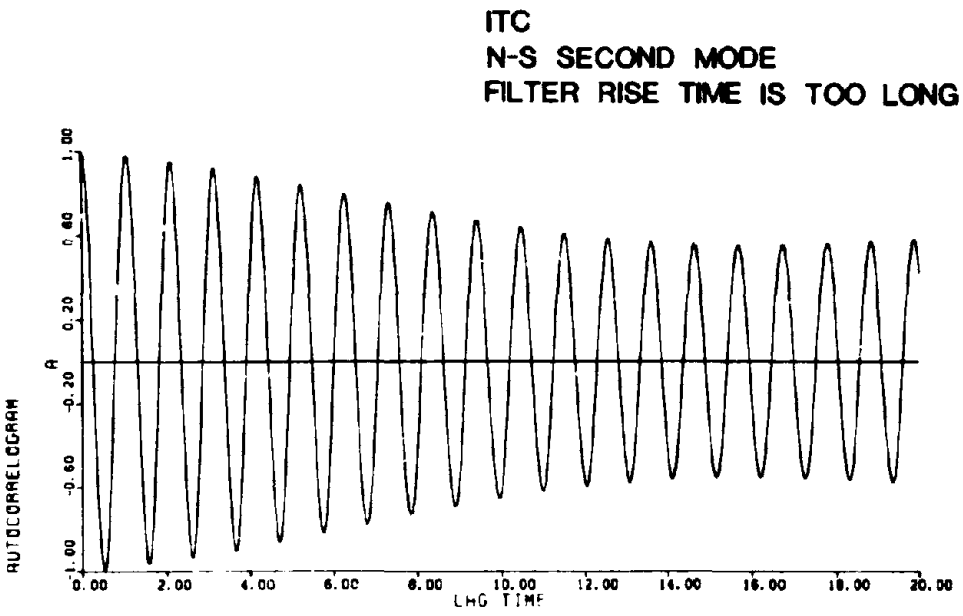
ITC
N-S SECOND MODE
FILTER RISE TIME IS TOO LONG
AUTOCORRELOGRAM
A
1.00
0.60
0.20
-0.20
-0.60
-1.00
0.00
2.00
4.00
6.00
8.00
10.00
12.00
14.00
16.00
18.00
20.00
LAG TIME

FIGURE 28

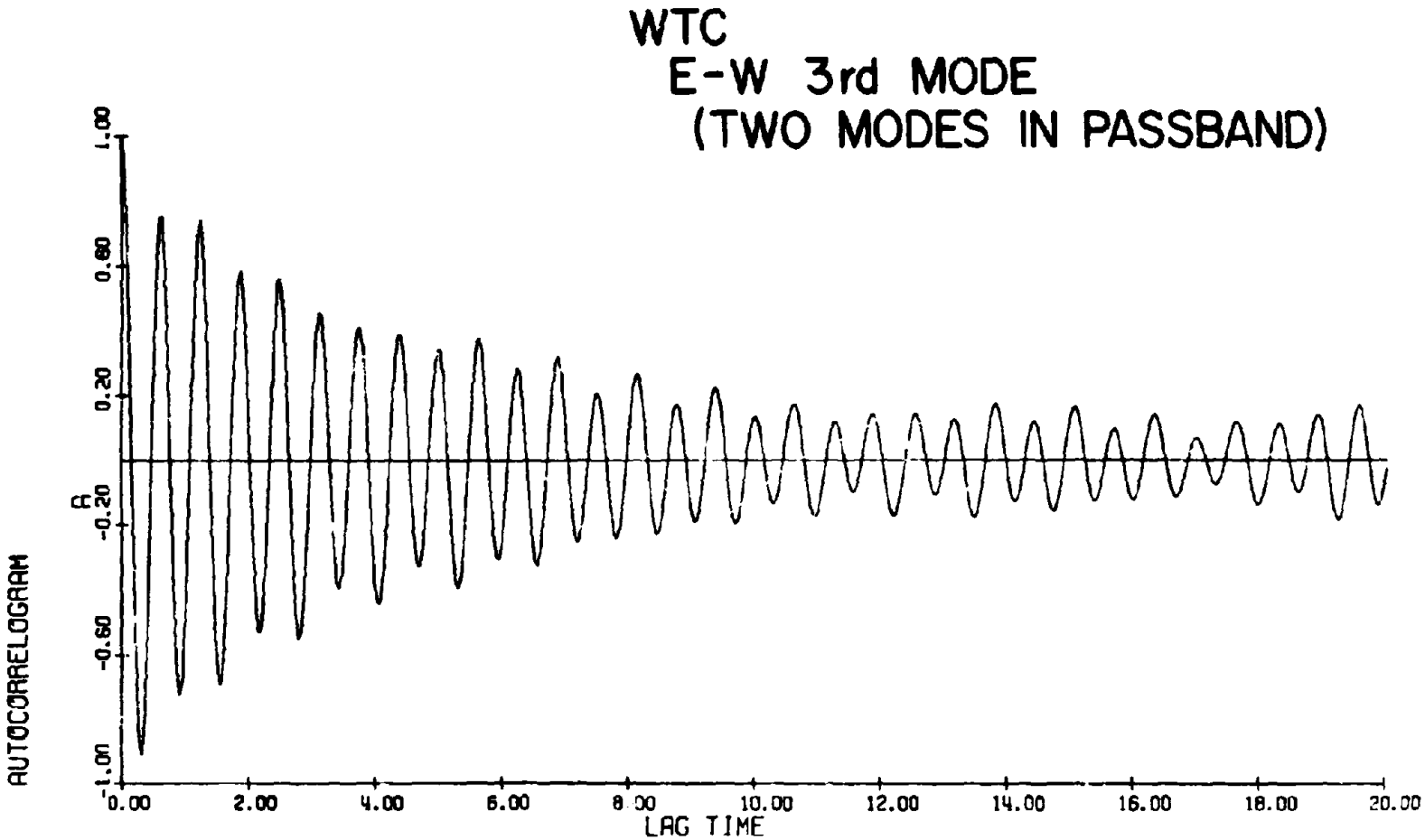
WTC
E-W 3rd MODE
(TWO MODES IN PASSBAND)
AUTOCORRELOGRAM
R
1.00
0.60
0.20
-0.20
-0.60
-1.00
0.00
2.00
4.00
6.00
8.00
10.00
12.00
14.00
16.00
18.00
20.00
LAG TIME

FIGURE 29

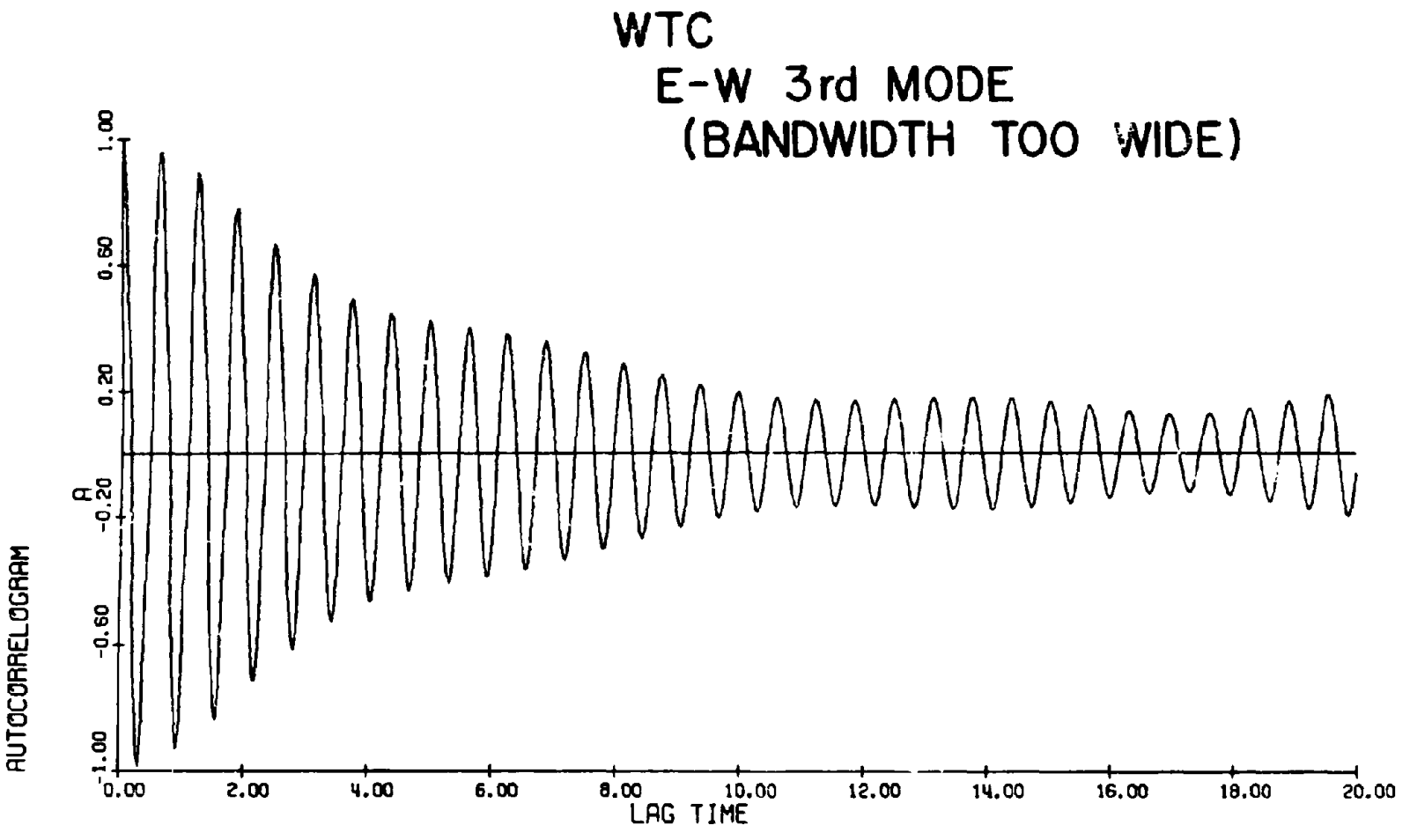
WTC
E-W 3rd MODE
(BANDWIDTH TOO WIDE)
AUTOCORRELOGRAM
A
1.00
0.60
0.20
-0.20
-0.60
-1.00
0.00
2.00
4.00
6.00
8.00
10.00
12.00
14.00
16.00
18.00
20.00
LAG TIME

FIGURE 30

TOKYO TOWER
N-S FIRST SHEAR MODE
WRONG CENTER FREQUENCY OF FILTER

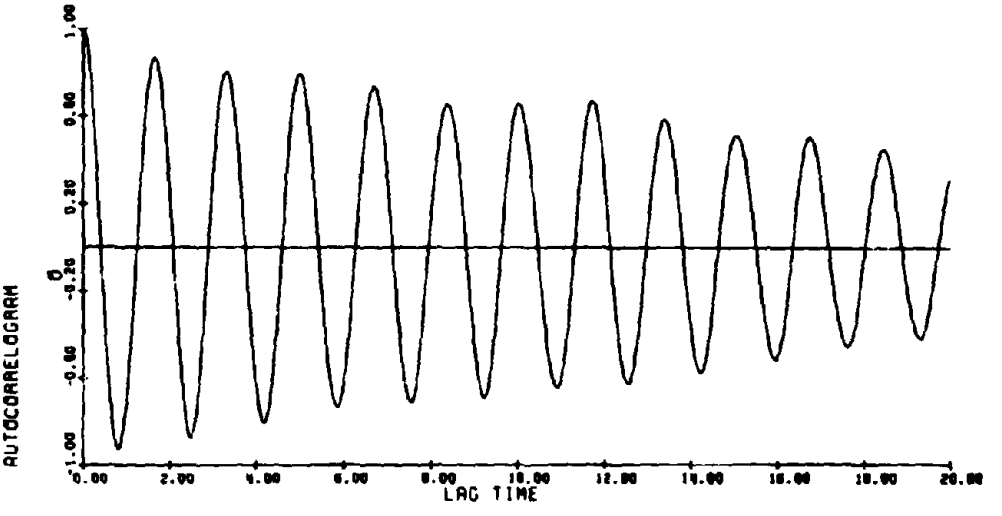

TOKYO TOWER
N-S COMBINATION OF FIRST BENDING
AND FIRST SHEAR MODES
BANDWIDTH TOO WIDE

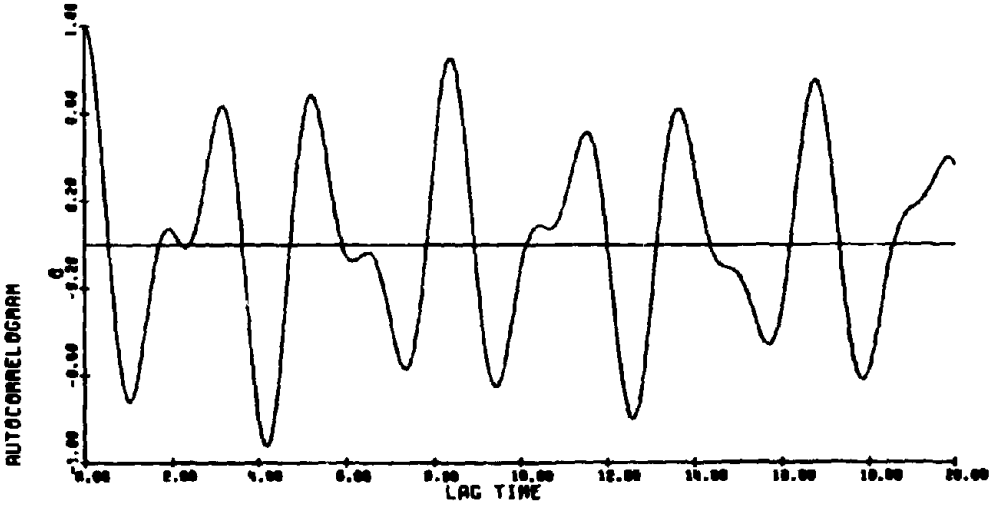

FIGURE 31